Università Ca'Foscari Venezia

Corso Di Laurea Magistrale In
Scienze E Tecnologie Dei Bio E Nanomateriali

Tesi di Laurea

ATOMIC LAYER DEPOSITION OF TiO_2 THIN FILM FOR BIOMEDICAL APPLICATIONS

Relatore: Prof. Patrizia Canton
Correlatore: Dr. Naida El Habra

Laureando: Giacomo Sagrini
Matricola: 858284

Anno accademico 2018/2019

It is not about the leg,
it is about the heart and the mind.
Eliud Kipchoge

TABLE OF CONTENTS

Abstract **1**

Sommario **3**

Introduction **5**

Outline of the thesis *7*

List of abbreviations **9**

Chapter 1 Atomic layer deposition: theoretical aspects **11**

1.1 History of ALD **11**

1.2 The mechanism **12**

1.3 Advantages and disadvantages **16**

1.4 ALD window **18**

1.5 Precursors **19**

1.6 ALD variants **21**

1.7 Industrial applications **23**

1.8 Titanium dioxide **25**

1.8.1 TiO_2 as biomaterial 26

1.8.2 TiO_2 deposition using ALD 28

Chapter 2 Experimental: optimization TiO_2 thin film deposition via ALD and characterization **29**

2.1 ALD equipment **29**

2.1.1 Precursors delivery system 30

2.1.2 The reaction chamber 31

2.1.3 Exhaust and vacuum system 32

2.1.4 The ALD precursor used 33

2.2 Deposition method ***34***

2.2.1 Temperature test 34

2.2.2 Substrate preparation: RCA cleaning 35

2.3 ALD deposition: optimization of titanium (IV) isopropoxide pulse time ***38***

2.3.1 Sims analysis 38

2.3.2 XRD: structural characterization 40

2.3.3 SEM: morphological characterization 40

2.4 ALD deposition: optimization of titanium (IV) isopropoxide purge time ***42***

2.4.1 XRD structural characterization 42

2.4.2 SEM: thickness investigation 43

2.5 ALD deposition: optimization of H_2O purge time ***44***

2.5.1 Spectroscopic Ellipsometry: thickness measurements 44

2.5.2 XRD: structural characterization 46

2.5.3 SEM: morphological characterization 46

2.6 Preliminary decomposition test of titanium (IV) isopropoxide ***47***

Chapter 3 Surface wettability study and neuronal biocompatibility test on TiO_2 thin film ***49***

3.1 Surface wettability study on TiO_2 thin film ***49***

3.1.1 Water contact angle measurements of as grown sample 51

3.1.2 Water contact angle measurements after UV exposure 52

3.1.3 Water contact angle after sterilization procedure 54

3.1.4 Water contact angle measurements after UV exposure on sterilized sample 55

3.2 Biocompatibility experiments: neuronal preparation procedure ***56***

3.2.1 Neurons dissociation and plating 59

3.2.2 Monitoring 60

3.2.3 SEM of neuronal cells *66*

3.2.4 Titania behavior in physiological medium: XPS and SEM investigations *67*

Conclusion ***73***

Appendix A: Characterization methods ***75***

A.1 X-ray Diffraction (XRD) ***75***

A.2 Scanning Electron Microscopy (SEM) *77*

A.3 Secondary Ions Mass Spectrometry (SIMS) ***78***

A.4 X-ray Photoelectron Spectroscopy (XPS) ***80***

A.5 Water Contact Angle (WCA) ***81***

Bibliography ***83***

Acknowledgements ***91***

ABSTRACT

Material Science is fundamental to properly functionalize the material surface through a suitable *bottom-up* approach in order to induce a targeted behavior. Among Chemical Vapor Deposition (CVD) techniques, Atomic Layer Deposition (ALD) is an attractive *bottom-up* process for the manufacturing of inorganic nanostructured thin films, with thickness theoretically down to a fraction of a monolayer. Thanks to its unique mechanism of growth, ALD is a powerful technique that has achieved a lot of interest: it allows the deposition of high quality thin films with atomic level control and high conformal coverage even on complex shaped surfaces. Semiconductor processing has been one of the main motivations for the development of ALD. Indeed, the miniaturization in the semiconductor industry has led to the requirement for atomic level control of thin film deposition on high aspect-ratio structures. In this regard no other thin film technique can approach the conformality achieved by ALD on these types of structures. It has also emerged as an important technique for depositing thin films for a variety of applications, from catalysts to electroluminescent displays, microelectronics, hybrid organic-inorganic materials and beyond.
In this work, a low pressure ALD process was employed to deposit titanium dioxide (TiO_2) for biomedical neuro-chips applications based on electrolyte-oxide-semiconductor field-effect transistors (EOSFET) and EOS-capacitor for stimulations of neuronal tissue. Specifically, the main aim of this work was the optimization of an ALD process for the deposition of high-*k* dielectric TiO_2 starting from titanium tetra-isopropoxide (TTIP) and deionized water. In particular, dense, pinhole-free and at controlled thickness thin films were deposited by working at controlled temperature ($T<300°C$) and by varying the process parameters
The structure-properties correlation of the grown thin films were widely studied by X-Ray Diffraction (XRD), Scanning Electron Microscopy (SEM), Energy Dispersive X-Ray Spectrometry (EDX), X-Ray Photoelectron Spectroscopy (XPS) and Secondary Ion Mass Spectrometry (SIMS), in order to evaluate the influence of the different process parameters on their physico-chemical properties.
Aiming to evaluate the functional biomedical applications of the deposited TiO_2 thin films via ALD, preliminary cellular/neuronal biocompatibility *in-vitro* tests were explored. In this regard, in order to study the influence on cell attachment/adhesion and growth, the surface chemical functionality was studied by wettability analyses. Water contact angle (WCA) has been used to establish the surfaces' wettability. All freshly prepared TiO_2 thin films showed super-hydrophilicity, even if the subsequent exposure to air induced a progressive decreasing of wettability. This behavior is ascribed to a progressive contamination by atmospheric hydrocarbons. To contrast this undesired behavior, the hydrophilicity (high-energy surfaces) was restored by exposing the contaminated surfaces to UV radiation and studying the WCA variation in relation to different exposure times.
Biocompatibility of TiO_2 was verified *in-vitro* by cultivating of neurons dissociated from rat's hippocampi and monitoring their development and morphology for 14 days in culture. The results showed that TiO_2 thin film is a biocompatible surface: neurons show developmental stages and morphology that are comparable to neurons seeded on standard Petri dishes.

SOMMARIO

La scienza dei materiali è il pilastro fondamentale per lo studio della corretta funzionalizzazione di un materiale attraverso un adeguato approccio di tipo *bottom-up* al fine di indurre nel materiale stesso nuove peculiarità. Tra le tecniche di deposizione chimiche da fase vapore, Chemical Vapor Deposition (CVD), si annovera la Atomic Layer Deposition (ALD) un interessante processo *bottom-up* impiegato per la produzione di film sottili inorganici e nanostrutturati, con spessori fino a frazioni di monostrato. Grazie alle sue caratteristiche di crescita uniche, l'ALD è una potente tecnica di deposizione che ha riscosso grande interesse poichè permette la deposizione di film sottili di alta qualità con un controllo a livello atomico e alta conformalità di copertura anche su superfici sagomate e complesse. L' impiego nel campo dei semiconduttori è stato uno dei principali stimoli per lo sviluppo di questa tecnica. Infatti, la progressiva miniaturizzazione nell'industria dei semiconduttori ha portato alla necessità di avere un controllo a livello atomico della deposizione su strutture ad alto *aspect-ratio*. A questo proposito nessun'altra tecnica di deposizione di film sottili è capace di ottenere un'uniformità così elevata su questo genere di strutture. È emersa anche come importante tecnica per il deposito di film sottili per diverse applicazioni: catalizzatori, display elettroluminescenti, microelettronica, ibridi organico-inorganico ed altre.

In questo lavoro viene presentata un'applicazione della tecnica ALD a bassa pressione per la deposizione di biossido di Titanio (TiO_2) per applicazioni biomediche di neuro-chip basate su EOFSET, electrolyte-oxide-semiconductor field-effect transitor. Più in particolare l'obiettivo di questo studio è stato l'ottimizzazione di un processo ALD per la deposizione di *high-k dielectric* TiO_2, partendo da titanio tetraisopropossido (TTIP) e acqua deionizzata. I film sottili *pinohole-free* con spessore desiderato sono stati depositati a temperatura controllata (T< 300°C) variando i diversi parametri di processo.

La correlazione struttura-proprietà dei film sottili è stata ampiamente studiata attraverso analisi di diffrazione di raggi X (XRD), microscopio elettronico a scansione (SEM), spettroscopia fotoelettronica di raggi X (XPS), spettroscopia a energia dispersiva di raggi X (EDX), spettroscopia di massa di ioni secondari (SIMS), con l'obiettivo di valutare l'influenza dei vari parametri di processo sulle proprietà chimico fisiche dello strato depositato. Al fine di valutare le applicazioni biomediche delle pellicole di TiO_2 depositate tramite ALD, sono stati eseguiti preliminari test di biocompatibilità *in vitro* tra cellule e neuroni e le superfici funzionalizzate. A tal proposito, per studiare l'adesione cellulare e verificare lo sviluppo e la crescita delle cellule stesse, si considera la bagnabilità della superficie come parametro diagnostico. Sono state effettuate misure di angolo di contatto (WCA) utilizzando gocce d'acqua. Tutti i film appena depositati hanno mostrato superidrofilia, mentre la successiva e progressiva esposizione all'aria induce una progressiva diminuzione della bagnabilità. È possibile attribuire questo comportamento alla graduale contaminazione da idrocarburi presenti nell'atmosfera. Per contrastare questo fenomeno indesiderato, l'idrofilia iniziale è stata ripristinata attraverso l'esposizione delle superfici contaminate a raggi UV ed è stata misurata la variazione dell'angolo di contatto in relazione ai diversi tempi di esposizione alla radiazione. La bioattività neuronale *in-vitro* è stata testata attraverso la coltivazione di neuroni estratti da ippocampi di ratti e monitorati per 14 giorni. I risultati mostrano che film sottile di TiO_2 è una superficie biocompatibile, la crescita e lo sviluppo dei neuroni sono infatti comparabili a quelli cresciuti su dischi Petri.

INTRODUCTION

The study of thin films encompasses many fields of research like Physics, Chemistry and Material Sciences and nowadays also biology and medicine are involved. In recent years this branch of technology is experiencing rapid growth in photovoltaics [Delft J. A. et al. 2012] and micro electronics devices [Hoivich N. D. et al. 2003]. We can find other simply application in decorative areas and in optics but also in protective and biocompatibility coating [Finch D. S. et al. 2008].
The new layer (i.e. the deposited film) on the substrate gives to the starting material new interesting features depending on the chemistry nature of the substance, on the specific characteristics of the deposition method, and physical parameter like temperature and pressure. The variation of the process parameters, the choice of the substrate, and the reagents, allow the operator to obtain a large variety of thicknesses and types of film, thus different applications and specific properties.
Thanks to its different applications, thin films can be created by disparate techniques each one with different features, and relative advantages and disadvantages. In particular, the most used and versatile techniques are: Chemical Vapor Deposition (CVD) [Choy K. L. 2003] and Physical Vapor Deposition (PVD) [Mattox D. M. 2010].
In the previous years, nanotechnologies' development has been increased thanks to the possibility to operate in atomic scale and the chance to obtain new devices with better and innovative performance. In particular, in nano-electronics, in which the continuously scaling down and the need for high quality and conformal thin film, required molecular manipulation. Different techniques are able to create film deposition material, but presently it is necessary very high thickness precision, pinhole-free films and elevate purity, so the standard CVD or PVD approach is not able to satisfy all the material specification. Only ALD (Atomic Layer Deposition) can fulfilled all these requirements. This deposition method allows to obtain crystalline material at relatively low temperature (from RT to 300°C), so permitting the employment of temperature-sensitive substrates (i.e. hybrid organic-inorganic systems) and/or minimizing unwanted inter-diffusion film to substrate processes. The advantages of ALD method include low impurity content, independence of line-of-sight, dense, smooth and pinhole-free depositions with high uniformity and conformity, even when thin film are grown on three dimensional complex structures. It is based on two successive surface reactions in a repetitive cyclic self-limiting process. This important aspect leads to excellent coverage because of the reaction take place only on the reactive sites and it ends by itself when all sites react. On the other hand, the majors drawbacks are high deposition time and not all chemical species can be used [George S. M. 2010].

OUTLINE OF THE THESIS

In **Chapter one** a general introduction about ALD technique from its discovery o to date is reported. ALD main application in different field of research, its evolution and diversification are explored. Specifically, atomic layer deposition is described in general, emphasizing a two reactants' metal oxide mechanism, highlighting the growth characteristics and limitations. The precursors properties mostly used are also presented

In **Chapter two** the experimental section is described in detail: several tests are performed to optimize the ALD deposition method to obtain compositionally uniform, conformal, dense, and pinhole-free oxide thin films. The various stages of optimization are described starting from the cleaning procedure of the substrates, moving then to the studies of the TiO_2 growth dependence in relations to titanium precursor pulse time, H_2O purge time, and titanium precursor purge time. In order to assess the influence of the different process parameters on physico-chemical properties, the structure-properties correlation of the grown thin films is widely characterized.

In **Chapter three** the attention is focused on the study of biocompatibility of titania through *in vitro* cellular cultivation experiments. A preliminary study of the deposited neurons behavior on the material and the influence of wettability surface properties on neuronal cell adhesion are studied.

Finally, in **Appendix A** the main characterization techniques, employed to analyze the deposited oxide films, are theoretically described.

LIST OF ABBREVIATIONS

ALD: Atomic Layer Deposition
ALE-LE: Atomic Layer Epitaxy-Luminescent Electro
ALE: Atomic Layer Epitaxy
CVD: Chemical Vapor Deposition
DMEM: Dulbecco's Modified Eagle Medium
DRAM: Dynamic Random Access Memory
EDX: Energy Dispersive X-Ray
EEPROM: Electrically Erasable Programmable Read Only Memory
EOS-capacitor: Electro Oxide Semiconductor capacitor
EOSFET: Electro Oxide Semiconductor Field Effect Transistor
FBS: Fetal Bovine Serum
GPC: Growth Per Cycle
LT-ALD: Low Temperature-Atomic Layer Deposition
MEMS: Micro Electro Mechanical System
ML: Molecular Layering
MLD: Molecular Layer Deposition
MOSFET: Metal Oxide Semiconductor Field Effect Transistor
NB: Neuro Basal
PE-ALD: Plasma Enhanced-Atomic Layer Deposition
PVD: Physical Vapor Deposition
ROM: Read Only Memory
SEM: Secondary Electron Microscopy
SIMS: Secondary Ions Mass Spectroscopy
TDMAT: Tetrakis Di Methyl Amido Titanium
TFEL: Thin Film Electro Luminescent
TTIP: Titanium Tetra Iso Propoxide
WCA: Water Contact Angle
XPS: X-ray Photoelectron Spectroscopy
XRD: X-Ray Diffraction

CHAPTER 1
ATOMIC LAYER DEPOSITION: THEORETICAL ASPECTS

Atomic layer deposition is a thin film growth technique characterized by unique capabilities. In this chapter the basics of ALD processing are described, investigating in particular the ALD concepts based on the use of two reactants for the synthesis of binary thin film materials, such as metal oxides (MxOy). In particular, the attention is focused, in general, on ALD growth mechanism, on advantages and disadvantages of the process, including the growth rate of ALD and the precursors' features. A brief review on the history of ALD, on ALD reactor variants and on its applications potentialities are also presented.

1.1 HISTORY OF ALD

ALD is a thin film deposition technique based on sequential self-limiting surface reaction, and it belongs to the large family of Chemical Vapor Deposition (CVD) processes. Atomic layer deposition was conceived independently by two research groups: it has been designed in Soviet Union by Prof. V. B. Aleskovskii while and Prof. S. I. Koltsov in 1965 defining it as Molecular Layering (ML), and in Finland by Dr. T. Suntola and his co-workers in '70 as Atomic Layer Epitaxy (ALE). More specifically, there is not much information about the development and the expansion of the discovery, especially about the "molecular layering" in Soviet Union. The first public announcement for "atomic later epitaxy" has been promulgated in '80s in San Diego, California, about a disclosure at the Society for Information Display (SID) [Suntola T. et al. 1980]. It has to wait until '90s at the ALE-1 conference [Niinistö L. 1990] for the meeting of two researchers. Dr. Suntola was invited in St. Petersburg to visit University of Leningrad to meet Prof. Aleskovskii, where works, dealing with oxide layer made-up with saturated surface reactions like ALE process, were presented. This meeting confirmed that the principle at the base of the modern atomic layer deposition, it had been separately and independently theorized and realized by the two researchers.
Thanks to the work by Riikka L. Puurunen and the collaboration of Dr. Suntola we have some information regarding the history and the development of ALE in Finland. The invention of the ALE evolved in early June 1974, Dr. Suntola said: "…*We had still an empty laboratory with just tables and chairs and a Periodic Table of the Elements hanging on the wall. Looking at the Periodic Table, and thinking of the overall symmetry in nature, to me came the idea of "serving" the complementary elements of a compound sequentially, one at a time, onto a surface. Monoatomic layers may be obtained if the complementary elements make a stronger bond with each other than they do with their own kind of atoms…*" [Puurunen R. L. 2014]. This idea was matured because of the need to produce a flat panel display (ALE-LE project). Once the equipment has been built, the first experiment was performed in August-September: the grown films showed better mechanical and structure properties than the material grown with conventional techniques, like sputtering or evaporation. On the wave of success, the discovery was protected by a patent, (*Finnish Pat. 52359, 1977; US Pat. 4058430, 1977*) and subsequently the ALE-LE project was sold to a company to increase the resource. After further refinements on ZnS –based TFEL (Thin Film Electro Luminescent) flat panel displays, their production started in Finland in 1983 and their first application was as information boards at the Helsinki-Vantaa airport (Figure 1.1).

Figure 1.1. Flat panel displays at Helsinki Vantaa airport.

Along its history, many different names were used to refer to the ALD technique, particularly to emphasize different properties of this unique technique. The name of ALD, which is most widely used, dates back to the early 1990s [Puurunen R.L. 2005]. In subsequent year the ALE process was spread of in USA and Japan, Dr. Suntola was invited in many conferences to present his invention. In the '90s with the birth of microelectronics and the advancement of new and more performing computer and electronics devices, ALE method has been increasingly success up to the present [Lim J. S. et al. 1999].
Notably, in the recent years, it has become the best and the most used method satisfying the high material performance. It also has been observed enormous growth in ALD application [Ritala M. et al. 2009] and a lot of available ALD equipment on the market. The main engine for the success of this technique has been the electronics industry and the continuous down scaling in microelectronics device. For example, the thin films are frequently used as part of MEMS (Micro Electro-Mechanical System) fabrication as etch stop and hard mask layers [Hoivik N. D. et al. 2003; Mayer T. M. et al. 2003]. In memory circuits for example ROM (Read Only Memory) and EEPROM (Electrically Erasable Programmable Read Only Memory), in which MOSFET (Metal Oxide Semiconductor Field Effect Transistor) are used as transistors: the thin film is a metal oxide that plays the role of insulating layer with a thickness order of 100 nm [Chen Y. -F. et al. 2009]. This powerful film growth is applied in organic solar cells [Delft J. A. et al. 2012], and also in medicine as a Brain Chips Interfaces (BCHIs) that are hybrid entities, where chips and cells establish a close physical interaction allowing the transfer of information in one or both directions [Vassanelli S. 2011].

1.2 THE MECHANISM

Atomic Layer Deposition technique belongs to the family of Chemical Vapor Deposition processes and it is suitable for the manufacturing of inorganic thin films with thickness control down to a fraction of monolayer. It can be defined as "*a film deposition technique that is based on the sequential use of self–terminating gas-solid reactions"* [Puurunen R.L. 2005].
ALD is known for its ability to deposit homogeneous, high quality, and conformal material layers on substrates even characterized by complex-shaped surfaces.

Concerning materials composed of two or more elements, the ALD chemistry is based on the use of one precursor for each element. More specifically, the chemical mechanism active in an ALD process, for a binary system, involves two vapor phase reactive chemical species: a metal precursor and a co-reactant agent. These precursors are separately and alternatively pulsed into the heated reactor containing the substrate surface where the reactions take place.
Atomic layer deposition technique is often defined as a low temperature process (LT-ALD), generally operating at temperature less than 300°C, so that the material deposition is driven by the chemical reactions.
Differently from a CVD process using binary reactions, in which the two reactants (i.e. A and B) are present at the same time and form the product film continuously on the substrate, a general ALD process consists of sequential alternating pulses of chemical precursors in vapor phase into the reaction chamber. They individually react with the substrate surface, and so they never react concurrently. Each ALD cycle consists of self-terminating reaction steps followed by a purge step to clean the reactor from unreacted and by-product species.
More specifically, for a binary system A B, it is possible to divide each cycle in four main steps:

1. in the first step, the first precursor (reactant A) is supplied to the growth chamber (under vacuum and for a definite time): the precursor is chemisorbed on the available active sites of the substrate surface (*self-terminating gas-solid reaction* occurs at surface only) and the surface is saturated with a monolayer of ligands;
2. in the second step, the reactor is purged by using an inert gas (typically nitrogen or argon – in flow-type reactors) or evacuated (in high-vacuum type reactors), to remove the unreacted reactants and the gaseous reaction by-products;
3. during the third step, the second reactant (reactant B) is pulsed into the reactor, where it reacts with the first precursor monolayer chemisorbed on the substrate surface: here again a self-terminating reaction of the second reactant occurs;
4. in the fourth step the reactor is newly purged or evacuated to remove any excess of unreacted precursor and gaseous reaction by-products.

As results, two half reactions lead to the growth of the desire material in each ALD cycle. The ideal reaction mechanism is here reported (equation 1 and 2). It takes as an example Al_2O_3 from Aluminum trimethyl and water:

$$n\text{-}OH + Al(CH_3)_3 \rightarrow \text{-}O\text{-}Al(CH_3)_2 + CH_4 \quad \text{first half reaction} \quad \text{(eq. 1)}$$

$$\text{-}O\text{-}Al(CH_3)_x + H_2O \rightarrow \text{-}O\text{-}Al\text{-}OH + x\ CH_4 \quad \text{second half reaction} \quad \text{(eq. 2)}$$

In the following Figure 1.2, a schematic representation of the conventional 4-step ALD process is reported.
In properly chosen process conditions, the surface reaction is self-limiting, this leading to a highly controlled film growth. In this regard, a finite number of surface sites are available and if the surface reactions become saturated, a constant thin film growth rate is obtained over the whole substrate surface, so films with excellent conformality[1] and good large-area uniformity are obtained. Indeed, it is important that during an ALD cycle, an efficient chamber purge (step 2 and

[1] The term conformality of a deposit means the capacity of a coating to perfectly respect the shape of the substrate and maintain a constant thickness along the entire profile of the substrate.

4) occurs in order to prevent undesired gas-phase reaction and/or possible CVD growth that leads to a non-uniform film.

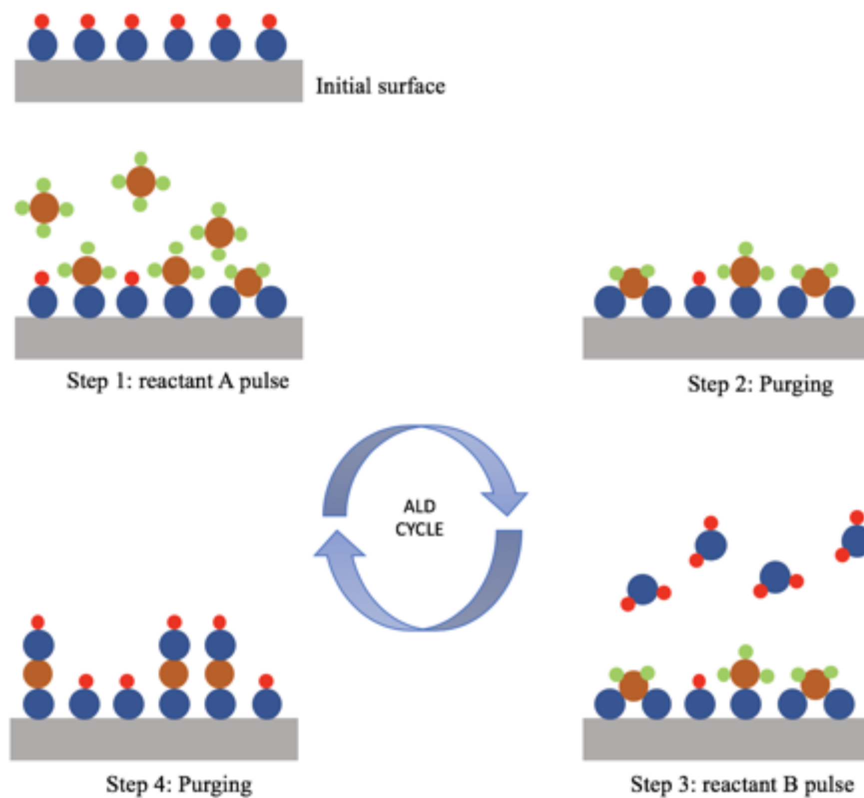

Figure1.2. Schematic representation of a conventional 4-step ALD process.

After the completion of one cycle, the surface is back to its original state and it is ready for the following cycles. This deposition mechanism results in layer-by-layer growth at atomic scale. As consequence, the thickness control is highly accurate and constant for each cycle, so that it can be digitally controlled by simply monitoring the number of ALD growth cycles.
Another important aspect regarding ALD cycle is surface absorption mechanism. The reactions that occur on the surface and the bonds between the reactants and the surface species influence the process. Self-saturation surface reaction is ensured only when a complete chemisorption of the species occurs. Indeed, in these conditions a chemical equilibrium on the surface is established and no more reactants can be adsorbed because all reactive sites are occupied. A possible deviation from the ideal process concerns the physisorption of the reactants. Under these side-conditions, precursors and reactive sites interact with no chemical bonds take place, but only a weak interaction takes place. In spite of this low interactions, good and uniform chemisorption results only when this collateral process is prevented. It is possible, by adjusting the temperature, to obtain a complete chemisorption: this process can be classified in the following three categories (Figure 1.3, Figure 1.4, Figure 1.5; with M=metal, L=ligand) [Puurunen R. L. 2003]:

- *Ligand exchange*: metal precursors ML_n loses a L and binds to the surface, in the same time the L binds a surface group released before and it forms a gaseous species (Figure 1.3a).

Other reactions between a ML_{n-y} species already linked to surface and another surface species are possible. Ligand exchange reactions release products in vapor phase (Figure 1.3b).

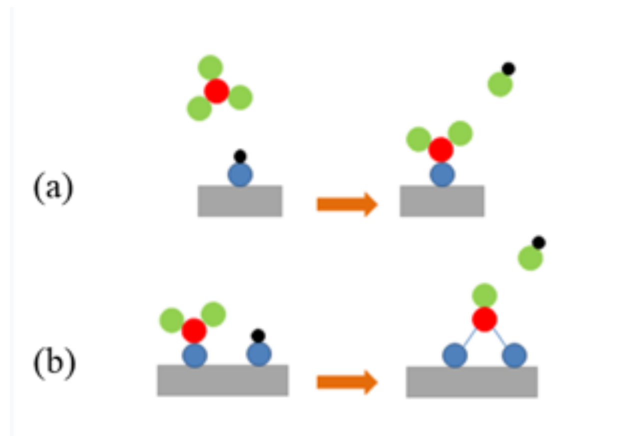

Figure 1.3. Ligand exchange reaction of the ML_n reactant with surface.

- *Dissociation*: ML_n binds a site and L ties a surface species (Figure 1.4a). If the reaction proceeds on the surface the number of M and L bonded does not change (Figure 1.4b). In this case precursor dissociate into several adsorbed species on the surface without releasing vapor phase products.

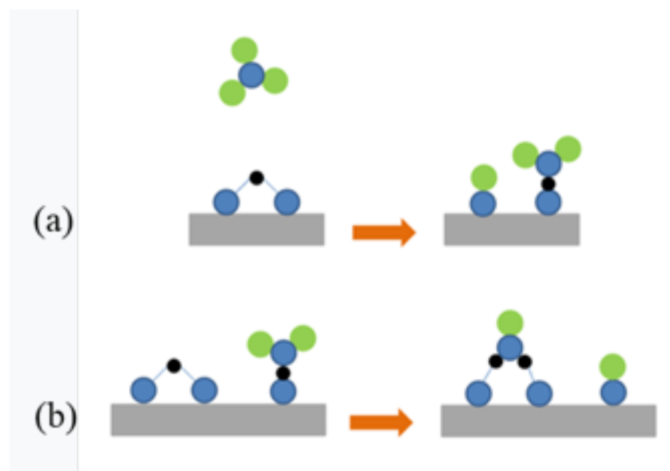

Figure 1.4. Dissociation of ML_n on the surface.

- *Association*: the bond between the precursor and the surface species is of coordinative type (i. e. hydrogen-bonding), with not L losing or between the ligand and the surface (Figure 1.5 a, b). The bond is between a surface species and an intact precursor with no ligand releasing.

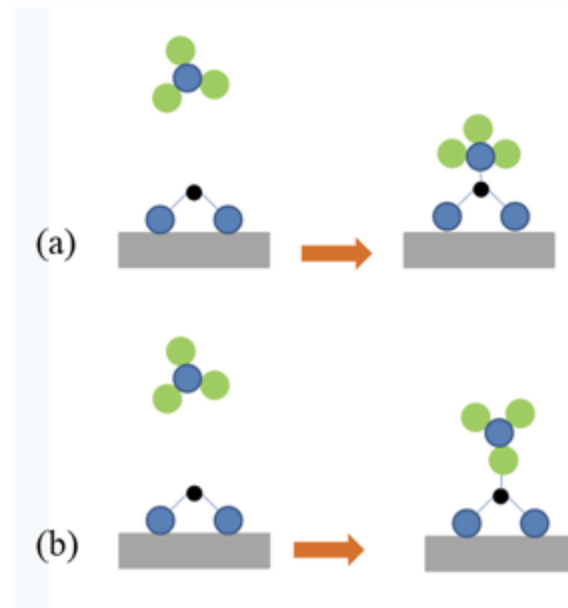

Figure 1.5. Association mechanism of ML_n on the surface.

1.3 Advantages and disadvantages

Atomic Layer Deposition is considered a growth method characterized by the greatest potential for producing very thin and conformal films with the possibility to control the thickness and composition of the growing material at the atomic level [Leskelä M. et al. 2003]

The main advantages of ALD derive from both the characteristic self-limiting reactions and the sequential operating mode and are listed below:

- self-terminating reactions happen at surface only: each precursor must undergo half-reaction at surface;
- the process is driven by chemical reactions: the growth temperature is generally low (under 300°C), so allowing also deposition on temperature-sensitive substrates. Moreover, the low temperature induces low stress, reduced inter-diffusion film to substrate, and permits the adsorbed precursor on surface not to undergo desorption or decomposition;
- the cyclic mechanism permits to accurately control the film thickness (GPC – growth per cycle), by simply changing the number of reaction cycles (digital control of thickness);
- ultrathin film thicknesses are possible, even less than 10 nm;
- high quality thin films are obtained, characterized by excellent reproducibility, 100% film density, and with amorphous or crystalline structure;
- excellent chemical composition control;
- excellent large area uniformity and conformal films are achieved also in complex 3-D structures with high aspect ratio;
- unlike CVD, there is a greater independence from small changes of growth conditions (i.e. temperature and precursor flows, precursor dose, small temperature variations etc.), thanks to the ALD processing window (characterized generally by a constant GPC, see below), that often is wide (allowing the processing of different materials in a continuous process);
- dense, pinhole-free films and interface control;

- elimination of gas-phase reactions, favoring the employment of precursors that are highly reactive towards each other;
- capability to prepare multilayer structures in a continuous process;
- the nature of this techniques makes ALD enable to scalability processes, and the unique limitation is on the reactor size.

Despite the considerable advantages, there are also disadvantages that limit a full application of ALD technique to thin film processing, as follows:

- slowness, in general the growth per cycle, i.e. thickness increment per cycle, is very low because usually only a fraction of a monolayer is deposited in one cycle. High deposition rate is usually due to a not ideal ALD process because of a possible competitive undesired CVD like growing. Deviation from ideality generally depends on various factors such as: precursor exposition/purge times, pressure, temperature and more;
- a wide range of thin film materials may be deposited by ALD, however not every material is possible: doped materials, or many technologically important ones (i.e. Si, Ge, and other metals etc.) are difficult or cannot be deposited. Moreover, ternary or more complicated multicomponent materials are difficult to be deposited, due to the availability of suitable volatile precursors able to react to a defined temperature (the reactor temperature cannot be modified during an ALD growth) [Leskelä M. et al. 2003; Niinistö L. et al. 2004];
- the availability/reactivity of suitable precursor can limit the ALD process development;
- impurities from precursors are typically may be included in the final film, whose content depends on the completeness of ALD reactions (for oxide depositions typically starting from metal halides or alkyl and using water as co-reactant precursor, the impurities are detected in the 0.1-1 atom% range) [Leskelä M. et al. 2003]. In contrast to PVD technique, nevertheless, the material not shows mechanical or electrical defects because they are in the range of 0.1%. Additionally, a more complexity in precursor molecule leads to higher potential by-products (and so contamination) and higher production costs which also need consideration. However, in general there is a real need of more support by synthetic chemistry to get new precursors;
- no thermal precursor decomposition is allowed, in order to avoid competitive undesired CVD-like growing;
- sometimes, due to the low deposition temperature, the grown films are characterized by low crystallinity;
- unlike other thin film deposition technique, ALD must work at low pressure, because at high pressure, it would be a competition between the vapors in the formation of the monolayer, and the times for the completion of each process cycle would be extremely long.

In the table 1.1 are summarized ALD the main advantages and disadvantages.

Table 1.1. ALD advantages and disadvantages.

Advantages	Disadvantages
Precise film thickness control	Slowness
Uniformity- Conformality	Low deposition rate (GPC)
Pinhole free	Low crystallinity
Atomic control	Limited precursor availability
Reproducibility	Impurities in 0.1-1%
Multilayer structure	Limited material selection
Dense film and good adhesion	Low pressure process

1.4 ALD WINDOW

"ALD window" is defined as the temperature region of nearly ideal ALD behavior in which best reaction conditions are employed. More specifically, self-limiting growth occurs, and the deposition has an ideal constant growth rate per cycle. The same term has been used to referring to a temperature range where the GPC is constant. The chemical species involved in the process, should react spontaneously on the substrate surface. Figure 1.6 shows the typical representation of the ALD window. Two non-ideal regions are shown, at lower and higher temperature with respect to the nearly ideal range (central horizontal line shown in Figure 1.6). Indeed, below the ALD window, lower reaction rate and slower mass transport occur. This means that the reactions might not be completed and resulting in a high deposition rate, due to the condensation of precursor molecules on the substrate surface. At higher temperature, a thermal unimolecular gas-phase decomposition of precursor molecules commonly happens, and the thermal decomposition is observed before the deposition on the surface. In this case, it is possible to observe a typically CVD-like growth mechanism, in which the growth rate increases with temperature. On the other hand, at high temperature it is also possible to find a decreasing of deposition rates due to the surface precursor desorption, which becomes the dominant surface process.
Working in the ALD window represents the ideal condition to operate in ALD regime, avoiding both condensation and decomposition problems; the chemistry is substantially independent of external conditions and it allows the deposition of a uniform and conformal coating, in self-limiting mode where precursor saturates the available sites. Finally, as reported by George [George S. M. 2010] it has to be mention that not every ALD process may work in self-limiting conditions due to decomposition phenomena, which may occur at the minimum temperature required for the surface reaction, so inducing additional adsorption. Moreover, other surface reactions never reach completion, so the self-limiting growth is followed also by the incorporation of a large amount of impurities in the deposited films.

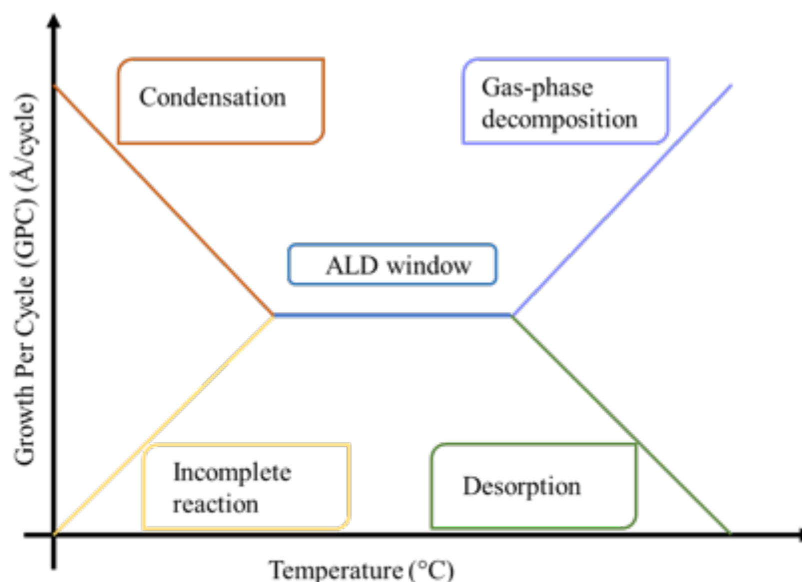

Figure 1.6. Temperature window of ALD process, indicated by the GPC as a function of temperature.

1.5 PRECURSORS

For all vapor phase delivery processes there are two main aspects to consider, such as the capability to convert a chemical source (precursor) in vapor state and the stability of the reactant during the gas-phase transport into the reaction chamber. On this basis, the key proprieties of a precursor are related to its volatility, thermal stability and reactivity. So, by considering the ALD technique, the success of the process relies on the underlying chemistry and on the self-limiting growth mode. Both the thermal stability of the precursors at the ALD processing temperature (to avoid self-decomposition) and an adequate volatility (at room temperature or at higher temperature) are key issues. They must be gaseous or vaporizable at T lower than ALD reaction temperature.
The precursors may be gases, liquids or solids characterized by sufficient volatility (vapor pressure) to be transported into the reaction chamber. Indeed, precursors must react in a fast and irreversible manner with the active sites on the substrate surface to guarantee a self-limiting process and complete reactions [Jones A. C. et al. 2008]. The reaction gaseous by-products should be inert and not interfere with the ALD growing film.
The precursors should be safe, easy to synthesize and to handle, not toxic, environmental friendly, and not corrosive toward both the reaction chamber and the substrate. For some application it is required a high purity; also the price is an important issue (Figure 1.7).
As the characteristics of the ideal precursors are manifold, it is evident that a compromise is needed. A typical precursor may be considered of the type ML_n, where M is a metal and the central atom, and L is the ligand. The metal atom is to be part of the grown material, and the ligand is released (totally or as a fragment) as gaseous side product during the deposition reaction. Moreover, the reaction by-products must be taken into consideration, because they have to be volatile in order to be easily removed from the reaction chamber.

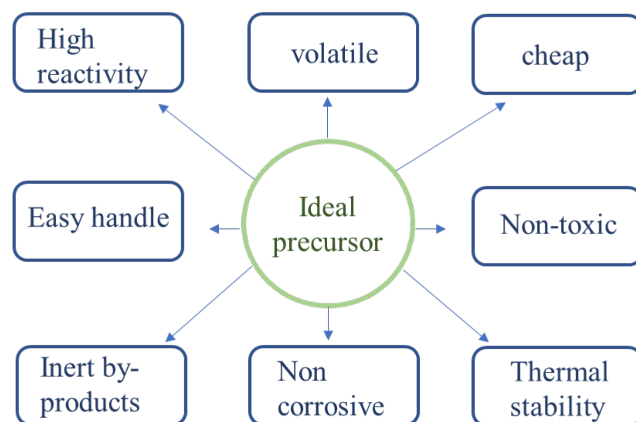

Figure 1.7. Principal characteristics of an ideal ALD precursor.

Typical precursors employed in ALD are organometallic[2]/metalorganic[3] compounds or inorganic [Hatanpää T. et al. 2013]. In particular, here we consider only the main ALD precursor classes, which are classified as follows:

- Halides (HX_n, such as $AlCl_3$, $InCl_3$, $TiCl_4$, $ZrCl_4$, etc.)
- Alkyls (MR_n, such as $[Al(CH_3)_3]$, $[Zn(CH_2CH_3)_2]$, etc.)
- Ciclopentadienyls ($M(Cp)_n$ such as $[Y(CpMe)_3]$, $[ZrCp_2Cl_2]$, $ZrCp_2Me_2$, $[Ru(CpEt)_2]$, etc.)
- Alkoxides ($M(OR)_n$, such as $[Ti(O^iC_3H_7)_4$, $[Ta(OC_2H_5)_5]$, etc.)
- Beta-diketonates ($M(acac)_n$, with -acac=acetylacetonate, $M(thd)_n$, with -thd= 2,2,6,6-tetramethyl-3,5-heptanedionate)
- Alkylamides ($M(NR_2)_n$ or $M(NRR')_n$ such as $[Ti(NMe_2)_4]$, $[Ti(NMeEt)_4]$, $[Ti(NEt_2)_4$, etc.])

Obviously, each reactant category has its merit and defect regarding stability, reactivity, and film contamination. For example, chlorides, which belong to the wide range of halides, (the oldest class of ALD reactants), are often used in ALD process: they have high reactivity, volatility, temperature stability and they are available for many metals. The high reactivity of halides allows the deposition of a large variety of materials, such as oxides, nitrides, sulphides etc. However, there are also some drawback. Indeed, they may ruin the reactor because of their gaseous by-products corrosiveness (such as HF, HCl and HI, which form when halides react with hydrogen-containing non-metal precursors, i.e. H_2O, NH_3, H_2S etc.). Moreover, many halides are solids, so they are sometimes difficult to maintain in vapor state and particles are easily incorporated into the growing film with its consequent undesired contamination.
Alkyls, that contain a direct metal carbon bond, present a strong reactivity, but their stability at deposition temperature is low and they are available only for a few metals. However, these precursors are widely used in this growth process (especially for deposition of Al_2O_3, ZnO, etc.) [Diaz B. et al. 2011].

[2] Organometallic: chemical compound containing at least one direct metal-carbon bond.
[3] Metalorganic: chemical compound with no direct bond with metal atom and carbon.

The non-metal co-reactants most used are water, molecular oxygen, ozone, hydrogen peroxide, alcohols, ammonia, hydrogen sulphides. Their choice depends on the nature of the material to be deposited (such as oxides, nitrides, sulphides etc.). The non-metal co-reactants' benefit is their high stability and reactivity, also at high temperature.
Metal oxides of the group 4 are the most studied material in ALD because their chlorides represent an important class of ALD precursors. They are stable, cheap, volatile at low temperature and show high reactivity. However, it cannot forget the high corrosivity of by-products such as HCl, as previously mentioned or that $ZrCl_4$ [Ritala M. et al. 1994] and $HfCl_4$ are solids, thus more difficult to use. They are industrially employed to deposit high-k oxides for transistors, photocatalysis, electroluminescent display and for protective coating.
Metal alkoxides represent another class of precursors widely used in CVD to produce oxide thin films but they are less employed because their lower thermal stability. Only Ti-alkoxides are successfully used with water to deposit TiO_2. Zr and Hf alkoxides are little used because their chlorides are most stable and cheaper. A trend is observable about the oligomerization that increases from Ti to Hf. It is known, for titanium alkoxide precursors, that the overall thermal stability (in term of decomposition onset temperature) under dynamic conditions in ALD process decreases with the increasing steric hindrance of the substituents, according to the order $Ti(O^tBu)_4 \leq Ti(O^iPr)_4 < Ti(OEt)_4 < Ti(OMe)_4$ [Pore V. et al. 2004].
Synthetic chemistry provides to stabilize Zr and Hf alkoxides by using donor ligands, that are bonded with amine or ether groups. These species are used in heteroleptic and homoleptic complexes, but the high stability achieved makes them not sufficiently reactive.
Alkylamides represent another important group of metal precursors, since they have the ability to increase the reactivity of the species. For example Zr- ethylmethylamide is used for Zr oxide deposition, it shows easy synthesis and high reactivity with water [Chen T. et al. 2008]. In contrast with alkoxides, the thermal stability of alkylamides is inverse: Hf and Zr are most stable than Ti.
The crucial point of ALD development has been and will be the availability of different opportunely tailored precursors species, because even small changes in molecular design may have a great impact on the final material properties and performance. In fact it is very important consider the properties of the species utilized to fulfill the desired needs of film deposition in relation to their applications.

1.6 ALD VARIANTS

As mentioned above, the ALD technique may be considered a particular variant of the CVD process. However, also ALD has its variants, all characterized by a chemical vapor deposition based concept, with a cyclic scheme of precursor introduction and a self-limiting mechanism.
ALE (Atomic Layer Epitaxy) is the first example of ALD, invented by Dr. Suntola in '70s in Finland, and the first application was for the deposition of ZnS thin film for electro luminescent displays [Suntola T. 1992]. Later, its use has expanded for the epitaxial growth of III-V semiconductors, besides II-VI ones, especially to layered structures (such as superlattices and superalloys).
As reported by Suntola [Suntola T. 1989] "*… atomic layer epitaxy is a method for producing thin films and layers of single crystal one atomic layer at a time utilizing a self-control obtained through saturating surface reactions. In conventional terminology, the term "epitaxy" has been used to describe the growth of single-crystal layers…*".

This technique possesses all ALD advantages: good homogeneity and thickness uniformity, conformality and a self-saturation reaction mechanism. The feature that distinguishes this technique from the common ALD is the particular structure of the thin growing material that has the same crystal lattice structure of the substrate.
The **PE-ALD** (Plasma Enhanced Atomic Layer Deposition) is another variant of ALD technique, more specifically it is the most widely used as alternative process to the thermal ALD. PE-ALD is characterized by the presence of a plasma source, which creates ions and radicals and activates the chemical reaction for the film growth; specifically, it improves the reactivity of the precursors. The use of the plasma gives some advantages such as, a lower deposition temperature, which allows both the use of some precursors, that normally are not usable because of their huge thermal activation request (so expanding the ALD thin film materials' selection) and the use of temperature-sensitive substrates. As mentioned before, plasma generates ions and radicals. Ions can produce a physical change in the final material and radicals can act like promoter for the growth. Nevertheless, species generated by plasma may undergo recombination and reagent leakage occurs. In thermal ALD this does not happen if it works inside the temperate range of ALD window. Moreover, when PE-ALD is used to cover HAR (High Aspect Ratio) structure, species recombination increase and inhomogeneous and not conformal film are deposited [George S. M. 2010]. In addition, it might also result in a reduced conformality and in a potential plasma damage to the substrate/growing film.
Photochemical assisted ALD is a different variant of the process, in which the supplementary activation energy is provided by light. At the same way, it can be used to remove layer-by-layer of material: ALD etching [Faraz T. et al. 2015]. The photochemical process consists of two mechanisms: photo-excitation and photo-dissociation. The first one consists in an absorption of a photon, so the chemical species gain energy and a chemical reaction may be promoted. Photo-dissociation, instead, is the process of absorbing light photon and the successive dissociation or breaking of a chemical bond in a molecule, so the formation of new reactive chemical species. Utility of photo-assisted-ALD is the high growth rates obtainable at the same substrate temperature, so it can operate at low temperature with higher GPCs. Other advantages are observed for example in ZnO thin films grown with UV-radiation: the material shows a very low resistivity and it is possible to operate at only 136°C [Yamamoto Y. et al. 2001].
The **MLD** (Molecular Layer Deposition) is the most recent ALD variants and it is based on the substitution of the non-metallic precursor (i.e. H_2O, H_2S, NH_3, H_2 etc.) with an organic compound to obtain a hybrid organic-inorganic material. In the event that both precursors are organic molecules, a pure organic material is obtained [George S. M. et al. 2011].
A typical example of hybrid organic-inorganic materials made by MLD are the Zincone (hybrid organic-inorganic polymer thin film of the form $(\text{-O-Zn-O-}C_2H_4\text{-})_n$, see Figure 1.8) [Peng Q. et al. 2009] and Alucone (hybrid organic-inorganic polymer thin film based on the reaction of trimethylaluminum and various alcohols) [George S. M. et al. 2009]. The main interest in this innovative material is the tunable range of physical and chemical properties available by varying the fractions of organic or inorganic precursor. It is possible to have different density and resulting different mechanical properties (such as stiffness). Moreover, electrical and optical proprieties including refractive index and dielectric constant should be modified by changing the composition.

An example of a completely organic compound made by MLD is Nylon 6,6. The growth film by adipoyl chloride and 1,6-hexanediamine is performed at 66°C [Du Y. et al. 2007].

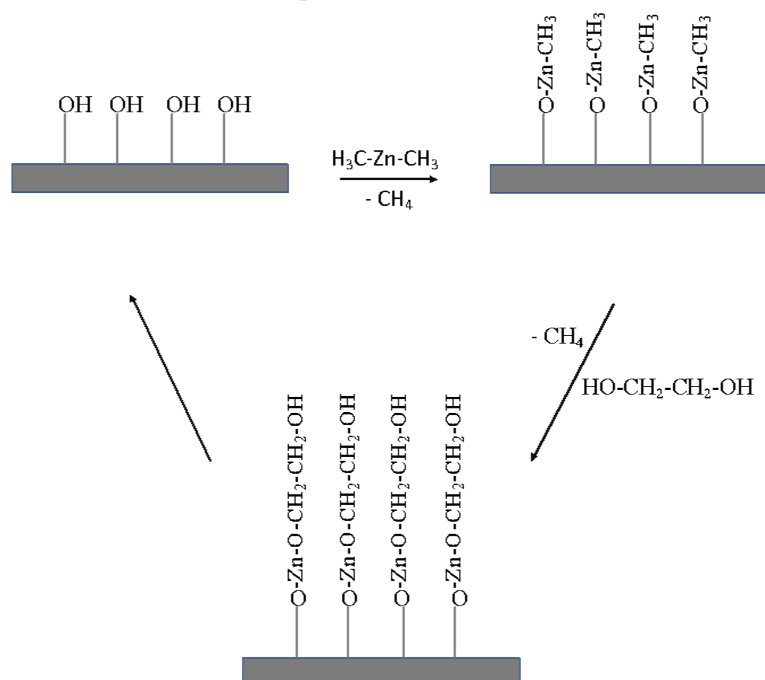

Figure 1.8: Schematic representation of the cyclic ALD reactions for Zincone synthesis starting from zinc(II) dimethyl and ethylene glycol.

1.7 Industrial applications

In last few years, atomic layer deposition has been explored a significant increase. Surely, the Microelectronic area was the most interested one, but also in protective coatings or magnetic heads this technique has taken hold. However, it cannot be said that this technique is widespread in the industry because of its major limitations: slow process and the patent (*Finnish Pat. 52359, 1977; US Pat. 4058430, 1977*) that preserved this technique for several years, makes hard to exploit it without possible legal trouble.

For sake of completeness, it is reported a short overview on the main industrial applications, based on articles, publications and conferences.

Microelectronics developed in the late 90s represented the major improvement for ALD technology. The continuous miniaturization in devices and the high precision required, lead to introduce new material and new deposition method. Only ALD has an atomic thickness control, a perfect and uniform coverage and a high conformality. MOFSET and DRAM have been the main role in ALD development and the first application was made public by Samsung in 1998 in DRAM production [Siltron L. G. et al. 2000]. Intel was the first to produce MOSFETs by ALD. They used it to deposit a high-k dielectric metal, hafnium oxide [Bohr M. T. et al 2007].

Magnetic heads are employed into hard disk to read and write information. The down scaling of it and the three dimensional structures made the sputtering inadequate and ALD was favored. Magnetic heads were covered by Al_2O_3 thin films, starting from $Al(CH_3)_3$ and H_2O [Kautzky M. et al. 2008].

TFEL (Thin Film Electro Luminescent) displays were in ‘70s the main reason for the birth and the development of ALD, by Dr. Suntola. The major advantages given by new approach is the formation of pinhole free films and a perfect and uniform coverage, which before was very difficult to obtain. In ‘80s TEFL displays manufacturing developed and its commercial use started. ZnS:Mn thin films were deposited as the luminescent layer, Al_2O_3 as the insulator and protective layer [Tiku S. K. et al. 1984]. The film thickness obtained was about 200 nm.
Protective coatings can preserve the material from ambient damage such as oxidation. As an example, protective films are used in jewelry to prevent silver tarnishing [Sneck S. 2007].
Optics needs high uniformity and precision thickness control so ALD would have been a good candidate in this field, but there no much application examples. Recently, multilayer stacks for infrared cut-filters are commercialized. In nano-optics ALD is used to fill nanogratings structure [Wang J. J. et al. 2005] and for Fresnel zone plates in X-ray microscopy [Vila-Comamala J. et al. 2009].
Solid oxide fuel cells represent the differentiation of usual fuel cells. These devices directly convert chemical energy into electrical energy. SOFCs consist of three characteristics layers anode, cathode and a conductive electrolyte. In general, these cells work at high temperature range 800-1000°C, because at lower temperature the conductivity goes down and the kinetic reaction becomes too much slower. To work at temperature range 300-600°C and to obtain good performance, the electrolyte film thickness must be reduced, so only ALD can do it [Beckel D. et al. 2007].

Finally, it must be stressed some other ALD applications in different fields. For instance, the synthesis of multilayer nanolaminates (Figure 1.9) with specific super-hardness until about 60-70 GPa are obtained only at low temperature and with a nanometric thickness control. only possible thanks to the ALD characteristics [Kim Y. S. et al. 2005].

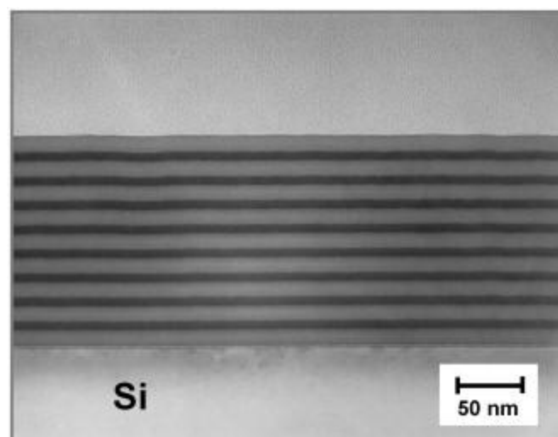

Figure 1.9. SEM cross section of alternately Al_2O_3-TiO_2 nanolaminates deposited by ALD process.

Coatings on biomaterial and polymer can be obtained only at low temperature, so for many years with common chemical and physical deposition method it was not possible to do this, because at the working temperature these materials would melt. Nowadays, thanks to ALD it is possible to cover material at range temperature of 100-150°C, so it has made potential polymer surfaces modification and achieve new interesting proprieties. For example, polymers coated with aluminum

oxide become more resistant to erosion. In biological field, thin film coverage renders the starting material biostable and adhesive proprieties are improved.
Another possible application is related to biomolecules' coating. For example, it has tried to cover, with metal oxide, tobacco mosaic virus and ferritin protein. Those molecules are highly temperature sensitive and it is required 60-70°C deposition temperature [Knez M. et al. 2006].
Photonic crystal, template by polymer nanostructures, is a low temperature ALD process and in contrast to CVD, highly conformal film grown and thickness control are obtainable. his approach for photon crystal production has been applied to a large variety of materials: Ta_3N_5, ZnO, GaAs, Al_2O_3, TiO_2 to obtain multilayer inverse opal structures with a periodicity ranging from 250 to 500 nm (Figure 1.10).

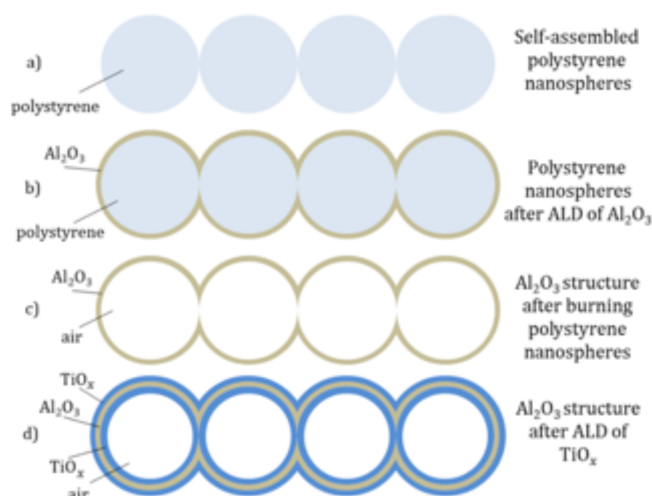

Figure 1.10. Schematic representation of the fabrication process of the Al_2O_3/TiO_2 inverse opal [Coll A. et al. 2018].

1.8 Titanium dioxide

Titanium dioxide (TiO_2, also called titania) is an indirect band-gap semiconductor material. It is easy to manufacture and at low cost in large amount. It is available in nature as mineral in amorphous phase and in three main allotropic crystalline structures: rutile, anatase and brookite. The three polymorphs' structures are characterized by three different distortions and assemblies of the base unit with a TiO_6 octahedral symmetry (Figure 1.10). It is possible to describe the structures in term of octahedron formed by O^{2-} ions around the Ti^{4+} ion (each titanium ion is at the center of the octahedra and the oxygen ions are at each of the six vertices). Brookite has and orthorhombic structure, whereas anatase and rutile have a tetragonal structure (more elongated in anatase phase) [Chen X. et al. 2007]. The different spatial arrangements lead to different distances between Ti-O and Ti-Ti, so it causes diverse mass densities and electronic band structure.
Rutile phase is the thermodynamically more stable crystalline form, whereas brookite and anatase are metastable. The conversion from the metastable forms to the stable rutile one is possible through thermal treatments at high temperature (600-800°C) [Asthana A. et al. 2010].
In the early twentieth century, titanium dioxide has been vastly used and technological applications have been proposed for the synthesis of titania in bulk and thin film forms [Asthana A. et al. 2010]. One of its main use is as white pigment [Pfaff G. et al. 1999; Braun J. H. et al. 1992] for varnishes, plastics and papers. It is non-toxic and it is used in textiles, drugs and foods (here as

additive E-171, [Rompelberg C. et al. 2016]), and being an UV absorber, it is employed in formulation for cosmetic and solar creams.
In thin film form, TiO_2 has been widely studied and it has a number of applications in optics and electronics (strictly dependent also on its crystalline structure), thanks to its good properties, such as chemical and physical stability, high refractive index, good transmission in Vis and NIR regions etc. In the '70s, the photocatalytic effects of TiO_2 were discovered and after this new application field, a large variety of researching of titanium dioxide material has been committed. This pulse opened vast research areas in new interesting field of application, such as electronics and photovoltaics; in recent years biomedicine, nanoscience and nanotechnology had also an explosive growth.

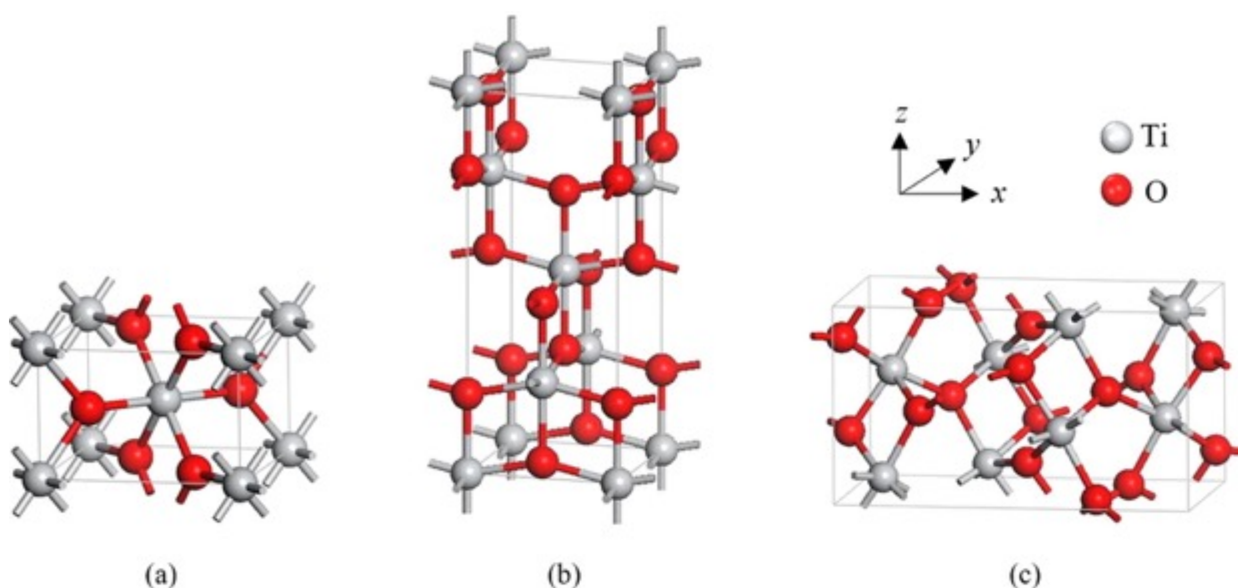

Figure 1.11. Three polymorph structures of Titanium dioxide, in particular the primitive unit cell of (a) rutile (100), (b) anatase (101), (c) brookite (210).

1.8.1 TiO_2 AS BIOMATERIAL

Thanks to emerging technologies and the continuous development of new materials, we assist to the use of synthetic new biomaterials, which interface with biological systems. They may be organic and/or inorganic and, generally, they are used in closed or direct contact with the body [Bauer S. et al. 2013]. They reside in the body for a significant amount of time with the task to interact in a controlled way with the host biological tissue and fluids. Nevertheless, this is a huge challenge because the body has to interact with the foreign biomedical devices and not to consider it as a negative invader (*i.e.* without rejection) [Roach P. et al. 2010]. In this regard, the correct choice of the biomaterial to build a biomedical device plays a key role; indeed, it must be specifically designed in relation to the functions that it must perform into the body (examples of biomedical devices are shown in Figure 1.11).

Figure 1.11. Examples of biomedical devices made of TiO_2. On the left a dental implant, on the right knee and hip joint protheses.

The primary characteristics, that a synthetic biomaterial must have, are biocompatibility, degradation characteristic, mechanical, chemical, non-toxicity and biological properties[4].
Among these, biocompatibility is a key property fundamental for all biomaterials. The biocompatibility definition has undergone several changes over the years. In general sense is defined as "*…the ability of a material, device, or system to perform without a clinically host response in a specific application*" [Samavedi S. et al. 2014]. However, a more complete definition has to consider the "biological performance" in term of host response and material response. So the biocompatibility may be defined again as "*…the ability of a material, device, or system to perform appropriately in an intended application and elicit a host response suitable to that application…*".
As result of the extension of life expectancy and the ageing of the general populations, many chronic and progressive physical and mental diseases are ever growing (such as cancers, diabetes mellitus, cardiovascular disease, orthopedic and neurological disorders) and consequently biomaterials with ever better performance are required [Wu S et al. 2014 and ref. therein].
In this thesis the attention is focused on TiO_2, in thin film form, as biocompatible nanostructured material and it is very attractive for its huge application in many biomedical fields, such as bone scaffolds, vascular stents, drug delivery systems and biosensors.
Specifically, crystalline TiO_2 thin films have been taken into consideration for the titania high-k dielectric properties. Indeed, in this field, crystalline titania may find interesting application for biomedical neuro-chips based on both electrolyte-oxide semiconductor field-effect transistors (EOSFET) sensors (for recording) and EOS capacitors for stimulation of neuronal tissue (i.e. technology based on the interfacing of neuronal tissue and microelectronic circuits with a bidirectional communication). Here, the dielectric material plays a key role for an efficient neuron-semiconductor coupling, thanks to its high permittivity to enhance the signal transfer from cell to chip and vice-versa [Cianci E. et al. 2012]. TiO_2 permittivity changes from k = 30 to 170, depending on both its crystal structure and deposition methods (rutile k-value = 90-170 depending on lattice orientation and anatase k-value = 30-40 [Cianci E. et al. 2012 and ref therein].

[4] Biostable material: resists to physico-chemical transformation. Biodegradable material: undergoes physico-chemical transformation. Biotoxic material: causes adverse reactions of the organism. Bioinert material: does not react with biological environment.

1.8.2 TiO_2 deposition using ALD

Titania is a material that can be prepared in the form of powder, bulk or thin film. In the field of research, the number of titanium synthesis methods are very numerous, each of which leads to the production of materials having different characteristics of structure, crystallinity, composition, contaminants, etc. Nanostructured materials with various morphologies have been synthesized by many different techniques, such as solvothermal and hydrothermal processes, sol-gel, anode oxidation, chemical vapor deposition (CVD), physical vapor depositions (PVD), spray pyrolysis and so on [Wu S et al. 2014 and ref. therein].

As already widely dealt with, ALD is the most promising technique for biomedical device application and it is now widely spread out. It finds high application thanks to its compatibility with the nano-scaling of biomedical components, with the biocompatibility of the materials that are deposited and with the tuning of the chemical reactivity in relation to the material to be deposited [Graniel et al. 2018].

In literature, a lot of references are related to TiO_2 growth via ALD by using different precursors. The main titanium precursors used are halides, alkoxides, and alkylamides.

Among halides, $TiCl_4$ is the most employed to deposit titanium dioxide thin films, due to its availability and low cost. A lot of works about its use have been reported generally with H_2O as oxygen source. One of the first works is reported a by Atomic Layer Epitaxy: $TiCl_4$ and water were used at two different temperature (175°C and 450°C) and the structure and the material properties were investigated [Haukka S. et al. 1993].

Another example of TiO_2 deposition starting from a halide precursor uses TiI_4 whit H_2O as oxygen source. It has been observed a self-limiting growth at 175-375°C temperature range, the crystalline structure was anatase, whereas rutile phase was observed at higher temperature (445°C). The TiO_2 GPC resulted to increase with substrate temperature, from 0.07 to 0.18 nm [Aarik J. et al. 2002].

Alkoxide precursors have been largely investigated owing to the need to have a substituent for $TiCl_4$, because its by-products high corrosiveness and the possible chlorine contamination of the films. $Ti(O^iPr)_4$ (TTIP)is the most used, because its high reactivity at low temperature and low cost. It is generally used with water or H_2O_2 to obtain the relative oxide. In general, the obtained GPC value of TTIP-H_2O system was constant at 0,30 Å/cycle in the temperature range 250-325°C [Rathu A. et al. 2002]. Moreover, a self-limited behavior was observed in the 100-250°C temperature range and the independence of the growth per cycle on the use of water or H_2O_2 [Aarik J. et al. 2002].

Alkylamide use, as titanium precursor, has been driven by the nature of the low energy Ti-N bond, consequently by its high reactivity. It allows to operate at low temperature and furthermore by-products are not corrosive. TDMAT (Tetrakis dimethylamido titanium) for example, was explored for TiO_2 deposition using H_2O, varying temperature from 90°C to 210°C. The ALD window was between 120-150°C, but the GPC linearly decreased outside this temperature range. Therefore, it was supposed, at deposition temperatures below 120°C, that this GCP decrease was due to a not sufficient water purging time. However, high purity and amorphous films were obtained [Lim G. T. et al. 2006].

CHAPTER 2
EXPERIMENTAL: OPTIMIZATION TiO_2 THIN FILM DEPOSITION VIA ALD AND CHARACTERIZATION

The activity here reported is focused on the realization of TiO_2 thin films on Si (100) wafer via Atomic Layer Deposition, starting from Titanium (IV) isopropoxide and water. The purpose of the activity is to define the deposition experimental conditions, that allow to work in ALD regime, by using a custom-made ALD reactor, which is briefly described. The final material has to be crystalline, pinhole free, with high uniformity and conformality.

The optimization process was divided into the following phases:

- substrate preparation (RCA cleaning procedure);
- study of the dependence of TiO_2 growth in relation to the pulse time of titanium precursor (TTIP);
- study of the dependence of TiO_2 growth in relation to the purge time after TTIP pulse;
- study of the dependence of TiO_2 growth in relation to the purge time after co-reactant (H_2O) pulse;

Different physico-chemical characterization methods were performed on the grown films:

- X-Ray Diffraction (XRD) to check the thin film crystallinity;
- Scanning Electron Microscopy (SEM) for the analysis of surface morphology and thin film thickness from cross-section measurements;
- Secondary Ion Mass Spectrometry (SIMS), to investigate depth profiles, compositional homogeneity and thickness of as-deposited thin films;
- X-Ray Photoelectron Spectroscopy (XPS), to analyze the chemical state and the chemical composition of the materials;
- Spectroscopic Ellipsometry to check the film thickness;
- preliminary TTIP decomposition tests via ALD.

2.1 ALD EQUIPMENT

In this work, to deposit thin films by atomic layer deposition a custom-made “cross flow” reactor was used. “Cross flow” means that in the reactor chamber there is a laminar flux of gas, that transport reactants species [Granneman E. et al. 2007].

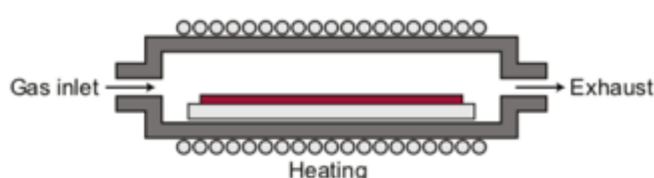

Figure 2.1. Schematic of the cross flow ALD reactor [Knoops H. C. M. et al. 2015].

The apparatus, reported in Figure 2.2, is formed by three main sections:

- a *precursor delivery system* consisting in a reactant supply system and a gas handling system;
- a deposition chamber;
- an exhaust and vacuum system.

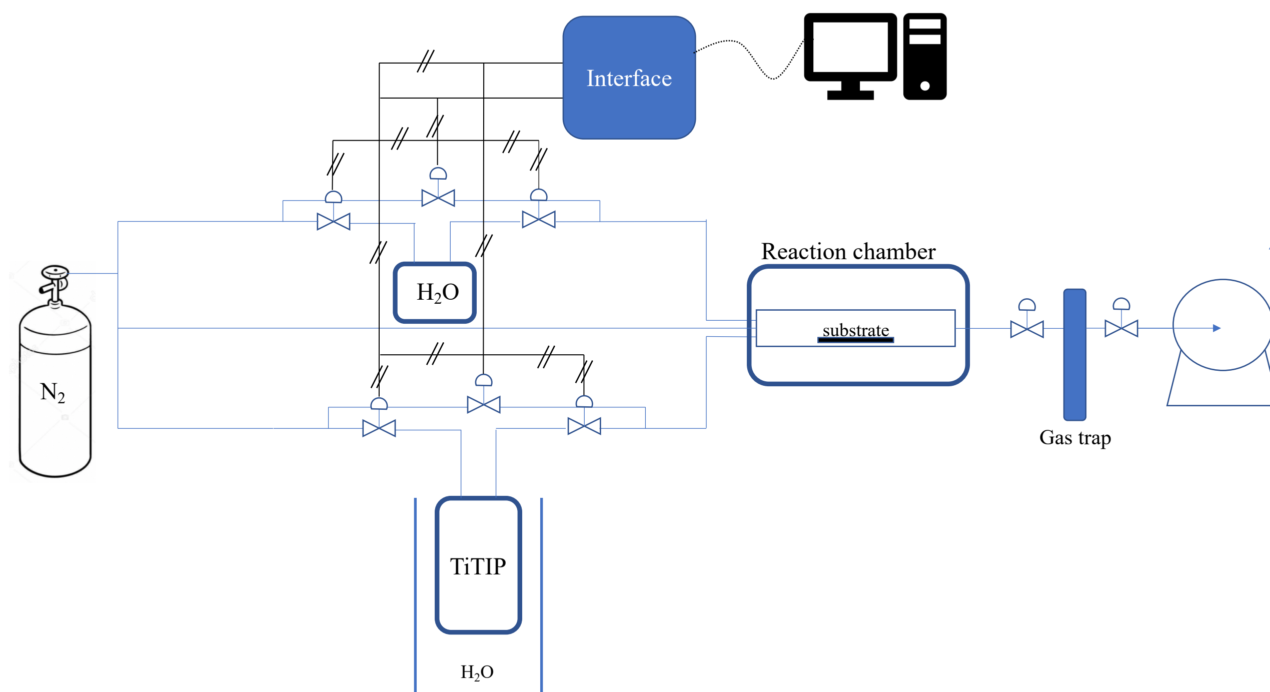

Figure 2.2. Schematic representation of ALD apparatus present at ICMATE-CNR in Padova.

2.1.1 Precursors delivery system

This first part of the ALD apparatus is characterized by pipelines with inert transport gas that pass through one or more bubblers to carry precursor vapors into reaction chamber. Inert carrier gases, such as N_2 or Ar, are generally used in order to ensure no reaction in the lines.
The system of precursor supply has the aim to generate precursor vapors and it consists in a series of temperature-controlled containers, called bubblers, which hold the precursors during the ALD deposition. The bubbler may be made of stainless steel or pyrex glass and their choice is made in relation to the nature of the precursor used (solid, liquid or gas). All the inlet gas pipelines (precursor line, co-reactant line, and dilution line are made of AISI 316) are equipped with mass flow meters (upstream the bubblers) controlled by mass flow controllers, to guarantee a precise gas flow rate of the precursor transport into the reaction chamber.
The used valves are pneumatic (Swagelock 6LVV-DPS4-C, Figure 2.3) and they allow repeated opening and closing cycles with fast response times.
In an ALD reactor, the possibility to set the time of gas injection into the reaction chamber is of particular importance. The pneumatic valves are controlled by pneumatic electro-valves mounted near and upstream them, in order to minimize the response times. A control unit manages the electrical control both manually and via personal computer. The control via PC allows the opening and closing of the pneumatic valve to regulate alternately both purge and precursor pulse times.

Figure 2.3. Swagelock 6LVV-DPS4-C pneumatic valve.

The Visual Basic software for the automatic management of the ALD process was entirely developed at ICMATE-CNR: it allows to manage one channel at a time, in a defined sequence and for a defined time of each channel. Figure 2.4 shows the interface of the Visual Basic software. The number of cycles is also preset and controlled via computer.

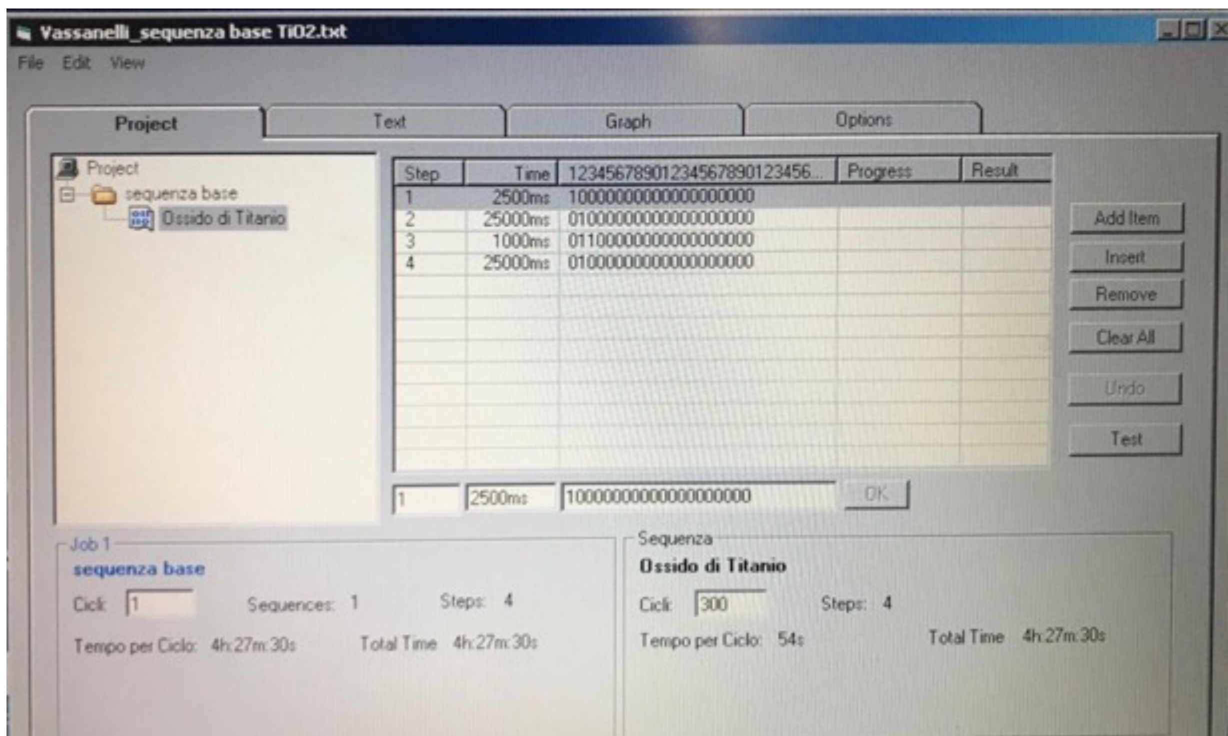

Figure 2.4 Visual basic software interface.

2.1.2 THE REACTION CHAMBER

The reaction chamber is constituted by a horizontal, hot-wall pyrex-glass tube and it is placed inside a tubular oven to ensure a constant and defined temperature (Figure 2.5). Into the glass tube is located a sample holder, where the substrates are positioned and everything is kept under vacuum. The glass tube is long 600 mm (300 mm reaction zone) and has a diameter of 50 mm. The deposition temperature is controlled in real time during the deposition by a K-type thermocouple, positioned inside the reactor in close proximity of the reaction zone.

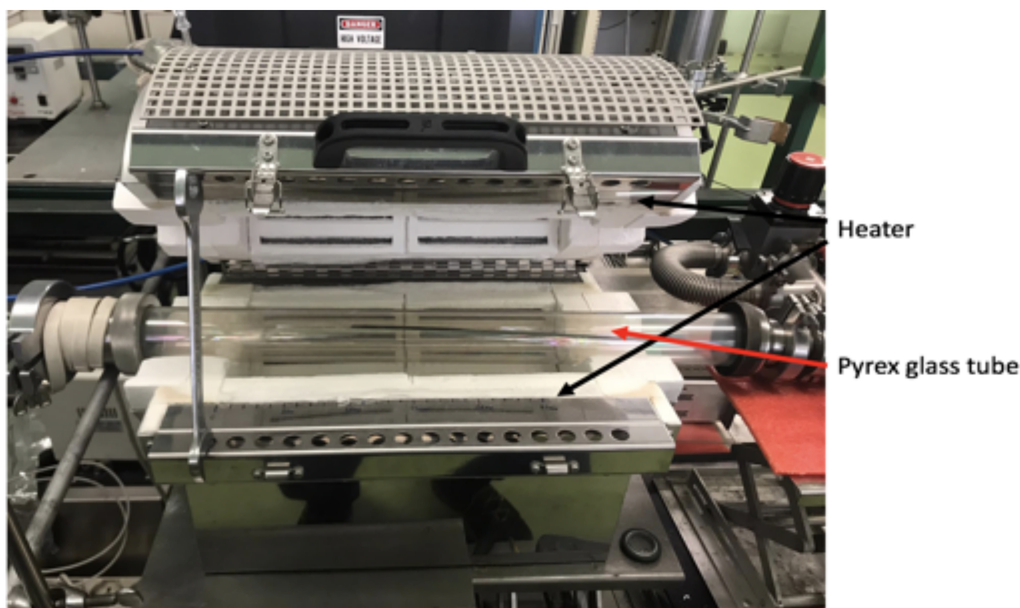

Figure 2.5. Reaction chamber of ALD apparatus used for the deposition.

2.1.3 Exhaust and vacuum system

The exhaust gas line and the vacuum system are positioned downstream the reactor.
The vapor trap is a stainless-steel cylinder, refrigerated by liquid nitrogen, to entrap and scrub the gas (Figure 2.6). The trap has the aim to protect the vacuum pump from possible particles (formed in the reaction chamber) or from residues of unreacted precursor and reaction by-products.
After the trap, and at the end of the whole deposition apparatus, there is a dry scroll pump (BOC-Edwards XDS 35*i,* peak pumping speed = 35m^3/h) that allows to make the vacuum necessary for the deposition. A MKS Baratron is close to the vacuum pump to measure the process pressure.

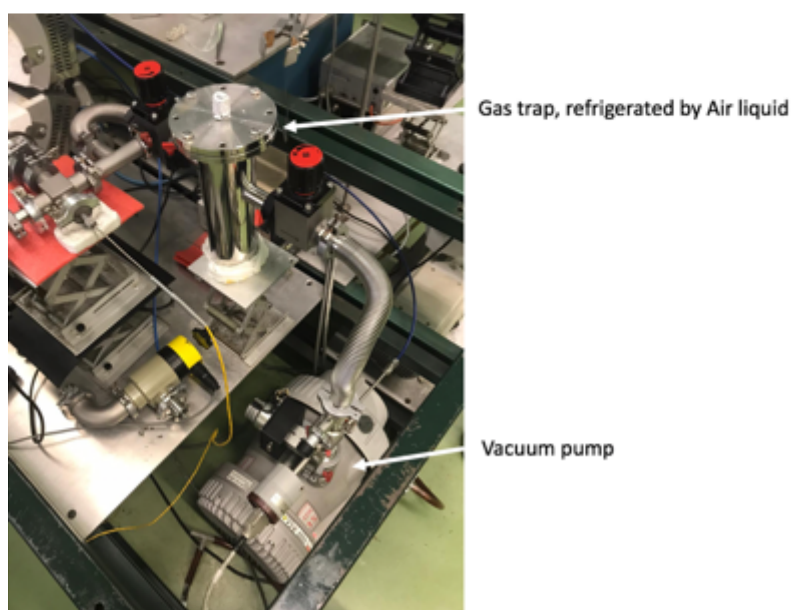

Figure 2.6. Gas trap and vacuum pump of the ALD deposition apparatus present at CNR-ICMATE, Padova.

2.1.4 THE ALD PRECURSOR USED

In this thesis deposition of TiO_2 thin films via ALD was carried out by using an alkoxide, in particular titanium(IV) tetraisopropoxide (by Sigma Aldrich) with the formula $[Ti(OC_3H_7)_4]$ (TTIP) as titanium source and its physical properties are reported in Table 2.1. The TTIP structure is shown in Figure 2.7.

Low price, high vapor pressure, high reactivity with H_2O, and the lack of corrosive by-products are the main reasons of the choice. Being moisture sensitive, TTIP can be stored almost indefinitely in a dry atmosphere (decomposition, when started, propagates throughout the entire precursor), so its handling has generally to be done in a Dry-Box (under nitrogen atmosphere).

The co-reactant precursor was water (for the reasons previously reported in Chapter 1). Notably, the oxidant power of water is enough to ensure a complete surface reaction, and namely it is able to restore active sites for the next grown cycle. However, other strong co-reactants, such as H_2O_2 or ozone, are available to synthetizes titania thin films. In this work, in relation also to the experience of the ICMATE-CNR laboratory, the ALD deposition were carried out by using deionized water (Deionized water at 18,3 MΩ).

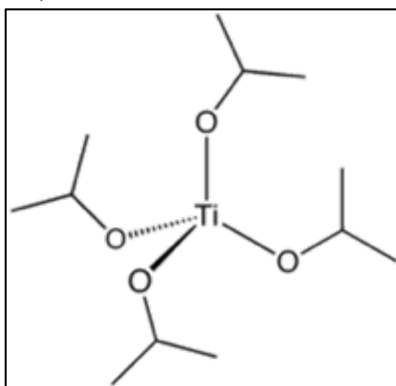

Figure 2.7. Schematic representation of chemical structure of TTIP

Table2.1. Physical properties of TTIP

Physical Properties	
Molecular weight	284,25 g/mol
Melting point	18 to 20 °C
Boiling point	232 °C
Freezing point	15 -19 °C
Vapor pressure at 100 °C	19 mm Hg
Vapor pressure at 50 °C	0.9 mm Hg
Density	0,962 g/cm $^{-3}$ at 20°C
Flash point	19 °C
Refractive Index	1.46
Appearance	Clear liquid

2.2 DEPOSITION METHOD

ALD is a high versatile technique, because it is possible to modulate different parameters, (once the desired material is fixed and the reagents are chosen), such as deposition temperature, purge time, pulse time, pressure, carrier gas flow etc. However, the optimization of the operation conditions in an ALD process, and especially in a custom-made reactor, is the most critical point, as it can influence the quality of the final material.

The definition of the experiments was dictated by the need to deposit crystalline, pinhole-free, dense and conformal TiO_2 thin films on Si(100) substrates.

Many experiments were carried out to find the best operating conditions, specifically addressed to the optimization of TTIP pulse time and purge times after both H_2O and TTIP exposures. Thanks to the previous consolidated experience at ICMATE-CNR some parameters were kept fixed as listed in the Table 2.2 [El Habra N. et al. 2015; Visentin F. et al. 2015].

Table 2.2. Apparatus parameter used during deposition

Fixed ALD parameters	
Deposition pressure	1,5 mbar
Deposition temperature	280° C
Ti source	TTIP- purity 99,999
Dilution N_2 flow	50 sccm
N_2 carrier flow through TTIP	110 sccm
N_2 carrier flow through TTIP	100 sccm
Substrate position	8cm
Cycles' number	300

2.2.1 TEMPERATURE TEST

Deposition method has been optimized trough the study of purge times and pulse TTIP precursor time. Firstly, the best substrate position into the reaction chamber has been investigated, in order to have a stable temperature during deposition. The working temperature, that has been chosen, was 280°C: at this temperature the material is crystalline (necessary property to have a high-k constant). In this thesis it has been taken into account the possible biomedical application as EOSFET and EOS capacitors, so to ensure the integrity of the device and for the correct functionality of it, we have to operate under 300°C, even if higher temperatures (until 300-350°C) could be used to obtain the same material characteristics.

Temperature test in dependence of the position inside the reaction zone is showed in the Figure 2.7. The oven temperature has been set at 270°C (ramp 1: from RT to 250°C, 5°C/min; ramp 2: from 250 to 270°C, 2,5°C/min) and, after a stabilization period of about twenty minutes, the temperature has been measured from the beginning of the reactor chamber to the end by using a thermocouple. Each point of the temperature profile shown in Figure 2.8 is the average of three repeated measurements. A not perfect insulation of the oven is observable, and it varies as function of the position.

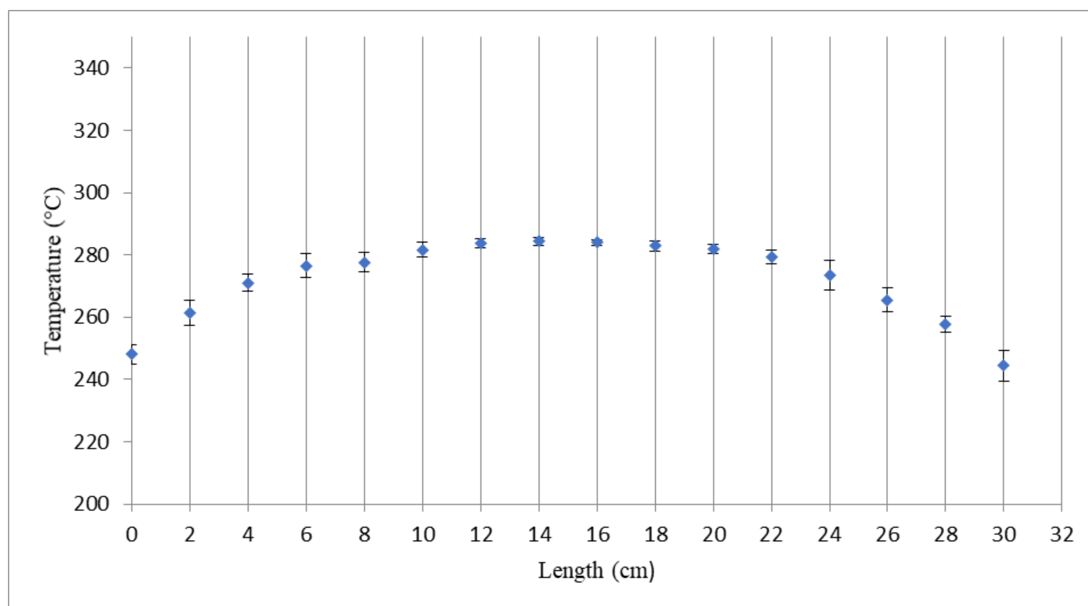

Figure 2.8. Temperature trend in the ALD reaction chamber.

In the position at around 8 cm from the entrance of the reaction zone, a quite stable temperature has been detected for the desired temperature target (280°C ± 3°C). Thus, for all the experiments the substrates were centered at 8 cm and horizontally placed parallel to the gas fluxes.

2.2.2 Substrate preparation: RCA cleaning

Silicon wafer by LG SILTRON INC. KOREA with the characteristics showed in the Table 2.3, were used as substrates for the TiO_2 deposition via ALD.

Table 2.3. Silicon wafer characteristics

Type	P
Orientation	(100)
Dopant	Boron
Res (Ω/cm)	5-30
Thickness (µm)	650-700

The samples, prior to loading in the ALD chamber, have been cut in rectangular shape, 25 x 12 mm, and cleaned according to Standard RCA Cleaning and then stored in N_2 atmosphere until their use.
The RCA (Radio Corporation of America) procedure represents a set of cleaning steps that were employed to remove all traces of impurities, which may be detrimental if present on semiconductor surfaces. Impurities on wafers may be of three types: (a) contaminants films, (b) discrete particles and (c) adsorbed gases [Kern W. 1990].

The procedure consists of three steps:

- Frist step: RCA-1: removal of residual organic contamination deriving from solvent cleaning or any other previous processing;

- Second step: removal of thin oxide layer grown during the previous RCA-1step; during this step silicon surface is highly reactive and immediately attracts particles and organic compounds from the solution and the ambient air;
- Third step: RCA-2 removal of ionic and metallic contamination and formation of a controlled passivated surface [Kern W. 1990]

Procedure

The RCA-1 solution is obtained by mixing:

- Deionized H_2O: 5 parts;
- NH_4OH (30-33%): 1 part;
- H_2O_2 (30%): 1 part.

Water and NH_4OH are mixed, heated at 70±5°C, and once hot, H_2O_2 is added. The resulting solution bubbles vigorously after 1-2 minutes and it is ready for use.
The silicon samples are soaked for 10 minutes in the ammonia-peroxide solution. After this time the surface is washed with deionized water several times and only if the surface is completely superhydrophilic (unbroken water test) it is possible to move to the second step; if the test fails the RCA-1 step must be repeated.

Second step consists in the preparation of a dilute solution starting from 37% HF (1 part) and deionized water (50 part)
Samples are immersed for 30-60 seconds, till the hydrophilic previously oxidized Si surface (During RCA-1) changes to be completely hydrophobic (water break test).

Finally, the RCA-2 solution is formed by:

- Deionized H_2O: 5 parts;
- HCl (37%): 1 part;
- H_2O_2 (30%): 1 part.

Water and HCl are mixed, heated at 70±5°C, and once hot, H_2O_2 is added. The resulting solution bubbles vigorously after 1-2 minutes and it is ready for use.
The silicon samples are soaked for 15 minutes in the chloride-peroxide solution.
Samples are then washed with water several times and the surface must be completely superhydrophilic (unbroken water test); if the test fails the RCA-2 step must be repeated.
At the end, all the specimens are gently dried by an N_2 flux and stored in glove box closed in tubes. In Figure 2.9 the apparatus used for the RCA cleaning is shown.

Figure 2.9. RCA cleaning apparatus used in our laboratory.

The RCA procedure ensures a uniform and homogenous silicon substrate surface. In Figure 2.10. SEM micrographs of two silicon surfaces, before and after the RCA cleaning, are shown: an evident changing of the surface aspect is observable. In the images on the left, before RCA cleaning, the Si surface presents imperfections and inhomogeneity, that during the growth could lead to an irregular film growth with consequent variable thickness on the whole substrate and possible roughness, due to probable residual contaminants and/or hydrocarbons. Whereas, the image after RCA cleaning (on the right) shows a regular and smooth surface, that ensure a homogeneous deposition. This process leads to the deposition of a uniform titanium dioxide layer on the silicon substrate.

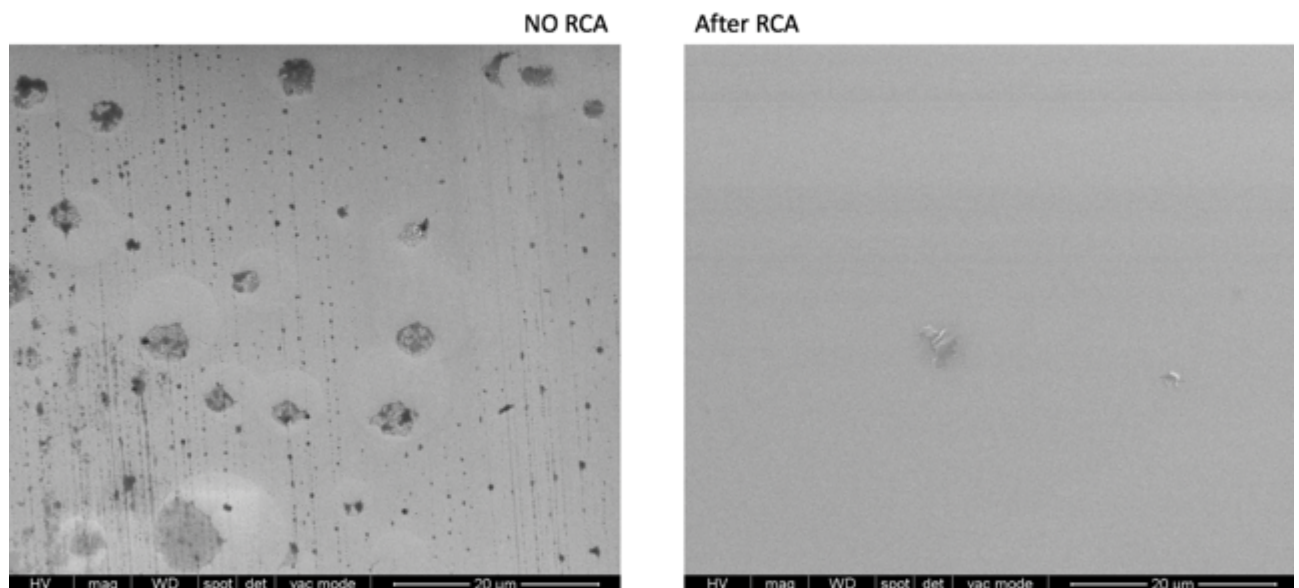

Figure 2.10. SEM micrographs (5000x) before and after RCA cleaning.

2.3 ALD deposition: optimization of titanium (IV) isopropoxide pulse time

Different growths have been carried out by varying precursor pulse time (and maintaining constant all the other process conditions, see Table 2.2), in order to find the optimal TTIP pulse duration to ensure an ALD regime and a constant GPC rate. More specifically, these preliminary experiments were performed to verify that the growth mechanism was really self-controlled (self-limiting) and not limited by the decomposition of the alkoxide.
In Table 2.4 are reported the used growth conditions.
All the deposited titania thin films were characterized by SIMS to estimate the film thickness, by XRD to check the crystallinity and by SEM to study surface morphology.

Table 2.4. ALD growth parameters by varying the TTIP pulse duration from 1 to 2,5 seconds (ALD cycles= 350)

Ti pulse time (s)	Ti purge time (s)	H_2O purge time (s)	H_2O pulse time (s)
1	30	20	1
1,5			
2			
2,5			

2.3.1 SIMS analysis

Information about the in-depth TiO_2 film composition and thickness was gained by SIMS measurements and representative depth profiles are displayed in Figure 2.11 as function of TTIP pulse duration. Secondary ions revealed were: C^- to estimate environmental pollution and/or incomplete precursor decomposition; O^-, Ti^- that are present in the film, and Si^-, deriving from the silicon substrate.
In all cases, Ti and O ionic yields were almost parallel from the deposit surface up to the interface with the Si(100) substrate. This highlights their common chemical origin and confirms the formation of compositionally homogeneous TiO_2 thin films. An apparent broadening of the film/substrate interface in correspondence of the Si signal increase is evident, however it may be considered as absence of interdiffusion between the silicon substrate and the deposited thin film.
Carbon trend shows a very low contamination in the TiO_2 film until the silicon interface (where it starts to increase) maintaining anyway, slow values indicating a good purity of the deposited material and a clean decomposition of the used TTIP precursor under the adopted conditions.
Titania film thicknesses referred to the SIMS Si signal (FWHM) are reported in Table 2.5.

Table 2.5. TiO_2 thin film thicknesses and GPC calculated from SIMS in-depth profiles (ALD cycles= 350).

Sample	Ti pulse time (s)	Thickness (nm)	GPC (nm/cycle)
VTiO13	1	21,4	0,06
VTiO15	1,5	47,4	0,13
VTiO16	2	42,8	0,12
VTiO17	2,5	46,0	0,13

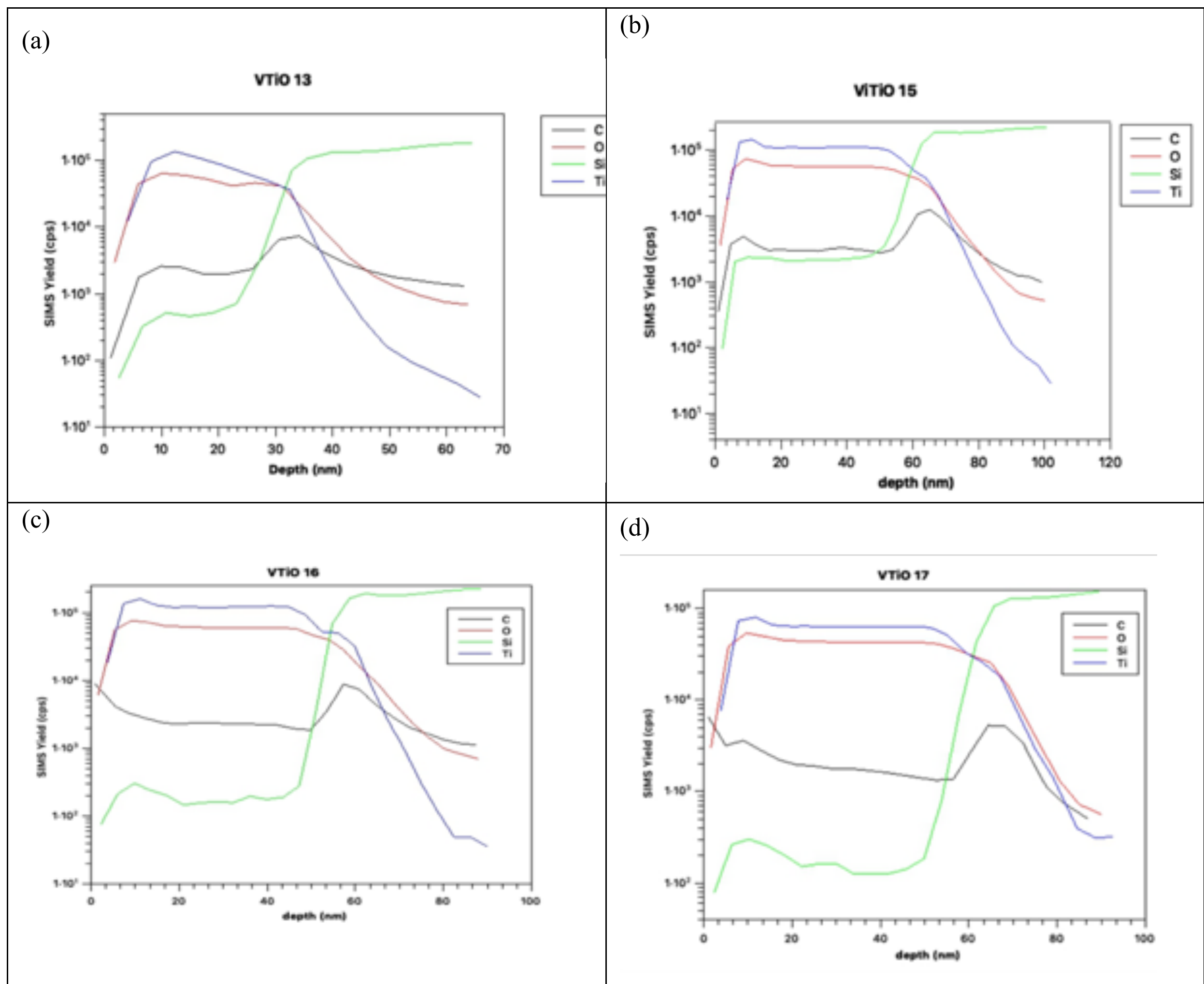

Figure 2.11. SIMS in–depth profiles of as grown TiO_2 thin films deposited at 280°C at different TTIP precursor pulse duration: (a) 1.0 s, (b) 1.5 s, (c) 2.0 s, and (d) 2.5 s.

Self-controlled ALD mechanism has been verified by varying TTIP pulse time. The saturation of the growth rate at a constant level when the pulse time is 1,5 s or above confirms that the growth is self- controlled at 280°C. As shown in the graph below reported (Figure 2.12) there is a constant GPC value starting from 1,5 seconds of TTIP pulse which remains unchanged for 2 and 2,5 seconds, too.

In accordance with the data just shown and taking into account the configuration of the ALD reactor in use, a 2,5 s TTIP pulse time was considered the best choice. A longer pulse time was preferred to ensure sufficient precursor quantity into the reaction chamber.

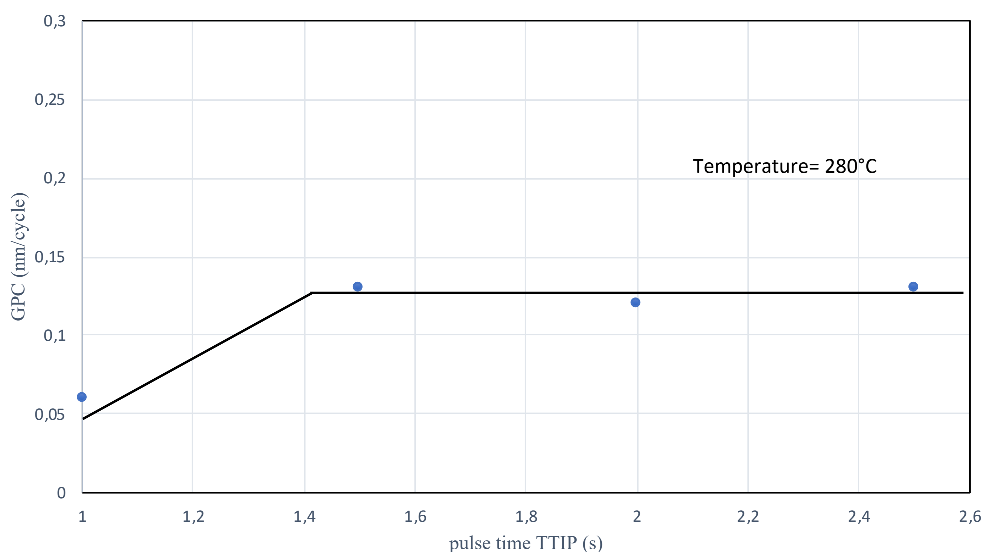

Figure 2.12. GPC of films grown by 300 cycles at 280°C as a function of pulse time TTIP duration

2.3.2 XRD: STRUCTURAL CHARACTERIZATION

Grazing incidence XRD analyses of the as grown TiO_2 films deposited on OH-terminated silicon at different TTIP pulse duration (1.5, 2.0, and 2.5 s) are shown in Figure 2.13. Diffraction patterns reveal that all the films are polycrystalline in anatase phase (ICDD n. 01-083-2243), with no evident preferential orientations and with the absence of rutile phase, as expected for thin films deposited at the chosen temperature [Ritala M. et al. 1993].

The (101) reflection (at 2θ= 25,32°) is the most intense one in all the TiO_2 films. In addition to the (101) main peak, almost all the reflections characteristic of anatase TiO_2 are evident: (112), (200), (211), (204), (220), and (215) at 2θ values of 37.60°, 48.08°, 55.11°, 62.73°, 70.34, and 75.12°, respectively.

The films analyzed have comparable thicknesses and their XRD pattern intensities are comparable (just a little less intensity is shown for the film grown at 2,0 s TTIP pulse duration, in accordance with the thickness observed by SIMS analyses).

2.3.3 SEM: MORPHOLOGICAL CHARACTERIZATION

SEM images of TiO_2 thin film grown on silicon wafer with 2,5 TTIP pulse time (GPC 0,13 nm/cycle) are shown in the Figures 2.14 at two different magnifications (50000x and 100000x). No structural defects, like cracks, were observed. The TiO_2 surface presented regular and non-planar morphology, pinhole-free with a repetitive shape. Homogeneity and uniformity of the film morphology was found on the whole surface.

The whole Si substrate surface was conformally covered by the dense and well-adherent TiO_2 films as shown in the cross-section SEM micrograph reported in Figure 2.15.

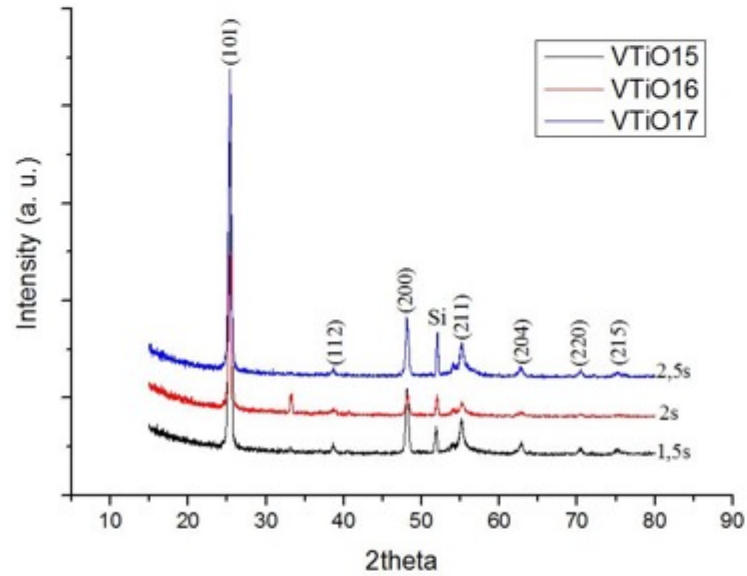

Figure 2.13. XRD patterns of TiO_2 films grown at 280°C at three different TTIP pulse durations (1,5, 2, and 2.5 s).

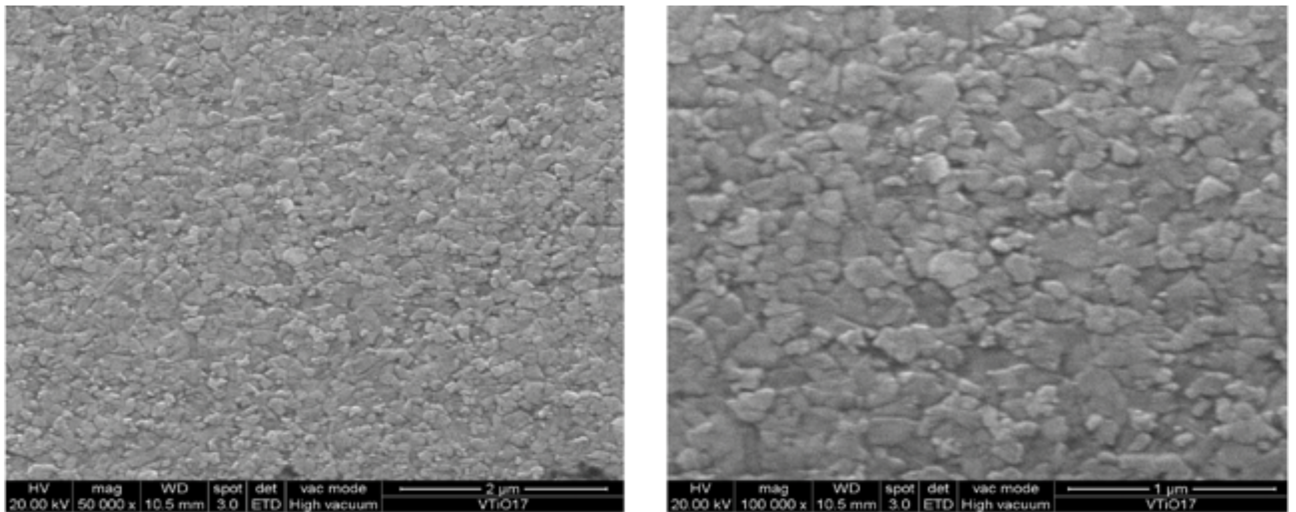

Figure 2.14 SEM micrographs of TiO_2 thin films (46 nm thick, VTiO17) at two different magnifications: 50000x on the left 100000x on the right.

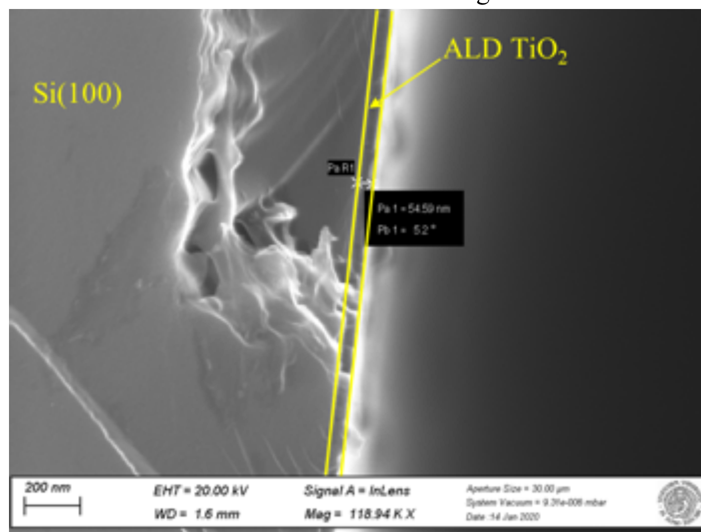

Figure 2.15. SEM cross-section of a Si substrate surface covered by ALD TiO_2 film.

2.4 ALD deposition: optimization of titanium (IV) isopropoxide purge time

Being the ALD TTIP/H_2O process self-terminating with respect to time, reactants' (TTIP and H_2O) purge durations (step 2 and 4 of one ALD cycle) must be sufficiently long in order to not affect, respectively, the amount of species adsorbed on the surface (and semi-reactions go to completion). In the case that the purge times are too short, the GPC tends to increase for a concomitant undesired CVD-type deposition.
In this regard, a series of experiments were carried out by changing the TTIP precursor purge time from 15 to 60 seconds. In the Table 2.6 growing conditions are reported.
The TiO_2 thickness was estimated by SEM cross-section investigations below reported.

Table 2.6. ALD growth parameters for TiO_2 deposition at 280°C by changing the TTIP purge duration from 15 to 60 s (ALD cycles = 300).

TTIP purge time (s)	H_2O purge time (s)	TTIP pulse time (s)	H_2O pulse time (s)
15	20	2,5	1
30			
45			
60			

2.4.1 XRD structural characterization

The films were analyzed by XRD in grazing incidence mode. Even in this case all the as-deposited films showed polycrystalline TiO_2 in anatase phase (ICDD n. 01-083-2243).
(101), (200) and (211) reflections (at 2θ= 25.33°, 48.09°, and 55.11°, respectively) are the only ones observed (Figure 2.16). No preferential orientations were detected.

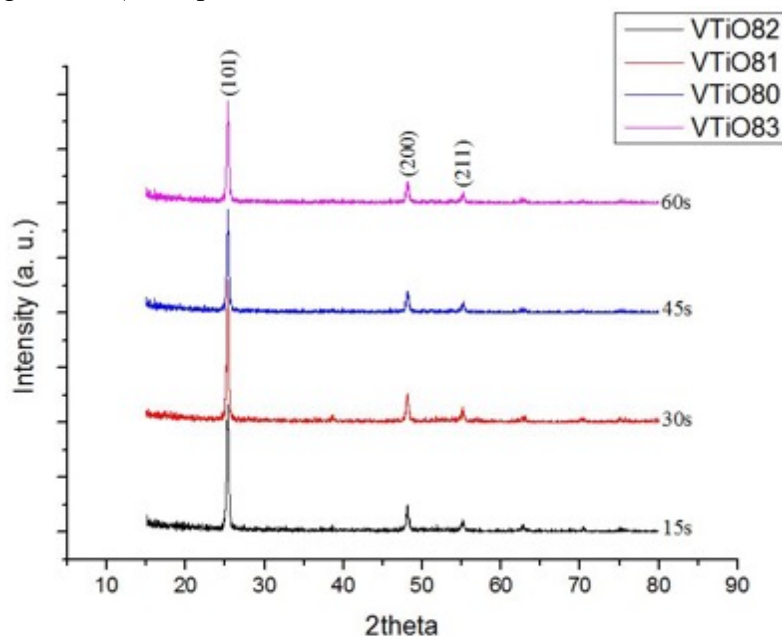

Figure 2.16. XRD patterns of TiO_2 films gown at 280°C at the different TTIP purge durations (15, 30, 45, and 60s).

2.4.2 SEM: THICKNESS INVESTIGATION

Not having an *in-situ* characterization technique in our ALD apparatus, SEM cross-sections were carried out to investigate the TiO_2 film thickness. The acquisition of micrographs in cross-section was not so simple, due to the low thickness of the deposited films, but the analyses gave however the possibility to have an estimation (Figure 2.17).

The thickness evaluation obtained by SEM cross sections are reported in Table 2.7. In Figure 2.18 the trend of the GCP in relation to the different TTIP purge durations is also shown.

From the analysis of the obtained GCP values, 60 seconds result to be the best TTIP purge time, because it represents the lowest GCP value obtained. Moreover, an unexpected 0.19 nm/cycle GCP estimation () has been obtained for the 45 s TTIP purge time; indeed, this value results to be higher than the ones obtained for 15 and 30 s purges.

Table 2.7. TiO_2 thin film thicknesses and GPC calculated from SEM cross sections (ALD cycles=300)

Sample name	TTIP pulse time (s)	Thickness (nm)	GPC (nm/cycle)
VTiO82	15	47 ± 4	0,16 ± 0,01
VTiO81	30	45 ± 6	0,15 ± 0,02
VTiO80	45	58 ±6	0,19 ± 0,02
VTiO83	60	43 ± 3	0,14 ± 0,01

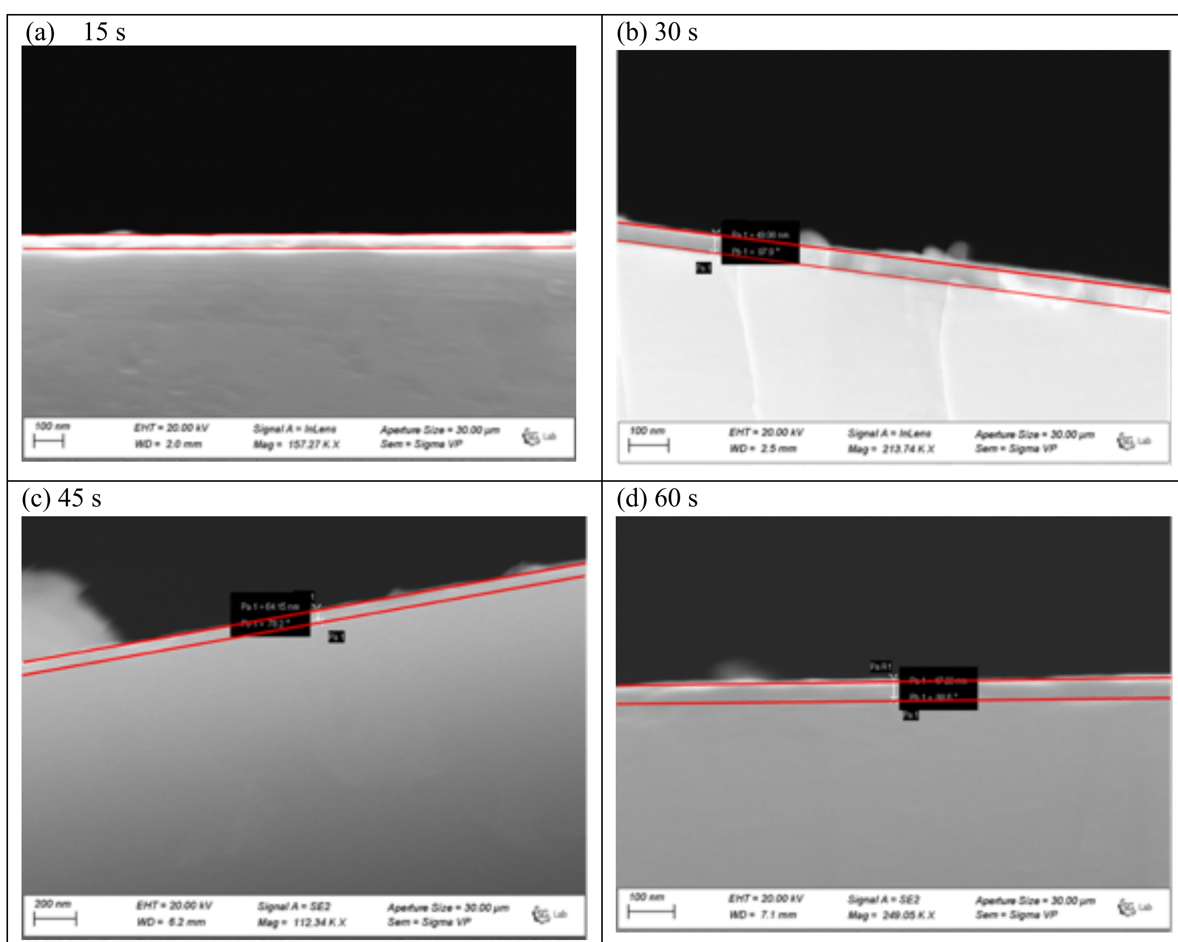

Figure 2.17. SEM cross-section images of TiO_2-films at different TTIP purges: (a) 15s, (b)30 s, (c) 45s, and (d) 60s (red lines mark the TiO_2 film).

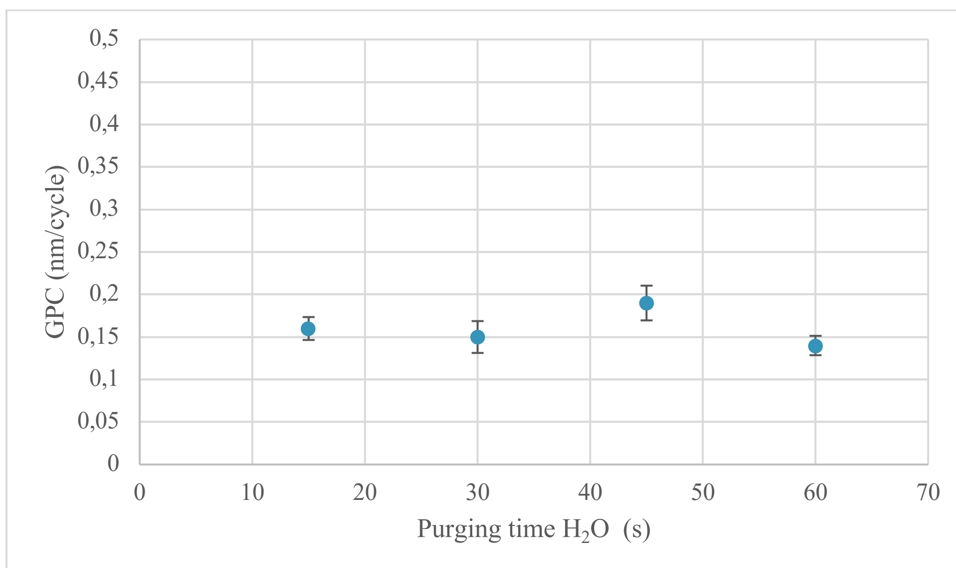

Figure 2.18. GPC of TiO_2 films grown (300 ALD cycles) at 280°C as a function of TTIP purge duration.

2.5 ALD DEPOSITION: OPTIMIZATION OF H_2O PURGE TIME

As exposed in the previous section, also water purges have been changed from 15 to 60 seconds in order to establish the ALD self-limiting conditions. In the table 2.8 growing conditions are reported.

The film thickness has been investigated by spectroscopic ellipsometry analyses.

Table 2.8. ALD growth parameters for TiO_2 deposition at 280 °C by changing the H_2O purge duration from 15 to 60 s (ALD cycles = 300).

H_2O purge time (s)	TTIP purge time (s)	TTIP pulse time (s)	H_2O pulse time (s)
15	60	2,5	1
30			
45			
60			

2.5.1 SPECTROSCOPIC ELLIPSOMETRY: THICKNESS MEASUREMENTS

The thickness of the TiO_2 layer was measured by spectroscopic ellipsometry analyses (Table 2.9) using a J. Woolham V-VASE variable angle spectroscopic ellipsometer. Spectroscopic scans were taken in reflection, in the wavelength range 300-1000 nm, at three angles 55-60-65°. To fit the data, the samples were modeled as follows: 1 mm – thick Si substrate, a TiO_2 thin film (the tabulated dielectric function for the anatase phase was used, while the film thickness was left as a free parameter of the fit) and a surface layer composed of 50% of TiO_2 and 50% air, introduced to mimic a possible surface roughness.

The GPC trend at different purging times of H_2O is detectable in Figure 2.19. A H_2O purge time of 15 s was not sufficient to ensure a self-limited control of ALD TiO_2 growth, whereas 30 and 60 s purges showed the minimum GCP, suggesting a self-terminating control of the reaction. Even

from this set of experiments, the unexpected GCP value (0.19 nm/cycle) for 45 s H_2O purge was detected, as just observed in the previous section. The explanation of this behavior is currently under study.

Table 2.9. TiO_2 thin film thicknesses and GPC calculated from spectroscopic ellipsometry data (ALD cycles=300)

Sample name	H_2O Purging time (s)	Thickness (nm)	GPC (nm/cycle)
VTiO78	15	57,36 ± 0,10	0,1912 ± 0,0003
VTiO77	30	45,10 ± 0,09	0,1503 ± 0,0003
VTiO76	45	64,30 ± 0,13	0,2143 ± 0,0004
VTiO74	60	48,26± 0,08	0,1609 ± 0,0002

The GPC trend at different purging times of H_2O is detectable in Figure 2.19. A H_2O purge time of 15 s was not sufficient to ensure a self-limited control of ALD TiO_2 growth, whereas 30 and 60 s purges showed the minimum GCP, suggesting a self-terminating control of the reaction. Even from this set of experiments, the unexpected GCP value (0.19 nm/cycle) for 45 s H_2O purge was detected, as just observed in the previous section. The explanation of this behavior is currently under study.

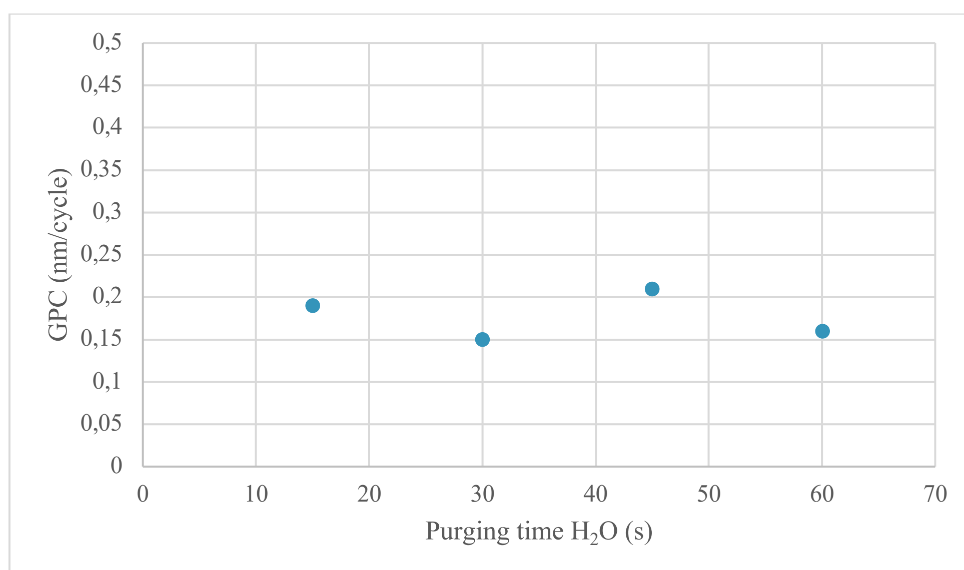

Figure 2.19. GPC of films grown (300 ALD cycles) at 280°C as a function of H_2O purge time duration.

2.5.2 XRD: STRUCTURAL CHARACTERIZATION

The experimental XRD patterns agree with the ICDD n. 01-083-2243 relative to TiO_2 in anatase phase and the relative intensities of the reflections are in good accordance with the theoretical data reported in the ICDD. X-ray diffraction in grazing incident have demonstrated a polycrystalline structure for all samples. No specific preferential orientation was observed (see Figure 2.20).

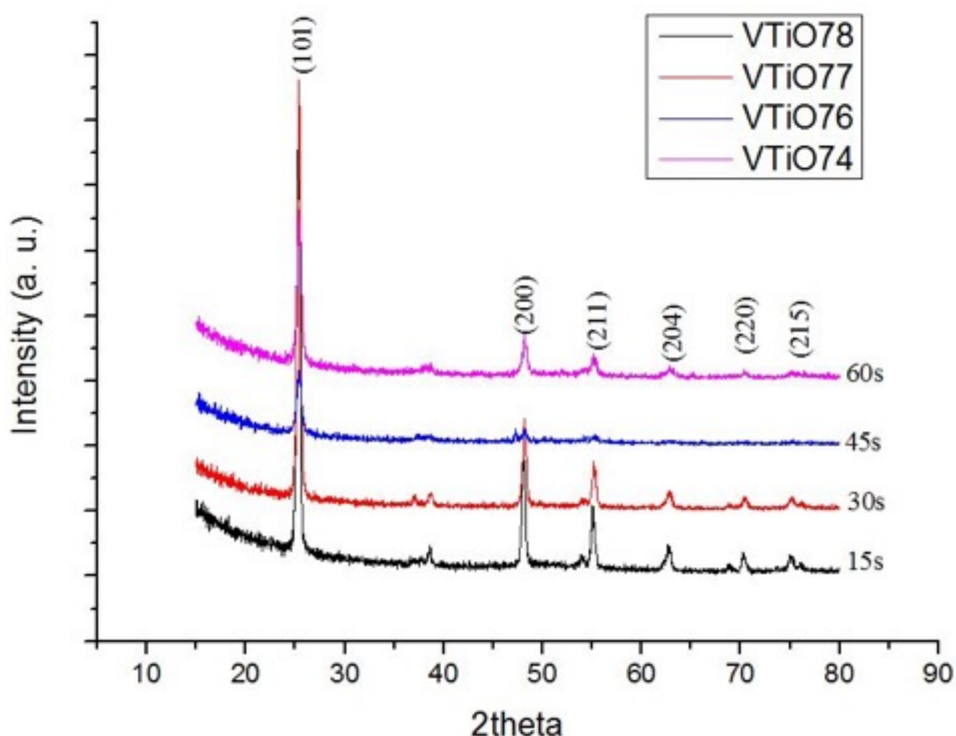

Figure 2.20. XRD patterns of TiO_2 films gown at 280°C at different H_2O purges (15, 30, 45, and 60 s).

2.5.3 SEM: MORPHOLOGICAL CHARACTERIZATION

SEM images of TiO_2 thin film deposited on Si(100) with only two different water purging times (15 and 30 seconds) are shown in Figure 2.121. They confirm once again a uniform surface morphology with no evident defects. The non–planar TiO_2 morphology is very similar for both deposits, even if the dimension of surface islands seems to be dependent on the film thickness.
The best ALD TiO_2 deposition conditions at 280°C are summarized in the following Table 2.10 They are the result of all the experiments done in this work for the optimization of our custom-made reactor configuration. It is worth of noting that our minimum GPC obtained of 0.15 nm/cycle is in contrast with literature data, because still high with respect to the generally obtained 0.3 Å/cycle in ALD commercial flow-reactor [Rahtu A. et al. 2002; Ritala M. et al 1993]. This probably may suggest us that the problem is related to both a not perfect optimization of the ALD regime and/or a concomitant possible TTIP precursor decomposition at the chosen deposition temperature (T=280°C).

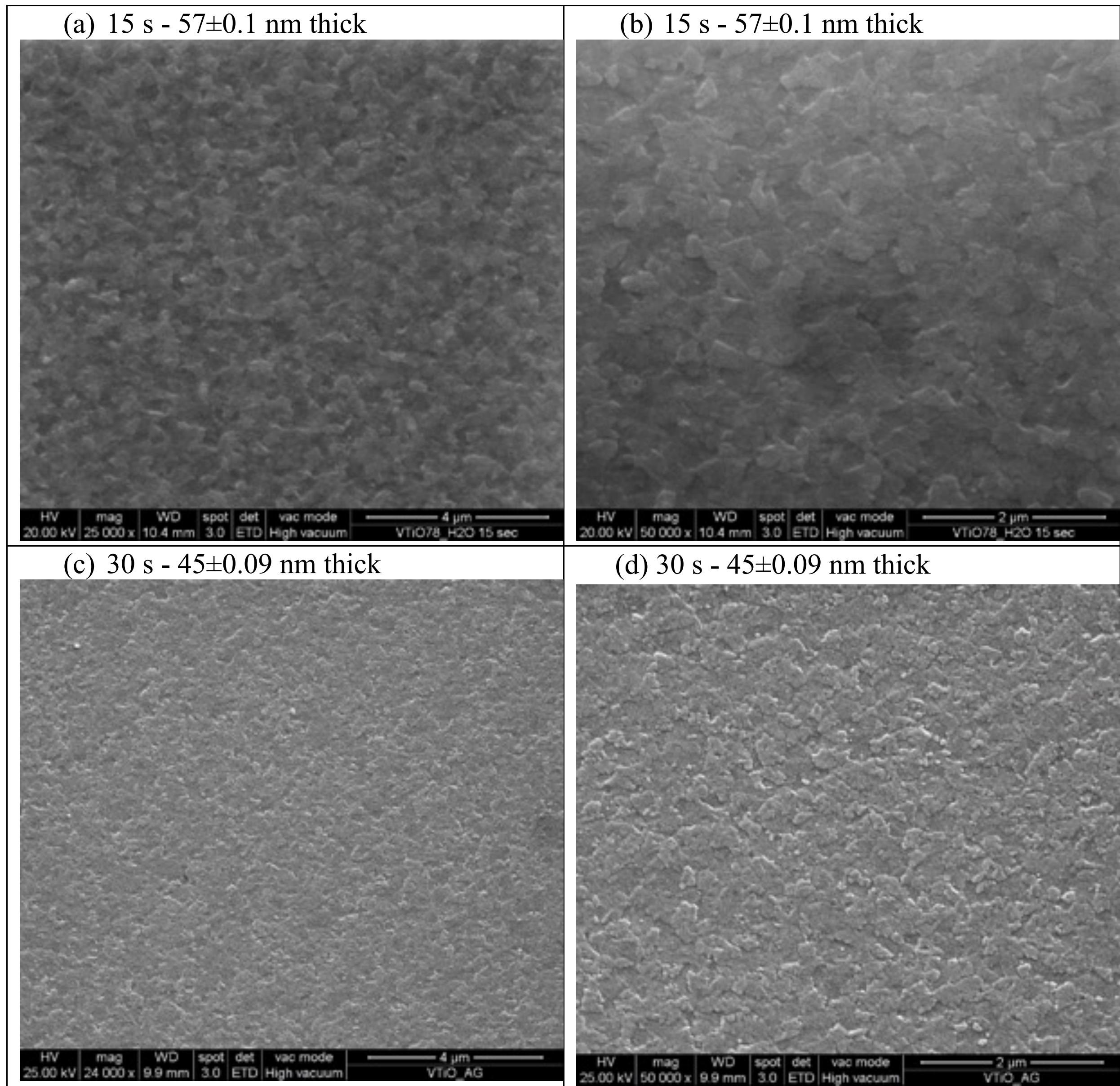

Figure 2.21: SEM micrographs of TiO_2 thin films on Si (100) obtained by changing H_2O purge durations: (a)-(b) 15 s (25000x and 50000x, respectively) and (c)-(d) 30 s (25000x and 50000x, respectively).

Table 2.10. Optimized deposition conditions for TiO_2 thin film deposition at 280°C (ALD cycles= 300)

TTIP purge time (s)	TTIP pulse time (s)	H_2O pulse time (s)	H_2O purge time (s)	GPC (nm/cycle)
60	2,5	1	60	0,15

2.6 Preliminary decomposition test of titanium (IV) isopropoxide

According to Rahtu et al. [Rahtu A. et al. 2002] TTIP precursor shows a constant 0.3 Å/cycle growth rate in the 250-325°C temperature range. At temperature below 250°C the growth rate was lower, whereas at T above 325°C the Ti precursor self-decomposition becomes a concomitant and dominant process, that ruins the self-limiting growth (self-controlled film growth is lost). However, in the 250 – 325°C temperature range, the precursor self-decomposition starts even if it is

not the dominant process. Since our ALD growths were carried out at 280°C and since the obtained GCPs are still relatively high, we decided to verify the possible concomitant contribution of the TTIP self-decomposition at our process temperature.
Three repeated experiments have been done making an ALD process with only $Ti(OCH(CH_3)_2)_4$ and nitrogen gas, and without the co-reactant water, operating at the same temperature and pressure conditions used during the previous depositions (Table 2.2). The optimized pulse and purges duration reported in Table 2.10 were also used. It turned out that, after 300 cycles, yellowish thin films were deposited on the Si surface during all the three experiments (Figure 2.23).
GIXRD analysis was carried out to investigate the nature of the film (figure 2.24) and the diffraction pattern exhibited the characteristic reflections of polycrystalline TiO_2 in anatase phase (ICDD n. 01-083-2243).
The growth of the film in these conditions is surely attributable only to the decomposition of the TTIP precursor, which behaves like a single-source one (Ti and O are both present in the TTIP molecule). Indeed, without water it is impossible to have an ALD like growth and a self-limiting process. Many studies [Fictorie, J. F. et al. 1994; Chen S. et al. 1993] explain the observed GCP fluctuations in classical TTIP/H_2O ALD deposition to a concomitant undesired TTIP self-decomposition with a CVD-like behavior.
More detailed studies will have to be carried out in our lab, in order to evaluate the weight that TTIP decomposition has on our ALD growth, also in light of the higher GCP values obtained with respect to the literature ones.

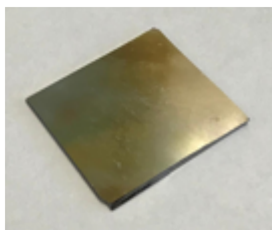

Figure 2.23: Thin film deposited on Si(100) deriving just only from TTIP self-decomposition.

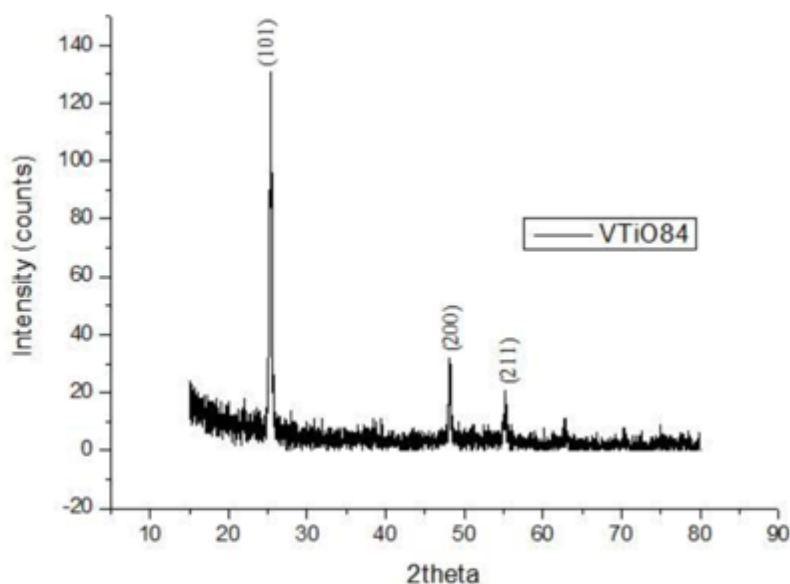

Figure 2.24: XRD pattern of TiO_2 thin film deposited on Si(100) deriving from TTIP self-decomposition

CHAPTER 3

SURFACE WETTABILITY STUDY AND NEURONAL BIOCOMPATIBILITY TEST ON TiO_2 THIN FILM

The study of functioning of the human body has always been a central topic of medical research. In the recent years, it has concentrated on studying the more complex apparatus: nervous system and the investigation, especially, of the multiple functions of brain.
This thesis, focused on the realization of a TiO_2 thin films by ALD, proposes a preliminary analysis of the biocompatibility of the prepared material with neurons and studies how UV radiation affects cellular adhesion, with a view of using it for the production of biomedical devices. Indeed, during the film preparation, fundamental physico-chemical properties were taken into account, for instance crystallinity, pinhole-free film and uniformity, required for clinical utilization.

3.1 SURFACE WETTABILITY STUDY ON TiO_2 THIN FILM

Particular attention has been paid to surface wettability. As we known, the contact angle affects cellular adhesion in accordance with Ho Lee J. et al., who observed maximum cell adhesion and growth at around 55° water contact angle, regardless of the cell types [Ho Lee, J. et al. 1997]. As mentioned in several studies, hydrophilic surfaces allow for better cell adhesion and subsequent proliferation compared to less wettable ones [Hakan N. 1996; Faucheux N. 2004].
Surface material properties influence neuronal cell adhesion, because the cells do not contact the bare surface, instead a pre-adsorbed protein layer. Indeed, concentrations and conformations of adsorbed protein control the cells response. Proteins during surface adsorption encounter displacement and conformational changes, thus kinetics and thermodynamics considerations should be study to rationalize the displacement and the adsorption of them.
In addition to Water Contact Angle (WCA) measurements, employed in this work, other analytical techniques can take into account to characterize surface charge, roughness, density of functional groups and other factors [Mei Y. et al. 2010].The water contact angle affects cellular adhesion, thus in these preliminary biological tests, WCA was used to check surface wettability. WCA analysis is characterized by a quick measurement, requiring inexpensive equipment and minimal expertise.
A surface wettability study has been carried out and, according to the needs to have hydrophilic surfaces also after ALD deposition, UV exposition was considered to restore the initial hydrophilic surface characteristics. By a custom-made apparatus and a dedicated software, the static water contact angle values were measured. Deionized water was used to form a drop of about 4μL.
In the Figure 3.1 a schematic representation of the possible behavior of a drop on the surface related on its wettability is shown. Different kinds of interaction with surfaces determine the shape of the liquid droplet and the resulting contact angle.
Initial tests were performed on as grown TiO_2 samples, i.e. such coming out of the reaction chamber and immediately stored into a vessel in controlled conditions (at a T = 20-25°C and at a Relative Humidity-RH ~ 43% ± 5%), during all the monitoring period. The vessel used to store all the specimen had a constant humidity of about 43%, thanks to a saturated solution of K_2CO_3

(potassium carbonate). Moreover, the equilibrium CA values were measured after 10 seconds from water drop deposition.

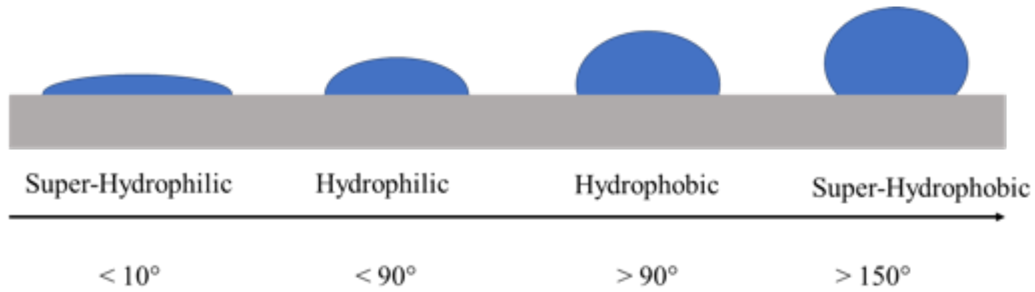

Figure 3.1. Schematic representation dependence of the surface wettability on the water contact angle.

Subsequently, the wettability behavior of also sterilized samples (according to a specific protocol) was observed and finally UV exposition effects have been studied. The same conditions were used for all the experiments: UV_C lamp (power 34 W/m^2 at the sample level and wavelength λ= 254 nm)

As an example, three images, acquired during water contact angle measurement are reported in Figure 3.2. Different surface wettabilities and the relative angle values can be noticed: the hydrophilicity increases from 74° of Figure 3.2 A to close to 0° of Figure 3.2 C.

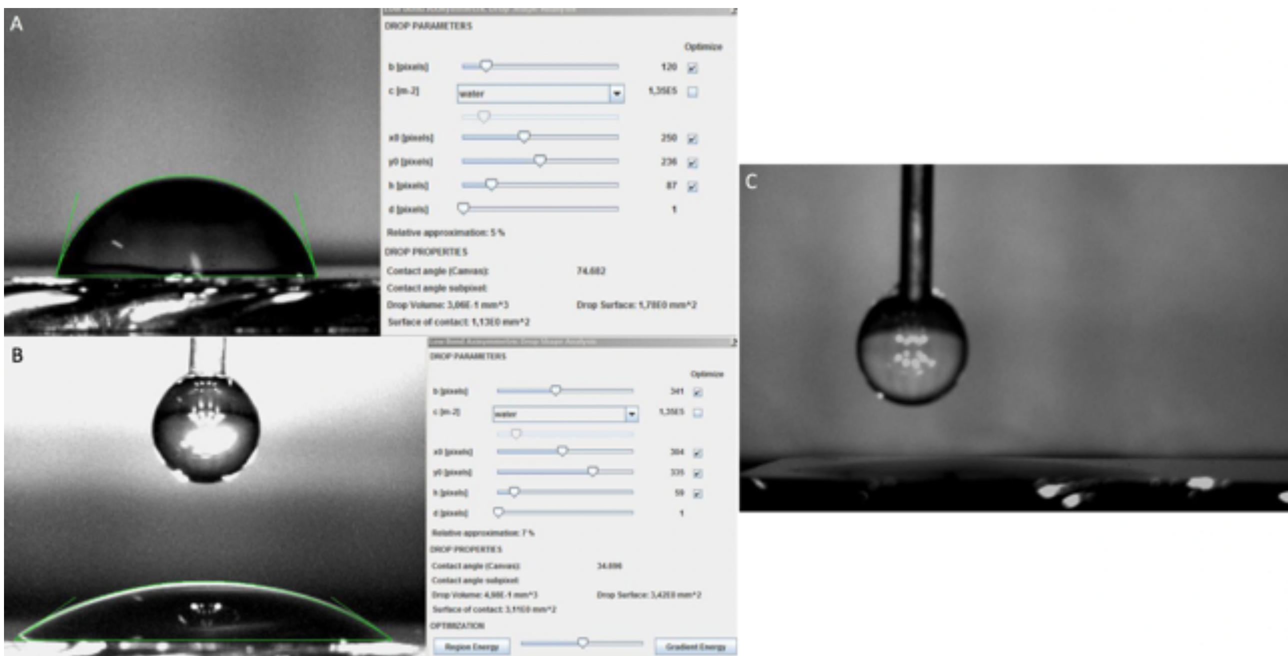

Figure 3.2Three different water contact angle measurements: A=74°, B=34°, C<10°= not measurable.

3.1.1 WATER CONTACT ANGLE MEASUREMENTS OF AS GROWN SAMPLE

For as grown samples, the water contact angles have been checked as a function of the time ageing until the achievement of a steady state. The analyses have been performed by monitoring of static water CAs during a period of about 2 months, and in the Figure 3.4 the general evolution observed is reported.
In Figure 3.3 contact angle values of the first twenty-four hours are shown, whereas in Figure 3.4 the general trend from the beginning to the last check after 65 days is reported. For each ageing time, three different samples were analyzed and the CA values are reported as mean value of three measurements.
It was noticed that, just after TiO_2 deposition (Figure 3.3), at time zero, the contact angle of water droplet was close to zero, suggesting a super-hydrophilic behavior for all the analyzed samples, and within one hour it retains low contact angle values, that can still be considered suitable for our purpose. After half an hour a progressive increasing of the water CA values was observed, to reach after 3 hours and for all the subsequent measurements (within 24 h) CA values quite stable at around the maximum observed of about 71°±1°. The wettability evolution, as a function of the time ageing until 65 days from sample preparation (Figure 3.4), highlights a progressive decrease. After about 50 days wettability stabilizes at WCA of about 86°±1. This behavior is ascribable to a progressive and unavoidable environmental contamination by organic pollutants, such as hydro-carbons, which are progressively absorbed on film settle and modify the surface [Lin X. et al. 2014]. Indeed, the surfaces which initially were hydrophilic gradually turned into hydrophobic ones.

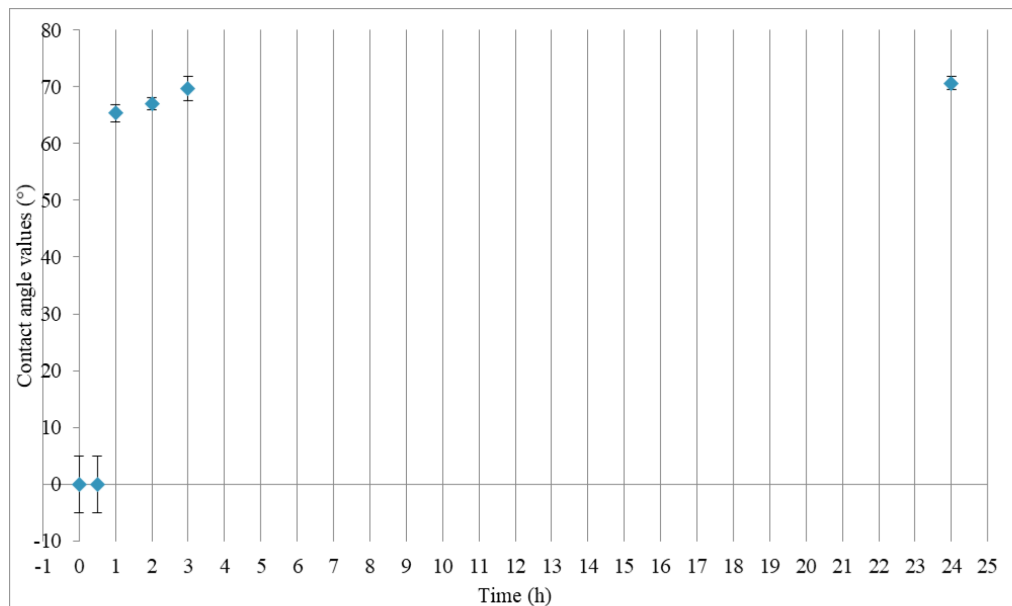

Figure 3.3. Water contact angle measurements just after TiO_2 ALD deposition as function of time (0-24h).

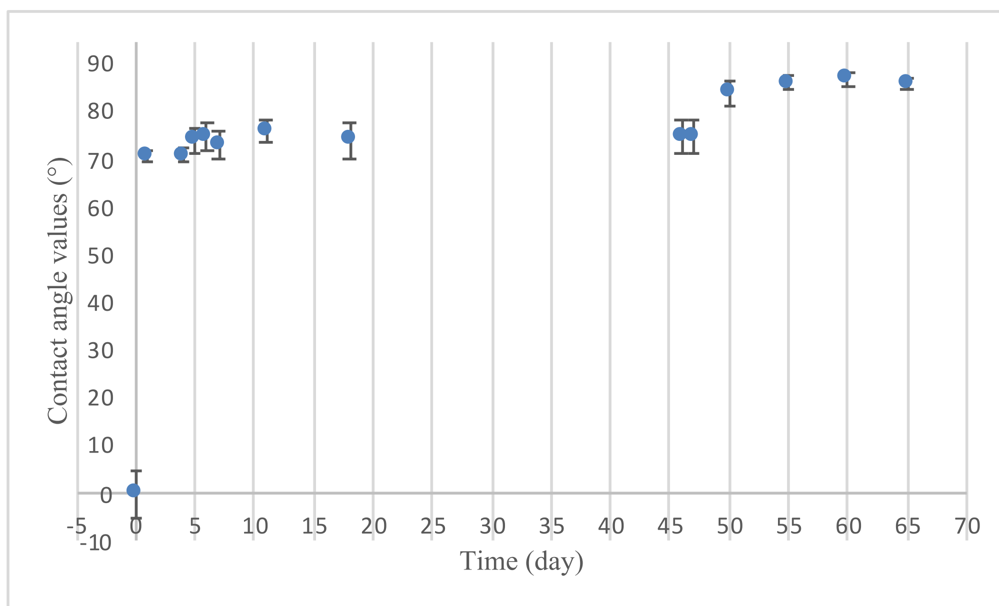

Figure 3.4. Water contact angle measurements just after TiO_2 ALD deposition as function of ageing time (0-65 days).

3.1.2 Water contact angle measurements after UV exposure

When exposed to suitable UV light (i.e. λ < 400 nm), titanium dioxide shows two distinct photo-induced phenomena:

- photocatalytic effect, that leads to the mineralize of organic compounds;
- photo-induced surface reorganization process that leads to increase the hydrophilicity of the surface, also reaching super-hydrophilic behavior.

These phenomena are attributable to the semiconductor nature of TiO_2. In fact, UV radiation shorter than λ= 400 nm (since E_g = 3.2 eV in anatase phase) can excite electrons from valence band to the conduction band and create pairs electron-hole. After this stage the two phenomena go on in different way.

In the first case, the photo-generated electron-hole pairs, in photocatalytic phenomenon, react with electron acceptors (i.e.: O_2, thus producing radical anions such as O_2^-, and electron donors, i.e.: H_2O to produce ·OH radicals). These reactive species start to carry on the contaminants' mineralization and also germs and microorganisms' death. This potential effect confers anti-pollutant and self-sterilizing feature to the material.

In the second case, super-hydrophilic mechanism follows three steps:

1. TiO_2 is irradiated by UV light, and an electron-hole pair is created:

   $h\nu \rightarrow e^- + h^+$
2. Reduction of Ti by a surface electron:
   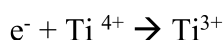
   $e^- + Ti^{4+} \rightarrow Ti^{3+}$
3. Formation of oxygen vacancy:

   $4h^+ + 2O^{2-} \rightarrow O_2$

In the end, Ti^{3+} is oxidized by atmospheric oxygen, and at the same time oxygen vacancies bond with H_2O creating new –OH terminating groups and thin water layer (Figure 3.5).

When TiO_2 is placed in the dark, the reverse reaction occurs, and the surface progressively return back, in the initial equilibrium [Fujishima A. et al. 2000].

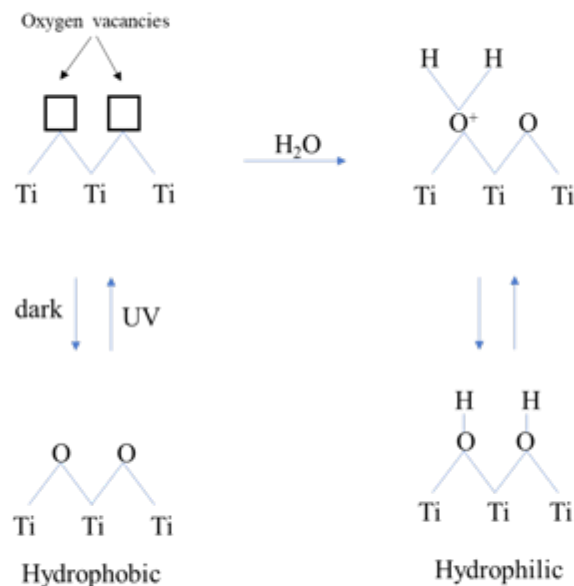

Figure 3.5. Schematic representation of hydrophilic mechanism of crystalline TiO_2 after UV exposition.

TiO_2 as-deposited thin films, previously stored into the dryer in controlled condition for above 65 days and with stable water CA values, were exposed to UV radiation (power 34 W/m^2 at the sample level, $\lambda = 254$ nm) for several different times (10, 20, 30, 60, 90, and 120 min).
As expected, UV irradiation completely restores surface hydrophilicity just after 60 minutes of exposure (see Figure 3.6) with average CA values lower than 10° (as previously observed for the freshly prepared TiO_2 samples). Indeed, for 60, 90, 120 min exposures, it may be assumed that a change of the surface in term of wettability has been found, because every samples displayed not measurable contact angles values (CA lower than 10°).

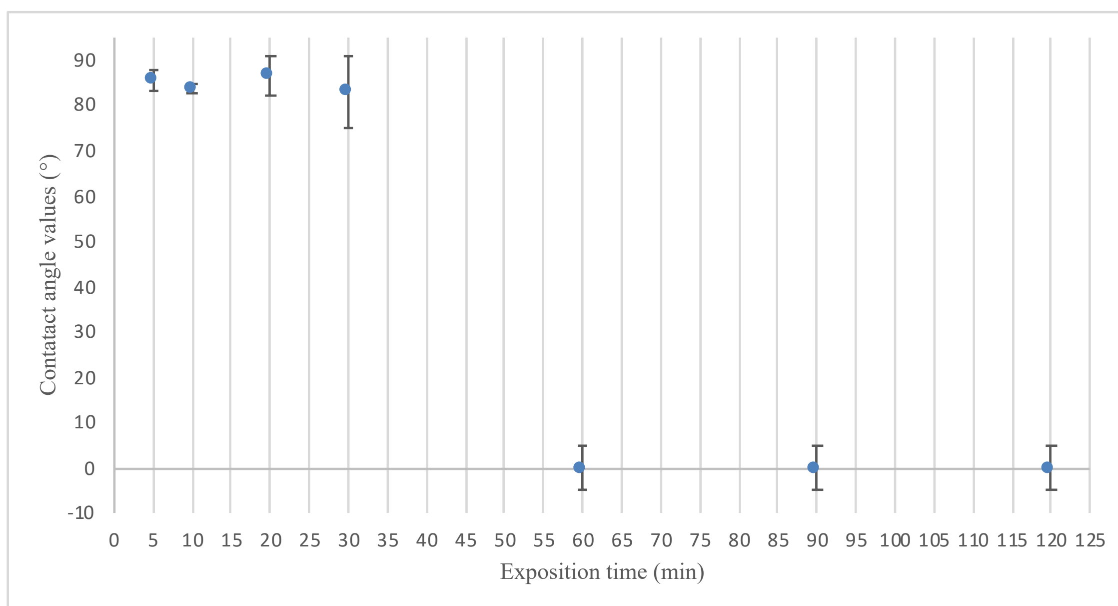

Figure 3.6. Contact angle values after UV exposition: 5min, 10min, 20min, 30min, 60min, 90min, 120min.

Indeed, for 60, 90, 120 minutes' exposure, a complete change of the surface in term of wettability has been found, as shown in the Figure 3.6, every samples displayed not measurable contact angles values. This means that all the surface sites are restored, and only OH sites are present on the surface.

3.1.3 Water contact angle after sterilization procedure

A dedicated cleaning and sterilization procedure have been carried out on as grown TiO_2 films to ensure a clean surface and avoid possible contamination.
The samples cut, to size of about 1cm x 1cm, were placed in Tickpour (5% v/v) at 70 °C for one minute. Tickpour is a detergent and this passage is necessary for removing generic dirty residues before the sterilization. Then the samples were rinsed three times in deionized water, air-dried and wrapped in silver paper. Finally, they have been put in a heater for one hour at 120°C, slowly cooled and placed in the dryer (with 43% ± 5% of relative humidity).
Water contact angle measurements on the sterilized samples have been carried out through the procedure previously described. The wettability was observed both after few minutes from the sterilization, to understand how this procedure affected surface properties, and after 24 h, because according to the biological needs the sample are used -one day after sterilization.
Just after the sterilization process (at time zero) the TiO_2 samples showed an interesting super-hydrophilic behavior of the surface (Figure 3.7), because thanks to the applied treatment the organic pollutants were completely removed. Even in this case, in order to establish the wettability behavior of TiO_2 film surface, water CA values were monitored at different ageing times within 24 h and the results are shown in Figure 3.7. The contact angle values after sterilization were not evaluable (CA<10°) at times 0, 10 min, and 20 min, whereas they exhibited a medium value of about 51°± 2 after 24 h.

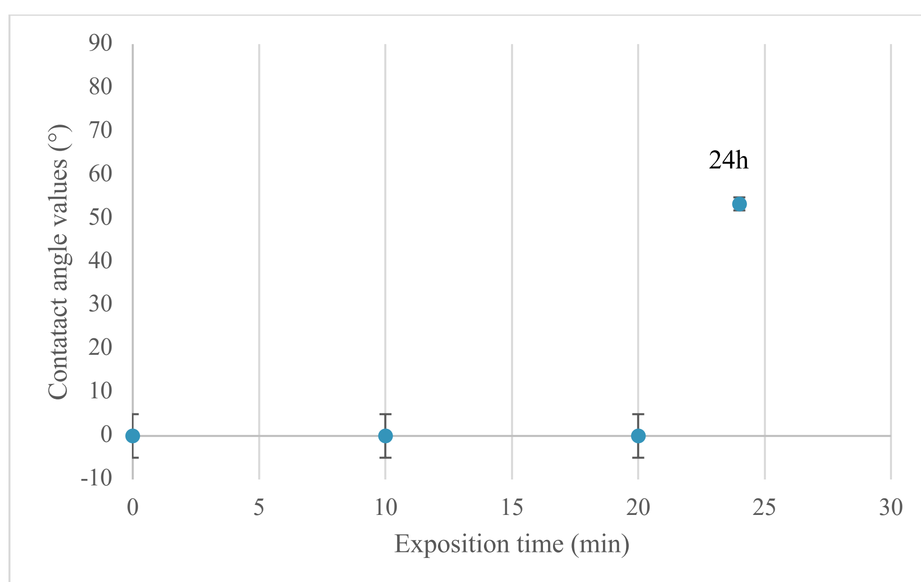

Figure 3.7. Water contact angle values of TiO_2 sample after sterilization procedure monitored at different times (within 24h)

The contact angle values after sterilization were not evaluable (CA<10°) at time 0, after 10 minutes, and after 20 minutes and exhibited a medium value of about 51° after 24 h.
The wettability was observed both after few minutes, to understand how the sterilization procedure affected surface properties, and after 24h because according to the biological needs the sample are used -one day after sterilization.
In accordance with the results, it has been decided to use UV radiation on sterilized samples and to study how the wettability changes, to ensure a hydrophilic surface for cellular deposition.

3.1.4 Water contact angle measurements after UV exposure on sterilized sample

In accordance with the obtained results, it has been decided to use UV radiation on TiO_2 samples after 24 h from the sterilization treatment, in order to study how the wettability changes with UV exposition time, to ensure a hydrophilic surface for subsequent neuronal cell deposition.
All the TiO_2 thin film just after the sterilization procedure were maintained in the dryer in controlled conditions and after 24 h three different UV exposition times were carried out: 30 s, 1 min, 2 min, and 5 min, that are compatible with the biological needs during the neuronal preparation procedure. The contact angle values after 30 s and 1 minute UV exposition show a hydrophilic behavior, with CA values in the range of about 45-50°, which are still acceptable for our purpose (see Figure 3.8). Whereas, for samples analyzed after 2 and 5 minutes of UV exposition the contact angles of water droplets plummet to zero, suggesting again a superhydrophilic behavior (CA<10°) for all the analyzed samples.
The neuronal cell biocompatibility tests, studied in the following section, were done tacking into account the results just obtained.

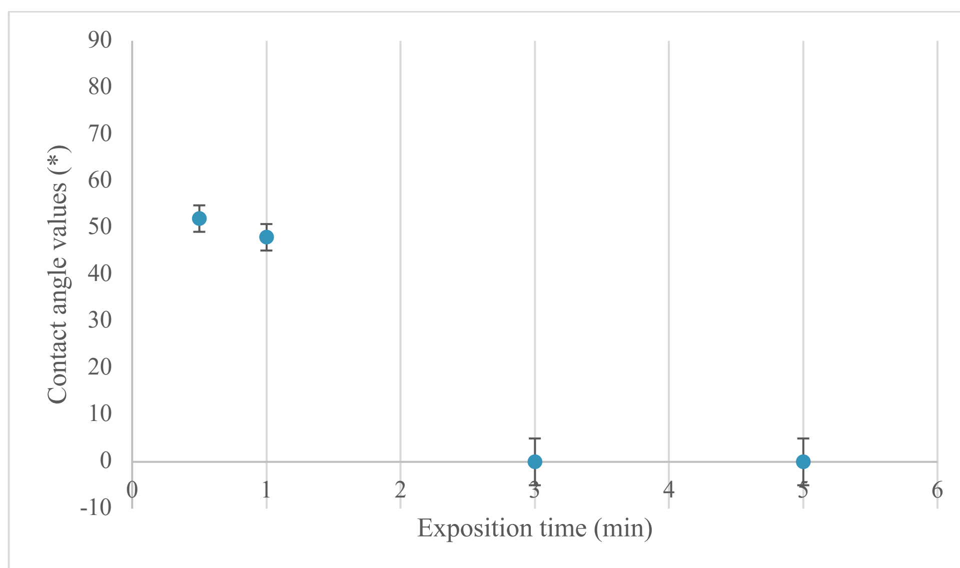

Figure 3.8. Water contact angle values at different UV exposition time (0,5, 1, 3, 5 min) on sterilized TiO_2 samples.

3.2 Biocompatibility experiments: neuronal preparation procedure

A total number of 24 samples divided into six groups of four were used. Each group is characterized by different experimental conditions as shown in the following table 3.1.
All samples have been sterilized, only group 1 has been preserved in open atmosphere and the solely group 3, 4, 5, 6 have been exposed to UV.
The plating density is the same for all samples, 15000 neurons/cm^2. In Table 3.2 the sample number, the exposition time and, relatively on the area of each sample, the approximate number of the seeded neurons are shown in detail.

Table 3.1. Group of TiO_2 with different treatments.

Group	Sterilization	Conservation in dryer	UV exposition
1	✓	x	x
2	✓	✓	x
3	✓	✓	✓
4	✓	✓	✓
5	✓	✓	✓
6	✓	✓	✓

Neurons plating consists in seeding a certain quantity of cellular culture on the substrate. To ensure a good adhesion, it is necessary to have a layer of poly-L-Lysine: this synthetic compound promotes cells adhesion by changing the surface of the substrates. 100 µL of the solution (20 µg/mL in sterile deionized H_2O) were deposited on the samples' surface; 2 hours later the excess was removed and after 10-15 minutes of air-drying under a sterile laminar hood the surface was ready for cellular deposition.

Table3.2. Numeration of different sample with relative treatments.

Group	Sample number	UV time exposition time (s)	Plated Neurons number approximately
1	1	No	9000
	2	No	9000
	3	No	9000
	4	No	9000
2	5	No	15000
	6	No	15000
	7	No	15000
	8	No	15000
3	9	30	15000
	10	30	15000
	11	30	15000
	12	30	15000
4	13	60	15000
	14	60	15000
	15	60	15000
	16	60	15000
5	17	180	15000
	18	180	15000
	19	180	22000
	20	180	22000
6	21	300	22000
	22	300	33000
	23	300	33000
	24	300	33000

A different behavior of the poly-L-Lysine drop was observed, in relation of the exposure of the sample to the UV radiation, suggesting different surface wettability. It was interesting to note that for the sample of the groups 1 and 2 (no UV exposition), the drop was well formed with the typical behavior for less hydrophilic surfaces. Samples A and B are shown in Figure 3.9. Both had no UV treatment, the only difference was in the storage: sample A, on the left, was preserved in open atmosphere, sample B, on the right, was maintained in the dryer in controlled condition.

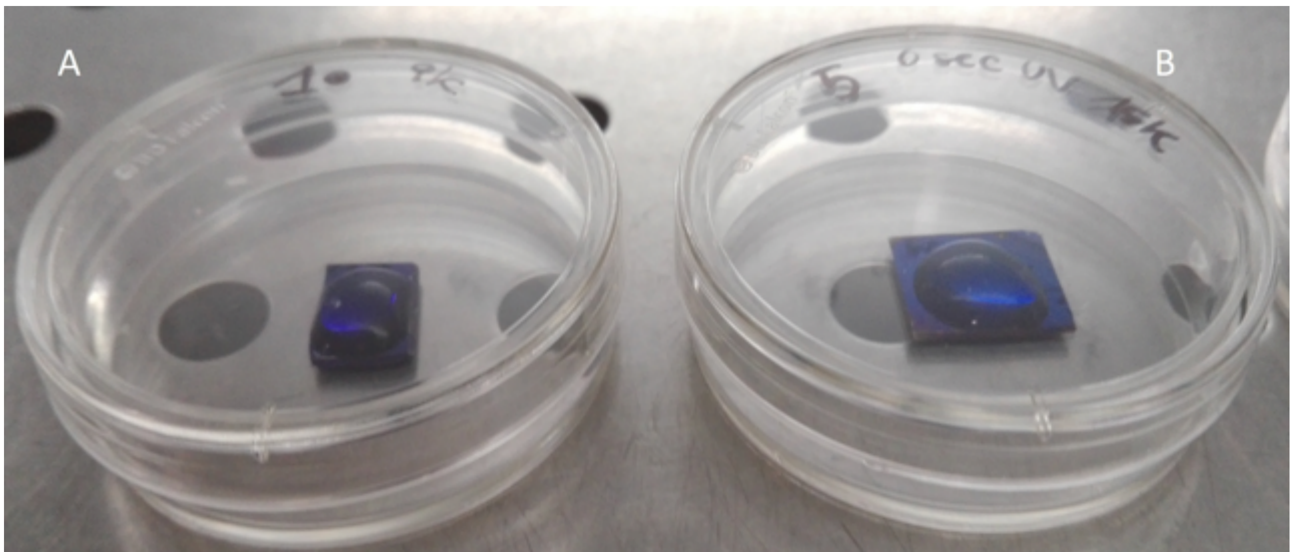

Figure 3.9. Sample A, group 1 and sample B group 2 after poly-L-Lysine deposition

In Figure 3.10, sample A of the group 3 is shown. It was exposed for 30 seconds to UV radiation and it appeared to be a little more hydrophilic, because the drop was thinner and more expanded on the surface. In Figure 3.10 B, the sample belongs to group 4, with 60 seconds UV exposition.

Figure 3.10. Sample A group 3 and B group 4 after poly-L-Lysine deposition, with 30 and 60 secondo UV exposition time respectively.

An increasing hydrophilicity was noticed by increasing the UV exposition time as revealed for samples A and B of Figure 3.11, with 3 and 5 minutes UV exposition, respectively. Indeed, in Figure 3.11 A the sample shows high hydrophilicity: the drop is distributed over the entire surface up to the edge, as for the sample B in figure 3.11. Thus, we can hypothesize that after 3 and 5 minutes of UV treatment the TiO_2 surfaces show a super-hydrophilic behavior.

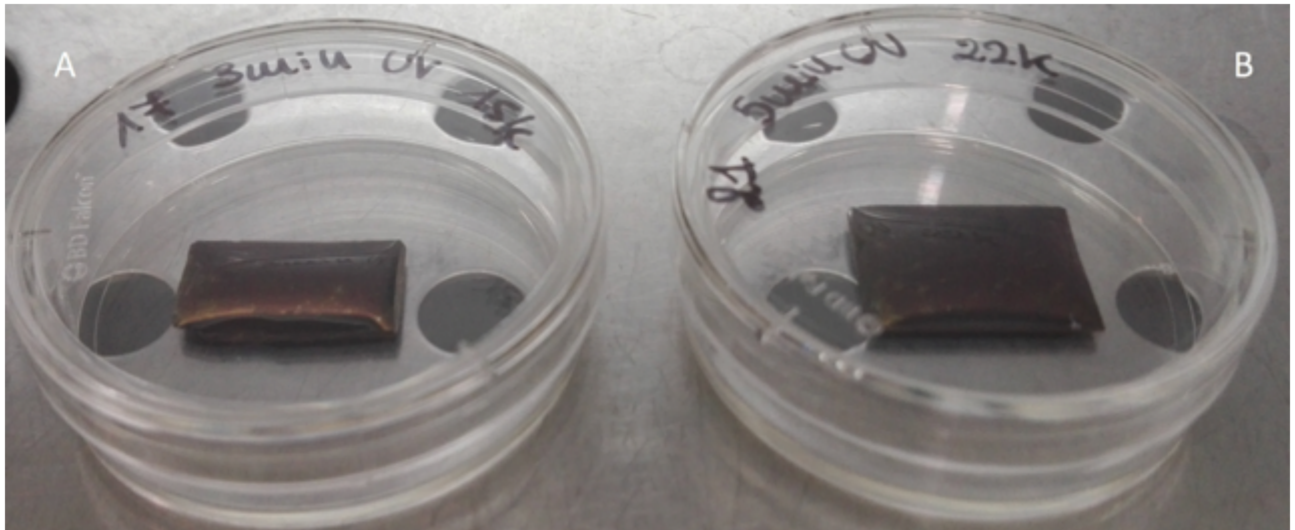

Figure 3.11. Sample A group 5 and sample B group 6 after poly-L-Lysine deposition, with 180 and 300 secondo UV exposition time respectively.

3.2.1 NEURONS DISSOCIATION AND PLATING

In this work for a preliminary biocompatibility study of TiO_2 thin film, neurons from rats (P1= one day life) hippocampi have been used (Figure 3.12). A brief description of the extraction procedure follows.

Hippocampi were dissected from the brains and maintained in cold HBSS (Hank's Balanced Salt Solution without Ca^{2+}/Mg^{2+}). Then the solution has been removed, 1 mL of Trypsin 0.08% has been added and incubated for 25 minutes at 37 °C. After Trypsin removal, 1 mL of Dulbecco's Modified Eagle Medium (DMEM) was added for mechanical neuronal dissociation by repeated and gentle passages through a pipette tip. After centrifugation for 10 minutes at 400 g, the supernatant has been discarded and the cells suspended in 10 mL of DMEM. The neuronal suspension was then seeded in a 100 mm diameter petri dish and incubated for 2 h at 37 °C: this procedure (called pre-plating step) allows a reduction in the number of glial cells and astrocytes in the final culture. Actually, most of the glial cells adhere to the petri surface, while neurons remain in suspension. The liquid was then put in a tube for the subsequent 10 minutes of centrifugation at 400 g. The supernatant was discarded and the cellular pellet was suspended in 1 mL of DMEM, then diluted in L15 medium and seeded on the samples, previously treated with the described procedures and coated with poly-L-Lysine. A parallel plating on standard petri dishes and glass coverslips was made for positive control. After 2 h at 37 °C in incubator the medium was replaced by Neurobasal (NB).

The cells have been maintained in the incubator and monitored for several days; two thirds of the maintenance medium (NB) are replaced every 3 days.

A list of medium and solution used during the experiments is reported. All are from Gibco – Thermo Fisher Scientific.

Figure 3.12. On the left hippocampi (from which neurons were extracted), on the right whole brain of rat used in the experiments.

A list of medium and solution used during the experiments is reported. All are from Gibco – Thermo Fisher Scientific.

DMEM added with:

- FBS (Fetal Bovine Serum), 10%
- Penicillin, 1%
- Streptomycin, 1%

L15 added with:

- FBS (Fetal Bovine Serum), 5%
- Penicillin, 1%
- Streptomycin, 1%

Neurobasal added with

- Glutammax-1, 1%
- B 27, 2%

3.2.2 MONITORING

After the deposition has been completed and the maintenance medium has been added, the samples are stored in an incubator at 37°C in a controlled humidified environment with 5% (v/v) CO_2 to avoid evaporation of the medium and ensure a constant pH. The cultures are observed after seven and fourteen days with the optical microscope Olympus BX51WI, using a standard physiological solution (PBS, Phosphate Buffer Saline).
All the samples, after seven days in culture (DIV_7), show neurons with typical shape and initial branching as described in Dotti C. G. [Dotti C. G. et al. 1988]. In some samples both neurons and little groups of glial cells are visible. TiO_2 thin films show good biocompatibility characteristics, indeed there are no differences between neurons grown on petri dishes or on TiO_2 substrate.

After 14 days in culture (DIV_14), an increase in ramifications has been noted and a highly developed neuronal network is present on petri dishes, on glass coverslips and on all TiO_2 samples. Cellular cultures on titania demonstrate that this substrate is suitable for neurons development.

Petri dish

Neurons on petri dish show dendrites and interconnections. Single neurons are shown in Figure 3.13, at DIV_7 the typical shape and dimension can be noticed, with the presence of main dendrites and the axon. In images acquired at DIV_14 the increase in secondary filaments (branching) and a more complex neuronal network should be noted.

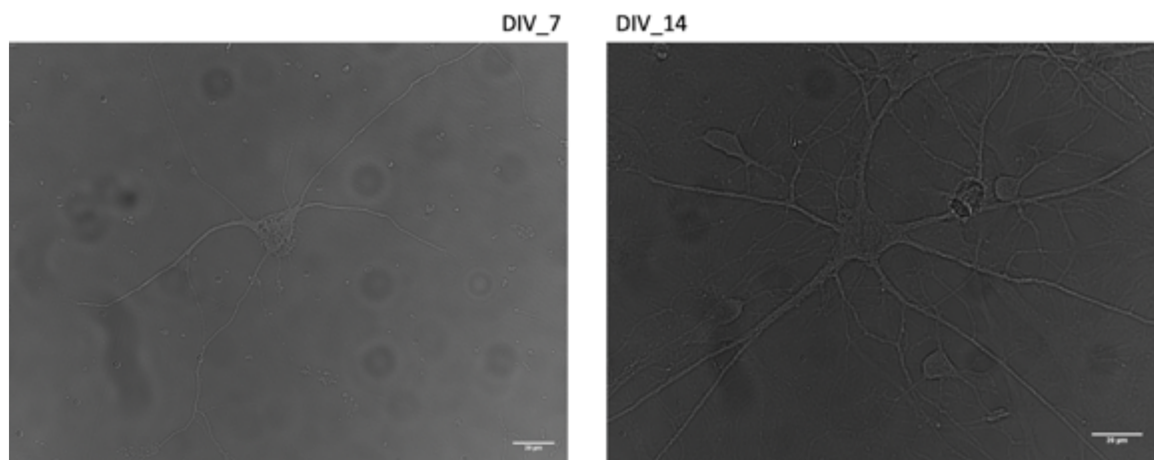

Figure 3.13. Images from optical microscopy of Petri dish, at 40x magnification after 7 and 14 day in culture.

Glass coverslip

Neurons on glass coverslips adhered and developed, showing their typical extensions and connections. In some areas of the coverslip few clusters (aggregated neurons) are present at seven days in culture. At DIV_14 neuronal network is very extensive and well formed, the image highlights the interaction between two neighbor neurons (Figure 3.14).

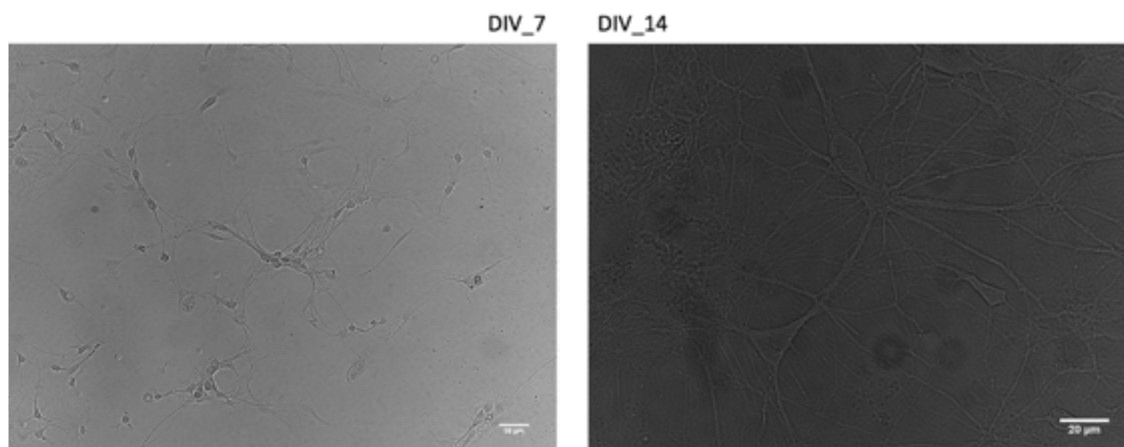

Figure 3.14. Images of glass coverslip, at DIV 7 and DIV 14 at different magnification.

TiO_2 sample, group 1

Group 1 samples were sterilized and stored in atmospheric conditions, without UV treatments. Neurons are developed, they present several extensions and a good network connectivity already

at seven days, and progressively increasing at 14 days in culture (Figure 3.15). Among the typical hippocampal neurons also few glial cells and astrocytes can be noticed: even if the pre-plating step has been performed to reduce the number of glial cells in the culture, the presence of few of them is necessary to ensure a good viability of neurons.

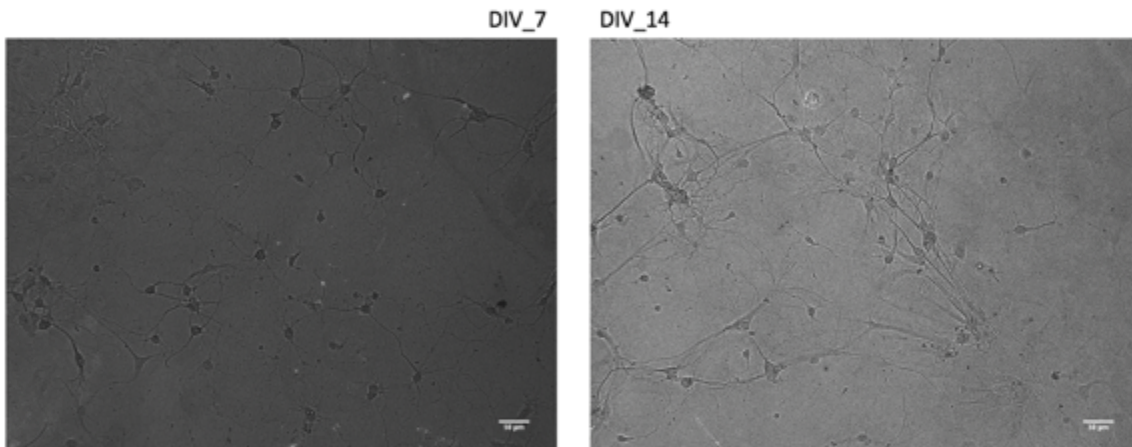

Figure 3.15. TiO2 sample at 10x magnification, showed neurons development at different DIV.

TiO_2 sample, group 2

The samples of group 2 were sterilized and stored in the dryer, without UV radiation. Neurons are present at a proper density (Figure 3.16). There are typical dendrites and axons, and various connections between neurons. In the magnified figure a good neuronal connection is already visible after seven days in culture.

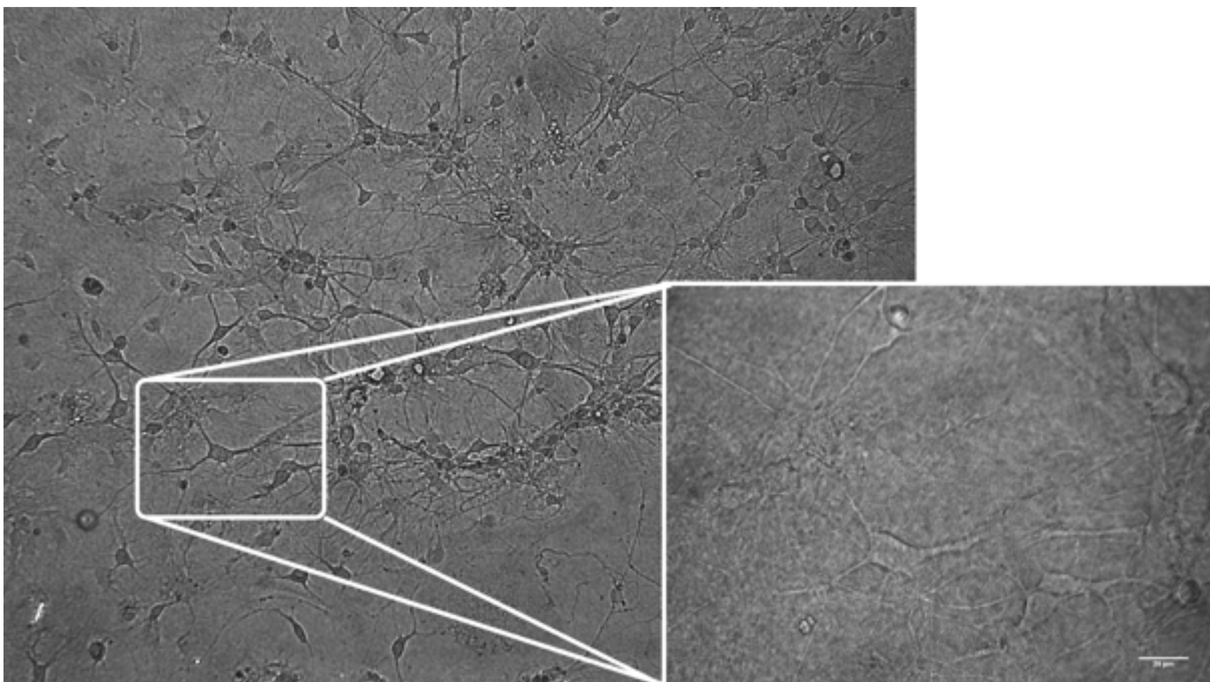

Figure 3.16. TiO_2 sample number 5, at DIV 7. Magnification at 40x showed neurons network already present at DIV 7.

The comparison between seven and fourteen days (Figure 3.17) wants to emphasize the elongation of the dendrites, although the neuronal density is different. Indeed, several factor can influence the neuronal density on the substrate and our aim is only to monitoring neuron growth and differentiation.

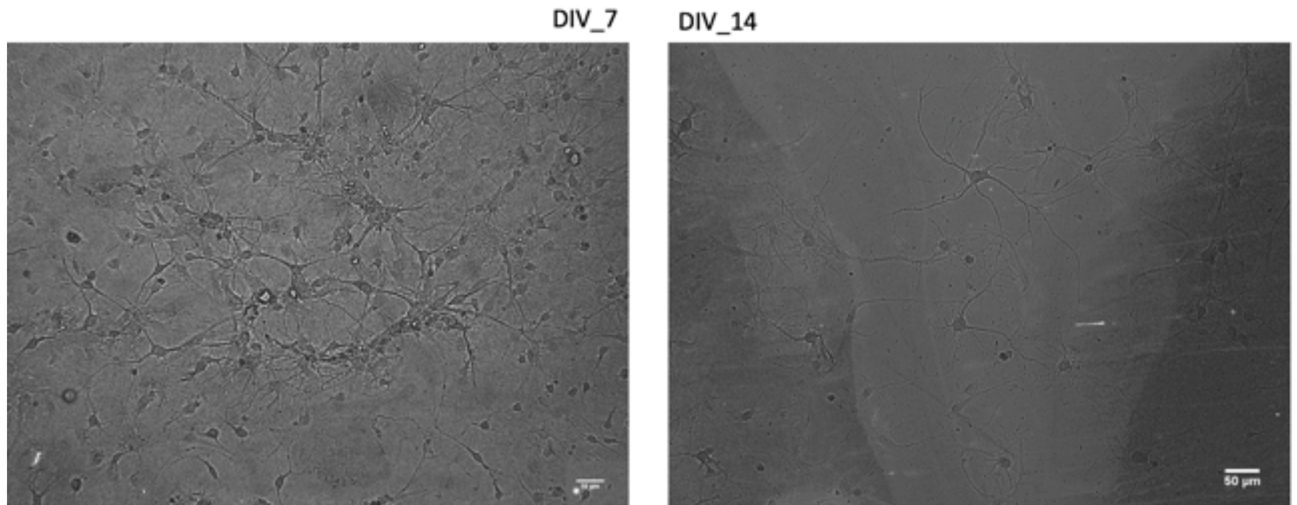

Figure 3.17. Comparison of dendrites development at 7 and 14 days in culture.

TiO_2 sample, group 3

This group has been sterilized and stored in dryer, moreover it has been exposed to UV radiation for 30 seconds. The neurons, reported in Figure 3.18, show the same characteristics of the other samples. Especially at DIV 14 neurons show large network and high branching, thus indicating that the substrate is highly biocompatible. Figure 3.19 showed a single neuron at DIV 14, neuronal networking is highly developed.

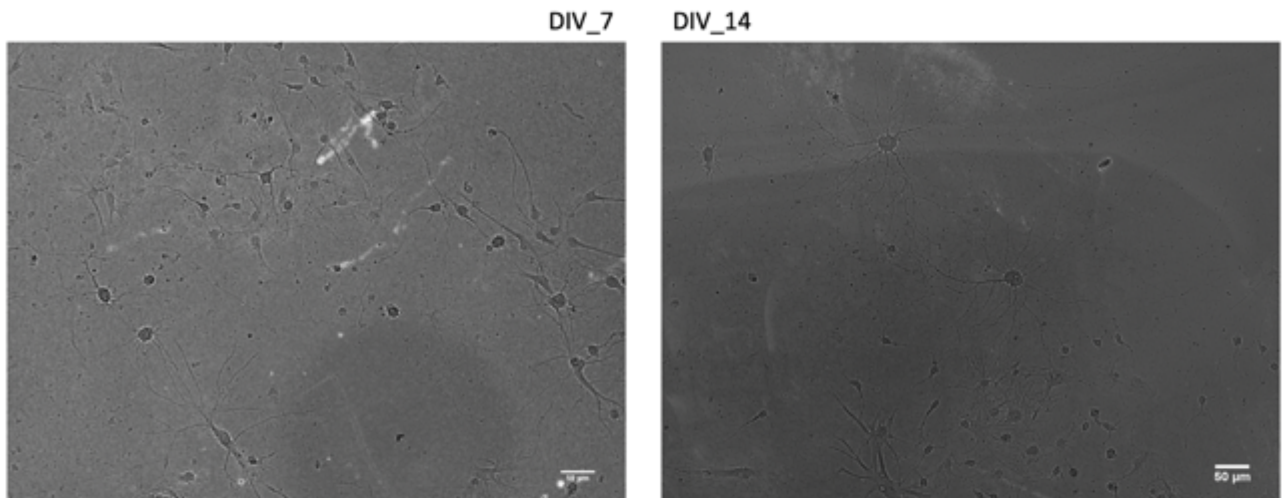

Figure 3.18. Neuronal development comparison at different day in vitro. At DIV 14 is visible a high neuronal network development.

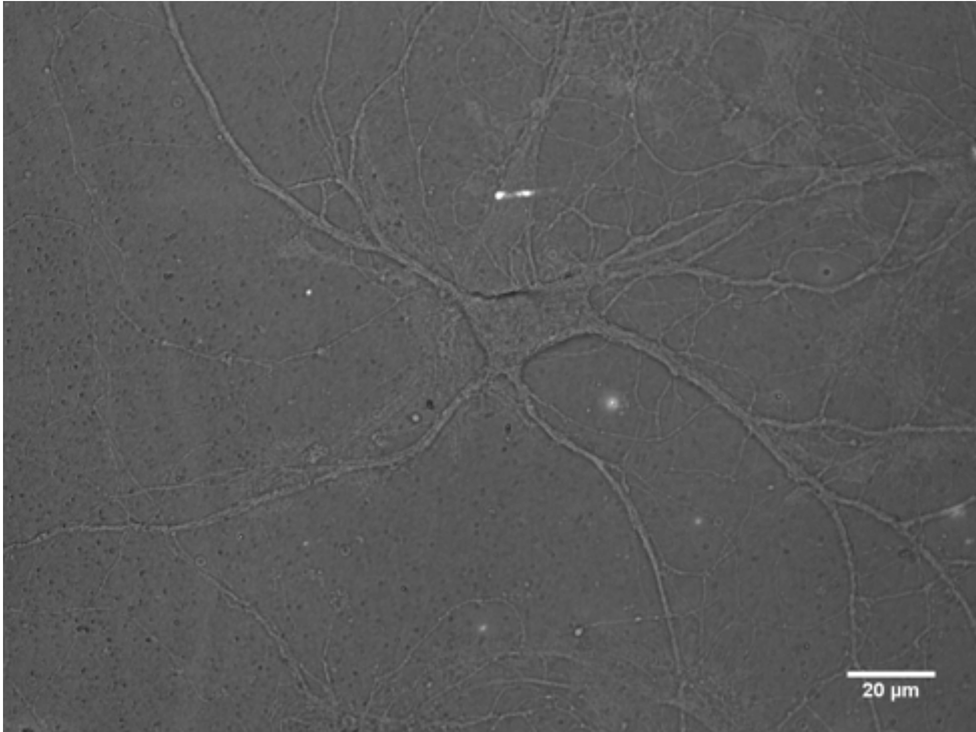

Figure 3.19. Single neuron with dendrites and axon on TiO_2 sample, group 3, DIV_14.

TiO_2 sample, group 4

Group 4 has undergone the same treatments of the others, but with UV exposition time of 60 seconds. Neurons are numerous and well developed after 7 as well as 14 days. At DIV 14 neuronal networking is highly developed, and the branching of the main filaments is very pronounced (Figure 3.20).

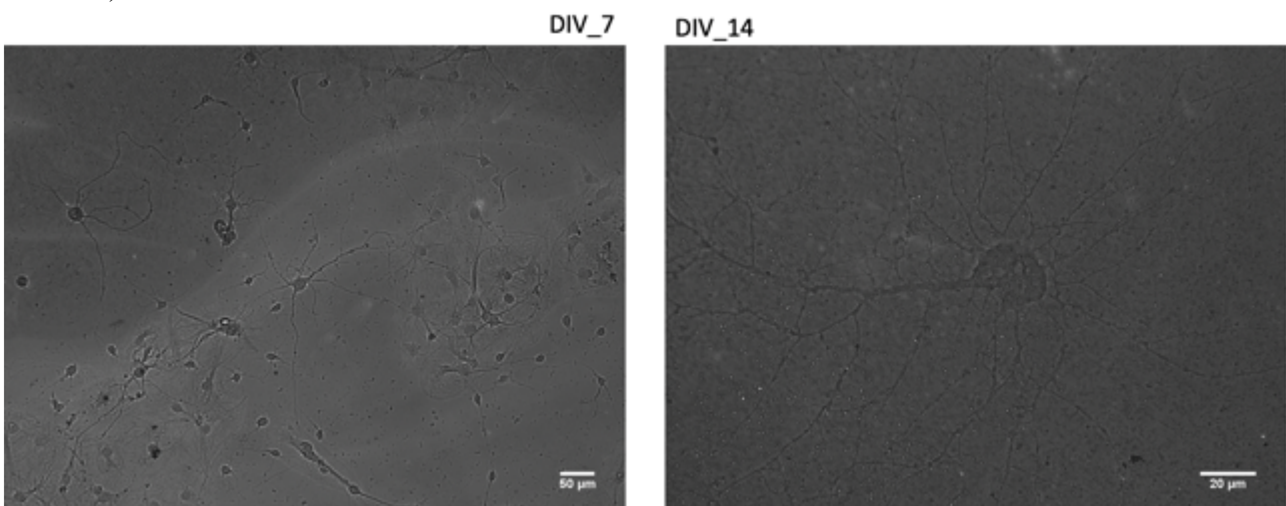

Figure 3.20. Neuronal development comparison at different day in vitro, on the left at day 7 and on the right at day 14 in cultivation.

TiO_2 sample, group 5

These samples were sterilized, stored in the dryer and exposed to UV rays for 180 seconds. At seven days a highly developed neuronal network is present. The magnification showed a single differentiated neuron (Figure 3.21).

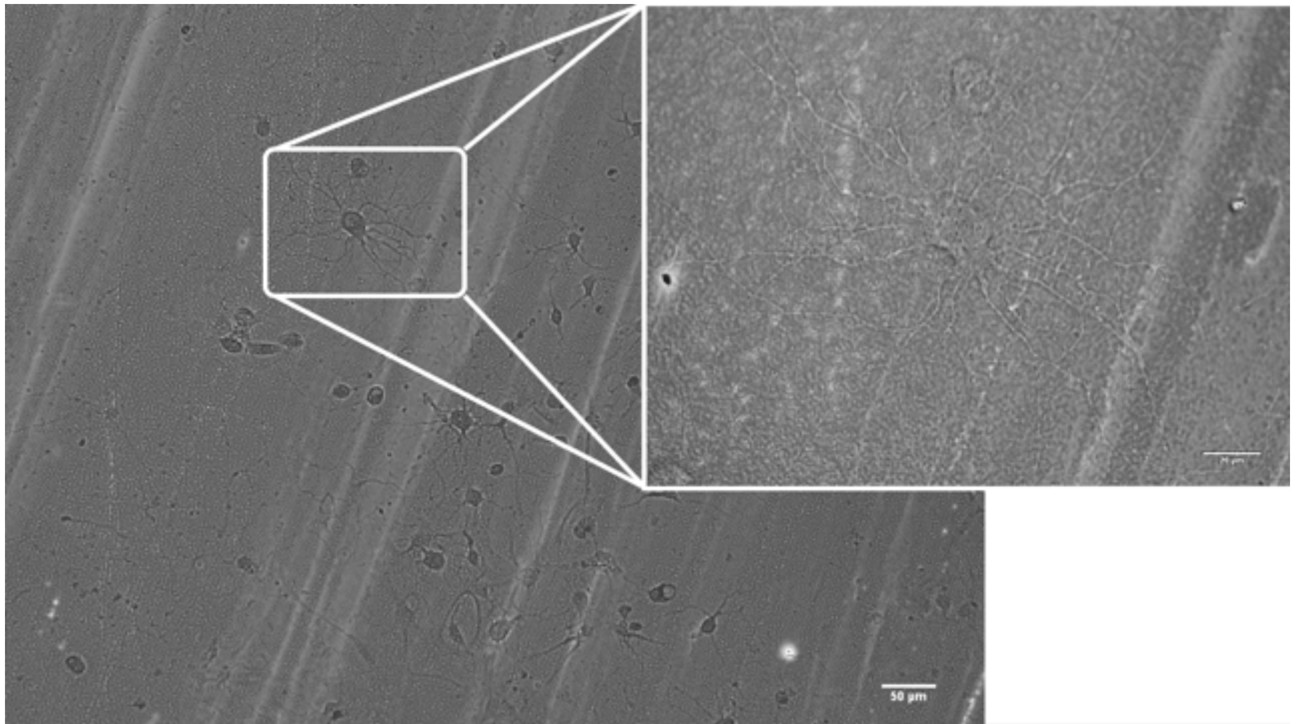

Figure 3.21. Neurons images taken after 7 days in vitro with different magnification

The images at DIV_14 wants to emphasize the presence of cellular adhesion on the whole surface, indeed there are neurons and glial cells up to the edge (Figure 3.22). It is possible to trace this behavior back to the fact that after 180 s UV exposition, the high hydrophilicity of the substrate allowed poly-L-Lysine to cover the all entire surface.

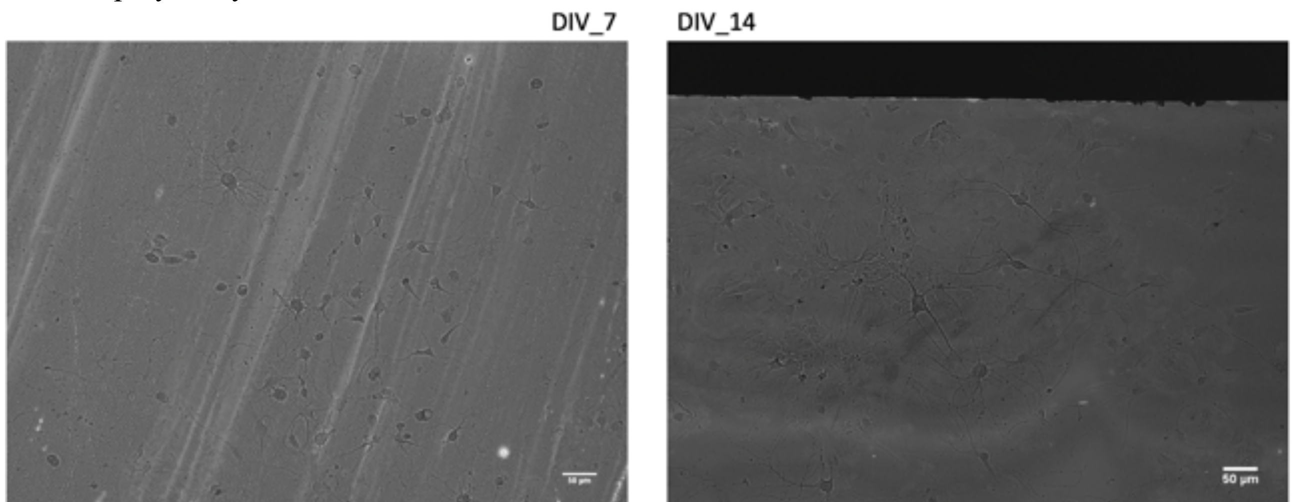

Figure 3.22. Neuronal development comparison at different day in vitro.

TiO_2 sample, group 6

Samples of group six have been exposed to UV radiation for 300 seconds. The comparison between seven and fourteen days in culture showed an increase in development of secondary filaments. The progression in neurons development leads to conclude that TiO_2 thin film is a biocompatible and not toxic material (Figure 3.23).

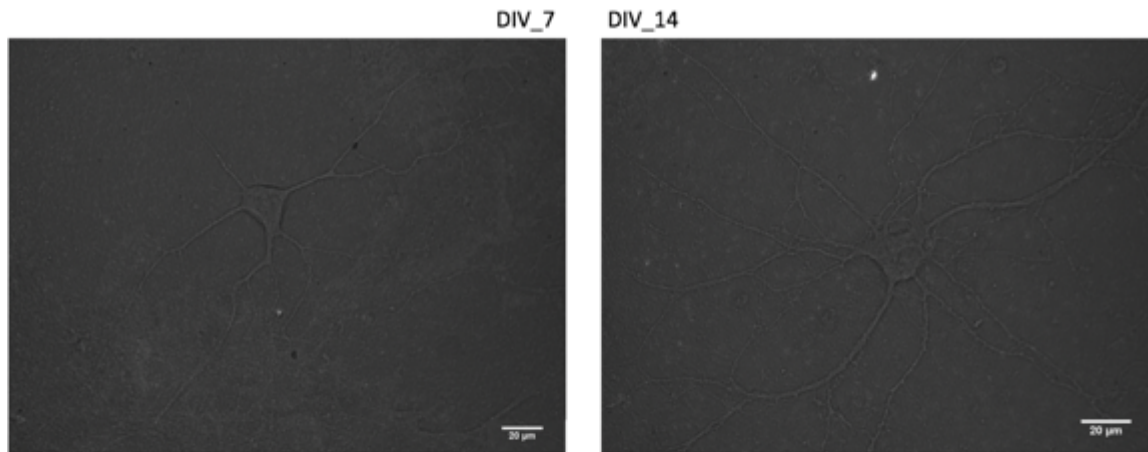

Figure 3.23. Comparison of neuron growth and development after 7 and 14 days in vitro.

3.2.3 SEM OF NEURONAL CELLS

SEM images were acquired to observe in detail neurons development and to investigate neuronal networks, especially examining particularly fine details such as dendrites and axons and the connections between neurons and glial cells.

SEM acquisition images of neuron samples were available after fixing with formaldehyde and dehydration in ethanol by the following procedure:

24h before SEM acquisition;

- Removal from culture medium;
- washing with PBS;
- fixing with formaldehyde 3.7% for 15-20 min;
- washing with PBS (three times)
- dehydration with ethanol at different step: 20%, 40%, 50%, 70%, 80%, 90%, 95% for three minutes each step.

Acquisition day: store the sample in ethanol 100%.

In Figure 3.24 SEM images of neuron culture grown on TiO_2 sample at DIV 15 are shown. Glial cells are in their typical structural organization as a carpet and some neurons are grown on the top. In Figure 3.23b a single neuron is taken. A very marked dendrites' development and a large network, in every direction on the surface, are formed. This particular dendrite organization suggests that it may be a stellate neuron.

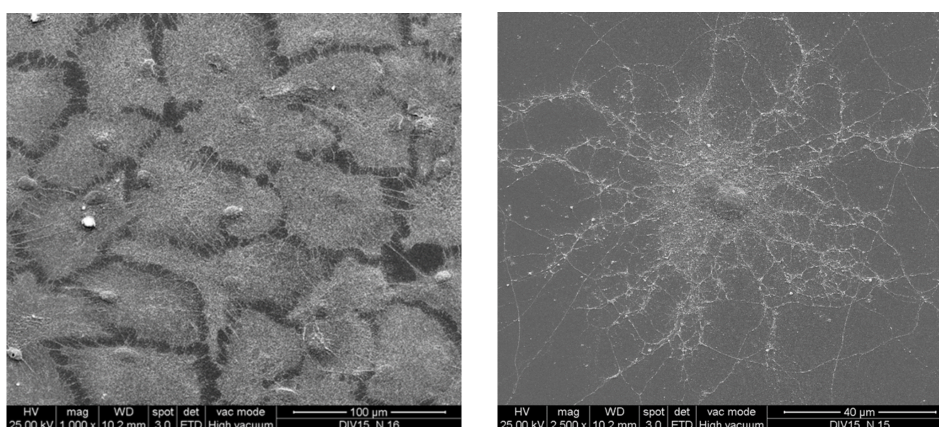

Figure 3.24. SEM images of neuronal culture on TiO_2 sample after Au metallization at DIV 15

3.2.4 TITANIA BEHAVIOR IN PHYSIOLOGICAL MEDIUM: XPS AND SEM INVESTIGATIONS

In order to study how the TiO_2 functionalized surface interacts when it is immersed in a physiological medium, here employed as an inorganic simulated body fluid (SBF), preliminary experiments were done by investigating the possible growth of phosphate related compounds on the sample surface after soaking in Krebs' solution. This solution is generally used to assess the response of the biomedical device during *in-vitro* neuronal tests.

Three TiO_2 thin films deposited via ALD on Si(100) were individually immersed in 15 mL of Krebs' solution (pH 7.4) and slightly shacked at 37 °C for three different incubation times of 1, 6 and 24 hours. Then they were maintained at room temperature in deionized water until the surface XPS characterization.

Krebs' solution composition:

- NaCl 119,99 mM
- KCl 1,99 mM
- $NaHCO_3$ 25.57 mM
- KH_2PO_4 1,17 mM
- $CaCl_2$ 2,00 mM
- $MgSO_4$ 1,20 mM
- Glucose 11.10 mM

XPS measurements were performed on as-grown TiO_2 and on the three TiO_2 samples maintained in the physiological solution for the different incubation times.

The extended spectra (Figure 3.25) suggest the presence of titanium and oxygen (and adventitious carbon, of course) in the bare sample (TiO_2 – green), while the precipitation of salts from the saline electrolyte medium in the soaked samples (TiO_2 1h, 6h, and 24h - black, red and blue, respectively) hide the substrate pristine element (titanium), but showing the presence of magnesium, calcium and phosphorous (Figure 3.24). No other foreign or unexpected elements are evident.

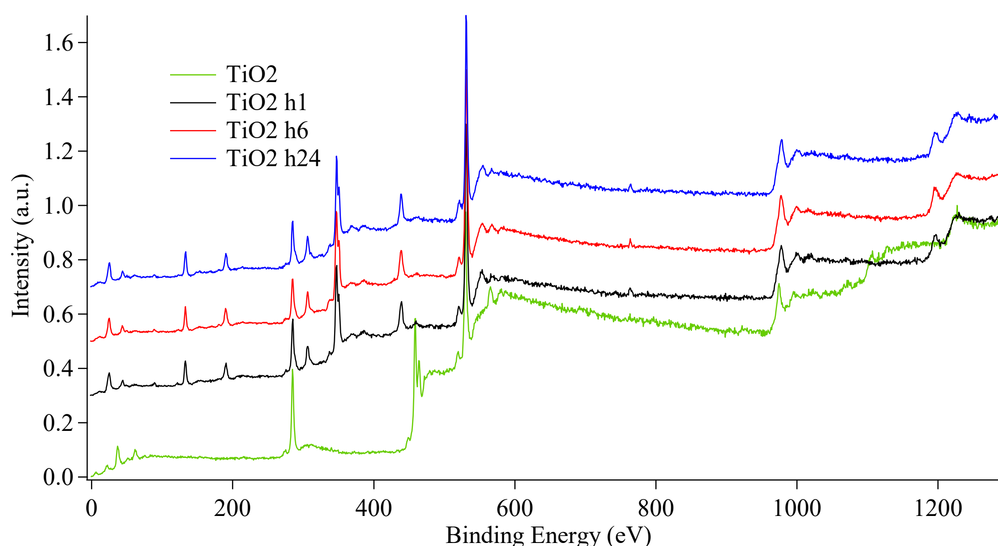

Figure 3.25. XPS measurement: extended spectra for the samples TiO_2 (green), TiO_2 1h (black), TiO_2 6h (red) and TiO_2 24h (blue). The spectra are shifted for a better comprehension.

The detailed spectra for Ti 2p, Ca 2p, Mg 2p, P 2p and O1s allow a deeper investigation of the element chemical state. Titanium $2p_{3/2}$ and $2p_{1/2}$ peaks are well evident only in the TiO_2 sample and the peak positions (see Table 3.3) well agree with Ti(IV) in TiO_2 (Figure 3.26). The analysis of the O 1s region (Figure 3.27) suggests the presence of oxygen as in TiO_2 oxide for the TiO_2 sample. The shoulder at higher BE (about 531.5 eV) also suggests the presence of hydroxyl surface groups.

In the samples TiO_2 1h, 6h and 24h, on the other hand, the main contribution for O 1s is centered at 531.3 eV. Considering the presence of calcium, magnesium and phosphorous, this peak position appears compatible with the presence of hydroxyls and phosphate-based compounds such as hydroxyapatite, calcium phosphate and calcium hydrogen-phosphate.

The Mg 2p region (Figure 3.28a) appears with a low S/N ratio, because the low amount of the element. The peak position suggests the presence of magnesium as Mg^{2+} in MgO. Calcium 2p XPS peak positions well agree with Ca^{2+} in calcium phosphates or hydroxyapatite (Figure 3.28b). The analysis of P 2p region (Figure 3.28c) confirms the hypothesis of phosphate-related compound presence: the peak position agrees with phosphorous as in phosphate environment.

The compositional analysis (Table 3.3) for TiO_2 sample indicates an oxygen over stoichiometry with respect to the theoretical value (67%). This is compatible with the presence of surface hydroxyl groups and molecularly adsorbed water. Concerning TiO_2 1h, 6h and 24h samples, the chemical analysis appears essentially constant, thus indicating that no surface composition evolution with the soaking time is present (but no comments are possible about the absolute amount of the phosphate-related compounds). The calculated Ca/P atomic ratio for the investigated samples is about 1.42, while the theoretical hydroxyapatite value is 1.67. This inconsistency is not surprising since the precipitated apatite is often non-stoichiometric with a phosphorus surplus. Furthermore, the presence of magnesium can also modify the precipitate nature [Moulder, J. F. et al. 1992; https://srdata.nist.gov/xps/].

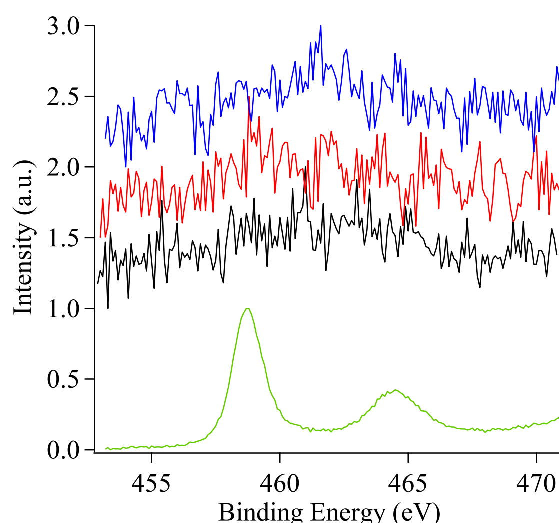

Figure 3.26. XPS measurement: detailed spectra for Ti 2p region for the samples TiO_2 (green), TiO_2 1h (black), TiO_2 6h (red) and TiO_2 24h (blue). The spectra are shifted for a better comprehension.

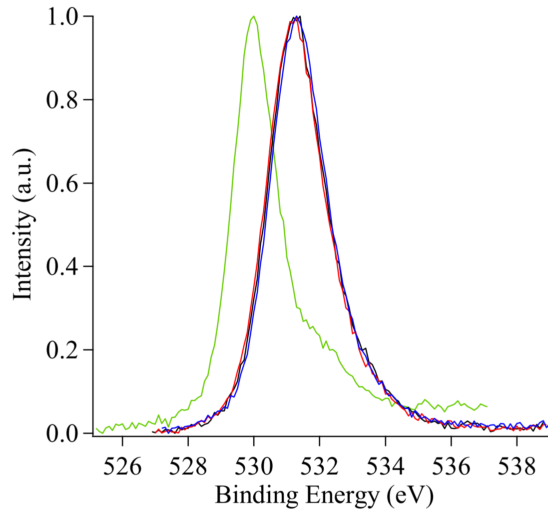

Figure 3.27. XPS measurement: detailed spectra for O 1s region for the samples TiO_2 (green), TiO_2 1h (black), TiO_2 6h (red) and TiO_2 24h (blue).

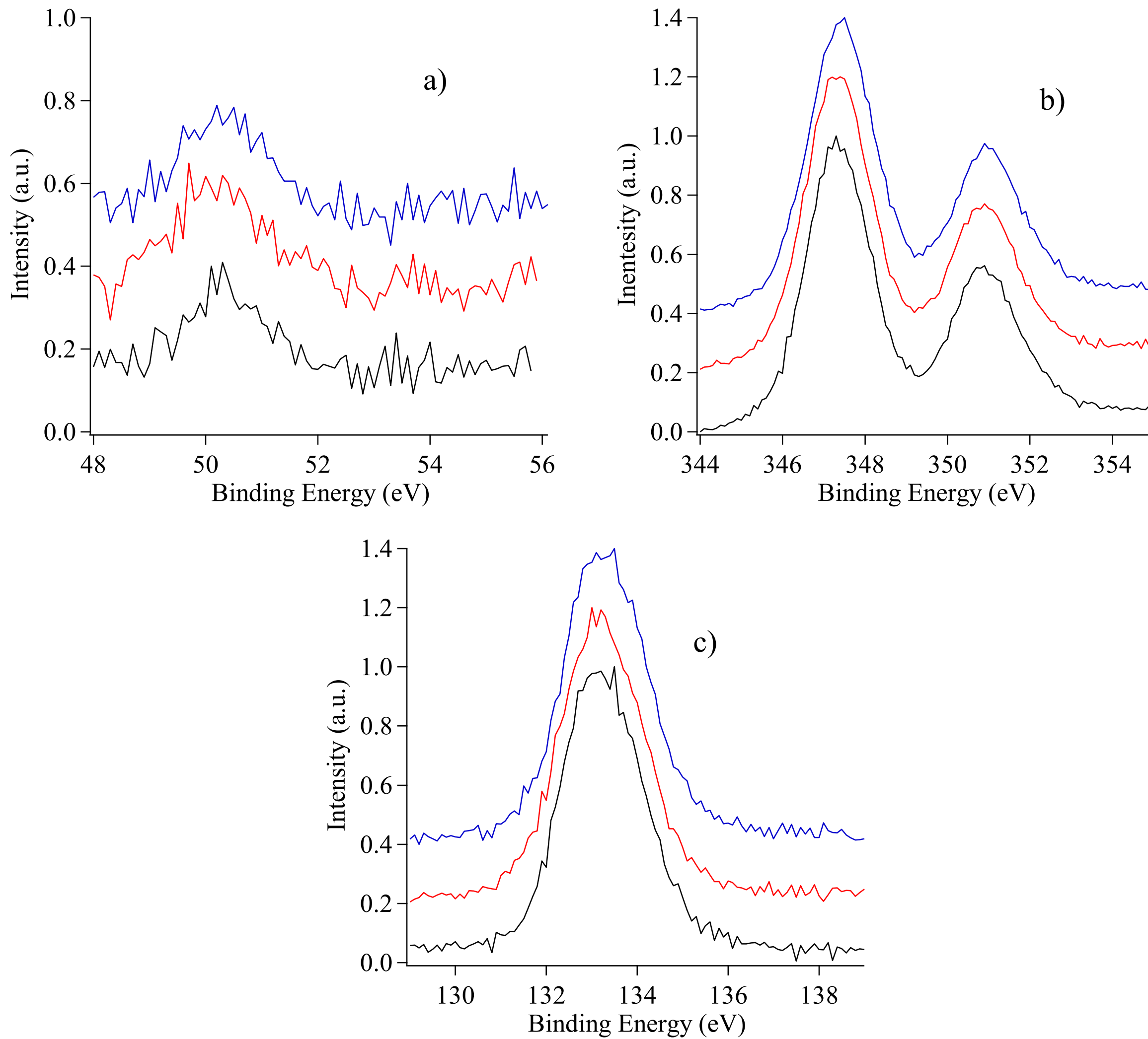

Figure 3.28. XPS measurement: detailed spectra for Mg 2p (3.27a), Ca 2p (3.27b) and P 2p (3.27c) regions for the samples TiO_2 1h (black), TiO_2 6h (red) and TiO_2 24h (blue).

Table 3.1. XPS peak position for TiO_2, TiO_2 1h, 6h and 24h. The atomic percentage are indicated in brackets. (ND = not determinable, NP = not present; the compositional data error is 1%).

Sample	O 1s	Ti $2p_{3/2}$	Ti $2p_{1/2}$	Ca $2p_{3/2}$	Ca $2p_{1/2}$	P $2p_{3/2}$	Mg 2p
TiO_2	530.0 (74)	458.8 (26)	464.4	NP	NP	NP	NP
TiO_2 1h	531.2 (68)	ND	ND	347.3 (17)	350.9	133.2 (12)	50.0 (3)
TiO_2 6h	531.3 (69)	ND	ND	347.3 (16)	350.9	133.3 (12)	50.2 (3)
TiO_2 24h	531.3 (68)	ND	ND	347.4 (17)	350.9	133.3 (12)	50.3 (3)

SEM investigation

Scanning electron microscopy observations were carried out for assessing the presence of phosphate-related compounds on the surface of the titania samples after immersion Krebs' solution, as found in XPS analyses. Figure 3.29 shows the scanning electron microscopy of as-deposited TiO_2 coated silicon surface and of TiO_2 coated silicon surface incubated in Krebs' solution at 37°C for 1 h, 6h, and 24 h. To compare the morphological features of all the different surfaces, the images are reported at the same magnification (25000x and 50000x).

It can be seen that, following immersion time in Krebs' solution, a newly formed layer of calcium phosphate-related compound was detected still only after 1 h of incubation. Analysing Figure 3.29 it is clearly evident the loss of the characteristic morphology of the as grown TiO_2 deposit (Figure 3.29a) and the progressive coverage of the TiO_2 surface, in relation to immersion time, with a thick enough layer of calcium phosphate related compounds. After 24 h immersion (TiO_2 24h, Figure 3.29d) TiO_2 surface was completely covered.

Even if still not sufficient, EDX analysis was used as a tool regarding compositional aspect. Indeed, Ca/Ti at% were assessed by EDX analyses, by mapping different areas, all at the same magnification (500x). It was observed an increase of the Ca/Ti at% ratio with time of immersion in Krebs' solution, and the highest value was detected for TiO_2 24h samples. The Ca/P at% ratio was approximately varied within the 1,0-1,5 range (suggesting possible formation of $Ca_3(PO_4)_2$, $Ca(HPO_4)$ and /or hydroxyapatite $Ca_{10}(PO_4)_6(OH)_2$ phases).

Other characterization techniques are now necessary, in order to better study the material characteristics and composition: XRD is undeniably an important primary characterization technique for identifying the precipitated crystallized phases, combined to FT-IR measurements to identify the different calcium phosphate related compounds.

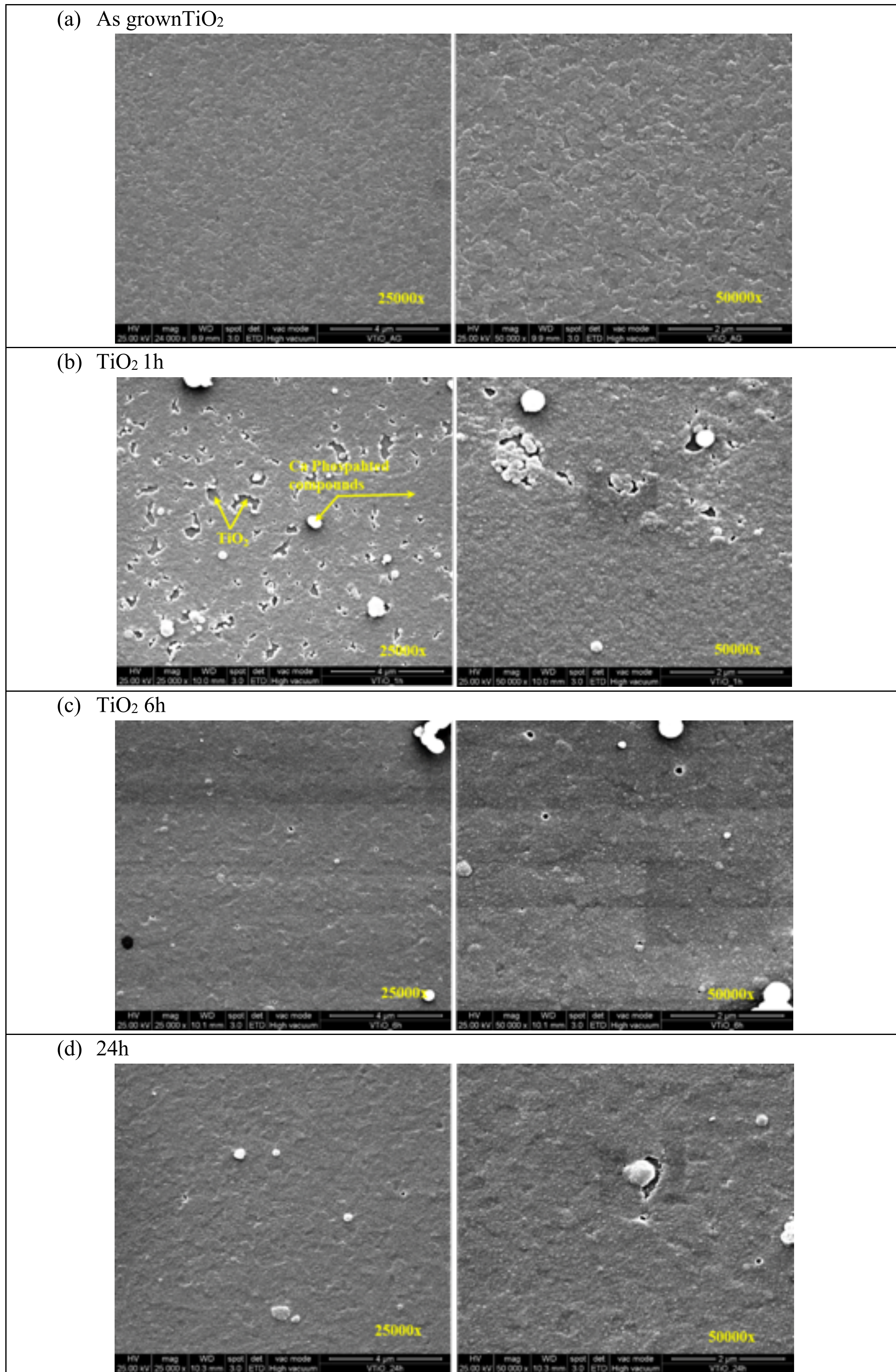

Figure 3.29: SEM surface morphologies (25000x) of the machined TiO_2 thin films deposited on Si(100) substrates: (a) as grown (TiO_2), after (b) 1h ($TiO_2$1h), (c) 6h (TiO_2 6h), and (d) 24 h (TiO_2 24h) immersion in Krebs' solution.

CONCLUSION

Regarding the innovation in nanoelectronics, Atomic Layer Deposition (ALD) is surely considered as one of the most promising growth techniques that could be employed to implement novel devices also for biomedical applications. The growth of the film with an atomic level thickness control and the possibility to obtain a dense pinhole-free and conformal material represents a notable advantage in the deposition of metal oxide.

In this thesis, the ALD TiO_2 film deposition has been optimized using a custom-made cross-flow reactor at low temperature (T= 280°C), starting from TTIP and deionized water on Si (100) substrate. Several experiments have been carried out in order to obtain optimal parameters of deposition, ensuring reproducibility, purity and physico-chemical characteristics. Biomedical neurochips based on electrolyte-oxide-semiconductor field-effect transistors (EOSFET) for recording and EOS-capacitor for stimulations of neuronal tissue, in fact, need well defined characteristics both from chemical and physical point of view. In particular, by varying deposition ALD parameters, dense, conformal, pinhole-free, and compositionally uniform thin films were deposited.

Polycrystalline TiO_2 films in anatase phase were grown, characterized by high purity along all the film thickness and without significant carbon contamination, indicating a clean precursor decomposition at the chosen growth temperature (280°C). Morphological investigations indicated a homogeneous surface morphology for all the samples, without cracks or pinhole. The optimization of process parameters, for our custom made reactor, were found and best GPC actually obtained is 0.15 nm/cycles. Preliminary experiments on precursor self-decomposition revealed the possible presence of a thin titania layer deriving from undesired CVD-like process, as already observed in literature data.

The second part of the research activity was dedicated to cellular/neuronal biocompatibility *in-vitro* tests on TiO_2 samples deposited via ALD. In this regard, the surface chemical functionality was studied by wettability analyses with the purpose to investigate the influence on cell attachment/adhesion and growth. Water contact angle (WCA) measurements were used to investigate surface wettability. Wettability studies demonstrated super-hydrophilic behavior of both freshly prepared and sterilized titania samples. However, their storing in air showed a decreasing wettability in relation to ageing-time, due to environmental organic pollutant contamination. In order to re-establish the hydrophilic/super-hydrophilic behavior of the deposited material, an UV treatment was applied allowing the complete restoring of surface wettability like that one of the freshly as-deposited samples.

Biocompatibility tests demonstrated that the material under study was highly biocompatible and non toxic, as confirmed by the progression in neurons development. Indeed, the monitoring of the neurons' progression after 7 and 14 days in culture revealed outcomes that are comparable to neurons seeded on standard Petri dishes. A clear influence of the wettability on neuronal cell developments was not found, however the more hydrophilic substrates have shown greater uniformity of cellular adhesion over all the sample surface. Moreover, preliminary experiments on the interaction between TiO_2 deposits and simulated physiological medium revealed the formation

of calcium phosphate-related compounds, as confirmed by XPS and SEM analyses, whose nature has to be deeply investigated.

Several aspects of this work need further study, especially some improvements in the ALD custom made apparatus could be the starting point for additional tests of deposition, in order to be able to precisely control the film thickness. Specifically, the installation of a Quartz Crystal Microbalance (QCM) is foreseen in the ALD reactor for the *in-situ* thickness study and control. Actually, a limit in our work was the accurate thickness control of the film, thus the upgrade with a QCM would allow us further optimization and understanding for an ideal ALD like-growth, with an in-real time feedback about the growing parameters effect. The use of diverse co-reactants such as H_2O_2 or O_3 and different metal precursors could be explored to study the variation in the physico-chemical material properties.

Regarding the biocompatibility aspects, more study is needed to find a relationship between the surface characteristics and neuronal cell vitality and response, in relation also to the employment of different high-k metal oxides.
Research activity has to be done in order to define the bioactivity effect of the TiO_2 deposits for the integration of the final biomedical device in human body. In particular, deep investigations regarding the response of the material, for example under acellular *in-vitro* experiments in different physiological medium (simulating human physiological fluids), will be surely of primary importance in order to investigate how the material can influence the neuronal cell development and its functional response.

Appendix A: Characterization methods

A.1 X-ray Diffraction (XRD)

X-rays are electromagnetic radiations with high energy and small wavelength. X Ray Diffraction (XRD) is a versatile technique to analyze material properties of mainly powders and solid samples. One its main application is the identification of crystalline phases in crystalline and semi-crystalline samples together with the determination of unit cell parameters.
This non-invasive technique is based on the phenomenon of diffraction; in particular, X-ray radiations interact with the atomic electrons that serve as scattering centers. If the atoms are ordered with a specific spatial arrangement (crystallites), an interference occurs among scattered rays, since the atomic distances are of the same order of magnitude of the X-ray wavelength.
In the beginning of the 20th century, W. H. Bragg, an English physicist, studied the diffraction phenomena. He noted that the wavelength of the incident radiation produced constructive interference only when the path difference of reflected rays is equal to an integer multiple of the incident ray wavelength, as show in Equation (A.1).

$$2d_{hkl} sin\theta = n\lambda \quad (eq.\ A.1)$$

In the Equation (A.1), d_{hkl} represents the inter-planar spacing between two adjacent planes; **θ** is the Bragg angle between the incident ray and the crystalline plane; **λ** stands for the radiation wavelength and n is the diffraction order number. Figure A.1 shows a schematic representation of Bragg conditions.
The result of diffraction is the *diffraction pattern* that, when collected with a mono-dimensional detector, reports in the majority of cases on Y axis the diffraction intensity and on X axis the 2θ angles; each diffraction pattern is thus characterized by different peaks, each one with its own intensity, position and width. The number and position of peaks depend on space groups, X-ray wavelength, crystal system of the material, lattice parameters, atomics species, and atomic positions, Reflection intensities, instead, are related to the atoms contained in the unit cell and their specific positions. Thanks to the Bragg's law, it is possible to calculate also the inter-planar distance d_{hkl}.
By means of XRD technique it is possible to carry out qualitative and quantitative analyses of the phases pure or present as mixture. Moreover, it possible to analyze the microstructure, such as preferential orientation, crystallite size, residual stresses etc.
Diffraction patterns are fingerprints of crystalline structures and so the comparison of the experimental spectrum with a calculated one (whose structure is known) allows the crystallographic identification of the analyzed sample. The most common databases archives are ASTM (American Society for Testing and Materials), ICDS (International Center for Diffraction Standards), JCPDS (Joint Committee on Powder Diffraction Standards), and ICDD (International Center for Diffraction Data).

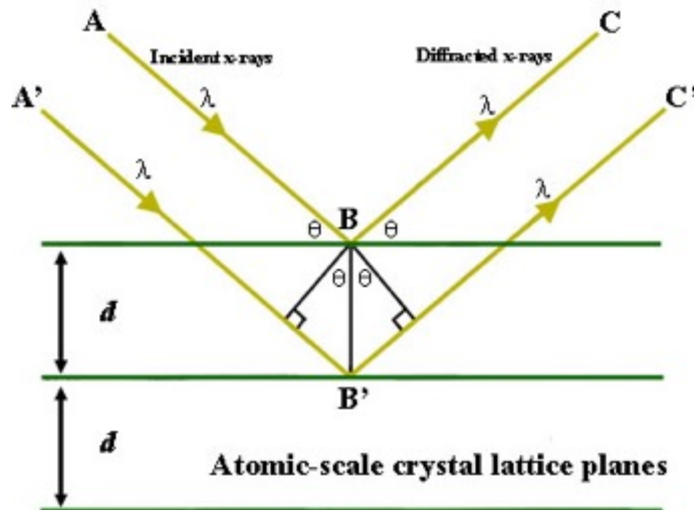

Figure A.1. Schematic representation of Bragg's law. The diffracted X-rays exhibit constructive interference when the distance between paths ABC and A'B'C' differs by an integer number of wavelengths (λ).

From the XRD pattern, it is possible to calculate the crystallites size, through the Scherrer's Equation (A.2)

$$D = \frac{k \cdot \lambda}{cos\theta \cdot \sqrt{FWMH^2 - B^2}} \qquad (eq. A.2)$$

where, k = coefficient addicted to the particles shape (dimensionless shape factor with a value close to unity);
λ = radiation X-Ray wavelength;
θ = Bragg's angle;
FWMH (Full Width at Half Maximum) = line broadening at half the maximum intensity (in radians);
B = instrumental line broadening (in radians).

In this work the XRD patterns were collected in grazing angle configuration, this is because thin film characterization using conventional Bragg Brentano setup (theta/2theta) generally produces weak signal from film and intense signal from substrate since wave penetration is considerable. Therefore, it is convenient to use grazing angle setup to minimize substrate contribution and contemporarily maximize reflections deriving from the thin film [Feldman L.C. et al 1986].
In this geometry, the incidence angle is fixed at a small angle and the angle between the incident and the detector is varied by moving only the detector arm. The signal originating from the substrate is significantly reduced.
Specifically, X-ray diffraction (XRD) spectra were acquired for qualitative structural characterization by using a Philips X'Pert PW 3710 powder diffractometer operating in grazing incidence mode (incidence angle = 1°). The used radiation was the Cu Kα (λ = 1.54056 Å) operating at 40 kV and 30 mA. All patterns were collected in the 15° ÷ 80° 2θ range and phase identification was performed with the support of the standard patterns reported in the 2002 ICDD database files.

A.2 Scanning Electron Microscopy (SEM)

Scanning Electron Microscopy (SEM) uses an electron beam to produce images of a sample through the scanning of the surface specimen. The electron beam interacts with the atoms of the specimen through elastic and inelastic interactions and produces various signals giving information about morphology, surface topography, microstrain and chemical composition. In general, elastic collisions generate backscattered electrons, that usually produce images showing contrast related to the different chemical composition of the specimen. The inelastic interactions produce, among different signals, secondary electrons. We focus on secondary electrons because they provide images with topographic contrast since they escape from a depth of few nanometers. The number of secondary electrons expelled depends on the chemical composition of the material, so different elements generate different amounts of secondary electrons. When a specimen is irradiated with a high-energy electron beam, interactions between the incident electrons (primary electrons) and the atoms in the specimen produce various signals (Figure A.2).

The electrons lose energy by repeated random scattering and absorption within a teardrop-shaped volume of the specimen. This is known as the *interaction volume*, which extends from less than 100 nm to approximately 5 μm into the surface. The size of the interaction volume depends on the electron energy, the atomic number of the specimen and the material density. The resulting interaction between the primary electrons and the surface or near-surface of the material at different levels of penetration results in the reflection of electrons with different energies, as well as electromagnetic radiation (mainly X-rays).

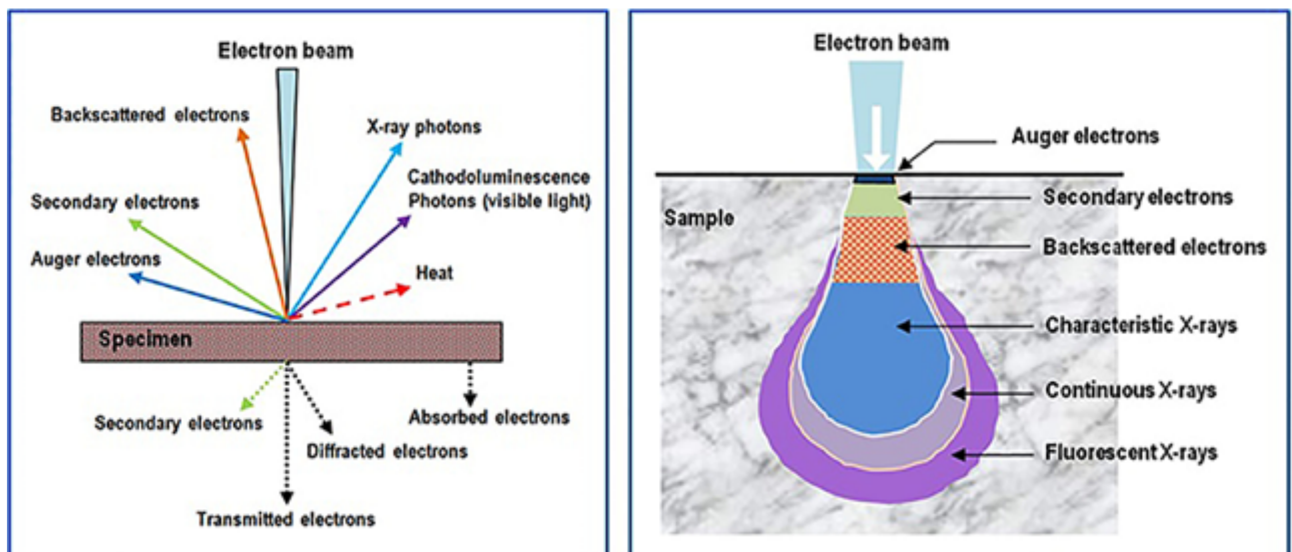

Figure A.2. On the left the results of the interaction between the incoming electron beam with the specimen is shown. On the right the interaction volume and the regions of the various signal that may be detected are represented.

SEM microscopy instrument is similar to the optics microscopy, it consists of:

- High vacuum system: used to eliminate possible interactions between electrons and air particles;
- Electron gun: generates electron beam thanks to thermoionic effect, usually composed by Tungsten filament (W) or crystal (LaB_6) cathodes, and Field Emission Guns (FEG);
- Optical system: made up by magnetic lens to focalize primary beam on the sample surface;

- Viewing screen: utilized to signal revelation and to collect images.

In this work, two different SEM instruments were used. Specifically, the surface morphology of titania coated silicon substrate was checked by using a FEIQuanta 200 FEG ESEM instrument, equipped with a field emission gun, operating in high vacuum conditions and at an accelerating voltage variable in the range of 20÷25 kV, depending on the observation needs. Before the analyses, the biological samples were coated with about 20 nm of an Au film deposited by Emitech K575X Turbo Sputter Coater.
Cross-section images to investigate the TiO_2 thin film thicknesses were examined by using a FE-SEM Zeiss Sigma VP, equipped with Everhart-Thornley, BSE and inlens detectors operating at an accelerating voltage of 20 kV.

A.3 Secondary Ions Mass Spectrometry (SIMS)

Secondary Ion Mass Spectrometry (SIMS) is a high sensitive elemental surface analysis technique able to detect elements concentrations up to the ppb level. A primary ion beam (e.g. Ar^+, Cs^+, Ga^+, N_2^+, O_2^+) with energy in the 0.1-20 keV range is sputtered onto the material surface at high vacuum. The ion beam permeates into the solid and generates elastic and inelastic collisions with the atoms. These collisions lead to a shift of the atoms from their reticular sites which, in turn, push other atoms, generating the so called *collision cascade* process. As a result, there is a certain probability for a surface atom to obtain enough energy to escape from the solid. This depends on the mass and energy of the primary ion beam, on both ionization energy and electron affinity of the surface atom and other instrumental parameters. In this way the solid is progressively eroded and a new surface is exposed. The ejected particles are composed by neutral species (atoms or molecule) or ions (secondary beam). A mass spectrometer detects the fraction of charged particles originated from the surface, separating the different ions on the basis of their m/z (mass to charge) ratio.
The chemical analysis of the upper monolayer makes SIMS specifically suitable for the investigation of thin films, with the detection of surface functionalities.
This technique is indispensable to the study of interface chemistry in a large variety of materials, both conducting and insulating, giving information about the diffusion of the chemical species by performing in-depth concentration profiles.
It can work in two different settings:

- Static: for surface analysis of the upper monolayer; low erosion rate, low current intensity, the sample is preserved;
- Dynamic: for in-depth concentration profiles; high erosion rate, high current intensity, the sample is damaged.

This technique is usually utilized to measure the in-depth profile for analyzing thin films features such as thickness, elements distribution, contaminants presence and inter-diffusion across the layer(s). As an example, in Figure A.3TiO_2 thin film deposited on silicon wafer (Sample 15 described in chapter 2) SIMS yield vs. depth profile is shown, where the trend of each ion species counts is displayed as a function of the erosion length. In the middle region of the graph in Figure A.3 the profiles of all the different ions are crossing each other: this region corresponds to the interface between the film and the substrate, so it allows the estimation of the film thickness and the relative inter-diffusion film-to substrate.

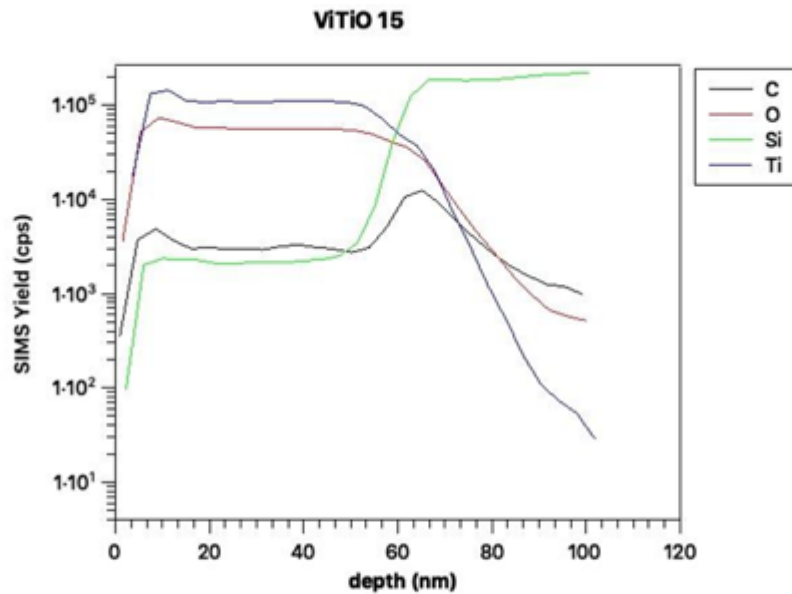

Figure A.3. SIMS profile of TiO_2 thin film on Si substrate showing the in-depth profiles of the different ions corresponding to the chemical elements present on the film.

In this work, secondary ion mass spectrometry depth profiles were obtained by an IMS 4f (Cameca) mass spectrometer working in UHV conditions by using a Cs^+ primary beam (10 kV, 20 nA) and negative secondary ion detection. Compensating charge phenomena were done by means of an electron gun. Measurements were performed rastering over a 150 × 150 μm^2 area, acquiring the signal from subarea 7x7 μm^2 to avoid crater walls interferences. Beam blanking mode and high mass resolution configuration were adopted to improve in-depth resolution and avoid possible mass interference artifacts (see Table A.1). Erosion rate was estimated by measuring the erosion depth at the end of each analysis by using a Tencor Alpha Step profilometer.

Table A.1: SIMS experimental conditions used for the TiO_2 thin films in-depth profile analyses.

Primary beam	Cs^+
Energy	10 kV
Sample potential	-4500 kV
Final impact energy	14,5 eV
Primary current	20 nA
Raster	150x150 μm^2
Secondary ions revealed	C^-, O^-, Ti^-, Si^-, TiO^-
Charge compensation	Electron gun
Acquisition mode	Beam Blanking

A.4 X-RAY PHOTOELECTRON SPECTROSCOPY (XPS)

X-ray Photoelectron Spectroscopy (XPS) is a technique used to investigate the chemical composition of solid surfaces, giving information of atoms chemical surround. It is based on the photoelectric effect that consist of an emission of surface electrons, when the material is hit by a photon beam. Figure A.4 shows a scheme of the interaction between the light beam (*hv*) and the material, where the photon is absorbed, and an electron is ejected

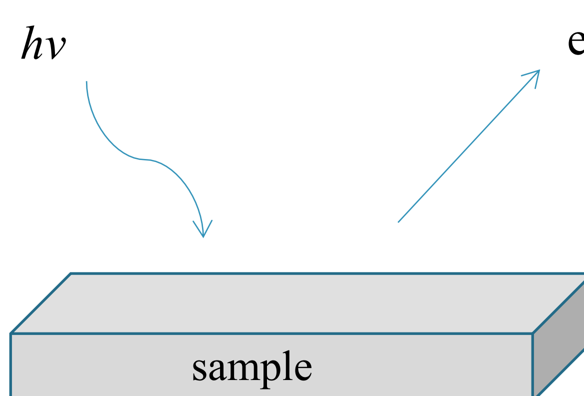

Figure A.4. Schematic representation of photoemission process

If the beam energy is high enough to expel electrons (photoemission process) they can be collected, and an electric current is measured. The kinetic energy of the photoelectron (E_k) is related to the electron binding energy (E_b) and the frequency of the photon (ν) by the Einstein relation, equation A.3:

$$E_K = hv - E_b - W \qquad (eq.\ A.3)$$

where W is the work function and describe the energy needed to remove an electron from a material Fermi level to the vacuum, hv is the energy of X-ray photon.
In the case of XPS the incident radiation is in the X-ray region (≈10^3 eV) of the electromagnetic spectrum, so it can be free electrons from the inner shells. The bond energies of these core electrons are specific for each core orbital and for each element. This fundamental assertion allows to correlate each XPS signal to a specific element. If no collateral impact occurs, core-level electrons escape from the sample, with an E_k value related to E_B by the Einstein equation.
The observed binding energies also depend on the chemical environment and on the oxidation state leading to small shifts of an element peak position, the chemical shifts.
Interestingly, the photoionization process, produces holes in the core levels, which can decay by the recombination with electrons coming from the outer energy levels (hole-electron recombination) and the excess energy release activates two competitive process:

- Auger emission, a non-radiative decay where an outer-shell electron is photoemitted. Its energy depends on both the element and valence state of the involved level, but it is independent of the nature and the energy of the source;
- X-ray fluorescence, a radiative decay where the excess energy is released as photons.

In this thesis, X-ray Photoelectron Spectroscopy (XPS) investigations were carried out with a Perkin Elmer Φ 5600 ci Multi Technique System using a standard Al anode working at 250 W. Extended spectra (survey: 187.85 eV pass energy, 0.5 eV/step, 0.05 s/step) and detailed spectra (for Ti 2p, Ca 2p, Mg 2p, P 2p, O 1s, C 1s, 23.5 eV pass energy, 0.1 eV/ step, 0.1 s/step) were collected. The standard deviation in the BE values of the XPS line is 0.10 eV. The atomic percentage, after a Shirley-type background subtraction [Shirley D. A. 1972] was evaluated by using the PHI sensitivity factors [Moulder J. F. et al. 1992]. The peak positions were corrected for the charging effects by considering the C 1 s peak at 285.0 eV and evaluating the BE differences.

A.5 WATER CONTACT ANGLE (WCA)

Static water contact angle (θ) measurements are used to determine the surface wettability of a solid by a liquid. It is defined as the angle formed by a drop of water on a flat, horizontal solid surface, at the boundary where the liquid, gas, and solid intersect. Hydrophobic and hydrophilic surfaces can be defined using θ values: high angles indicate poor wetting; low values indicate good wetting. In general, for $\theta < 90°$ the surface can be considered hydrophilic, while for $\theta > 90°$ the surface is hydrophobic. Ideal hydrophilic surfaces exhibit a contact angle close to 0°, whereas for ideal super-hydrophobic surface the angle is > 150°.
The system for the static contact angle determination is formed by a horizontal sample stage, a motor driven syringe to drop the liquid and a camera. This method is based on the analysis of the drop shape after few seconds (10-20 s) from its deposition on the sample. Once the liquid is dropped on the surface, the image captured by the camera is analyzed by a software which evaluates the angle formed between the solid/liquid interface line and liquid/vapor interface line. This technique requires low expensive equipment and information about surface properties may be easily obtained: by applying Young's equation (A.4) it is possible to relate the liquid/solid-, liquid/vapor- and solid/vapor-surface tension (γ_{ls}, γ_{lv}, γ_{sv}) to θ, (Figure A.5) [Kwok D. Y. et al. 1998]

$$\gamma_{lv} cos\theta = \gamma_{sv} - \gamma_{ls} \quad (eq. A.4)$$

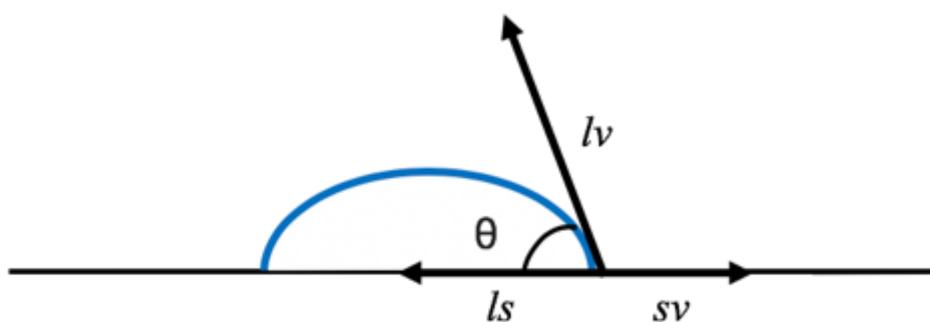

Figure A.5. Schematic representation of the three tensions formed from three states interface: solid, liquid and vapor.

However, this goes beyond the investigation scope of this thesis, which is to monitor the samples surface wettability over ageing-time.

In this work, water contact angles were measured to determine the wettability of ALD TiO_2 coated Si(100) substrates as function of ageing-time (by conserving all the samples in a dryer under constant conditions at RH= 43% ± 5%).
A custom-made apparatus was used with deionized water as liquid. All measurements were done in ambient conditions (T = 20-25°C). The drop deposited on the sample surface by the syringe was of 4 μL and the equilibrium WCA was measured after 10 seconds from water drop deposition. A CCD camera was used to observe the deposited drop. The reported values are the average of three determinations. The image was analyzed with the ImageJ software (plugin LB-ADSA, Low Boundary Asymmetric Drop Shape Analysis) (Figure A.6).

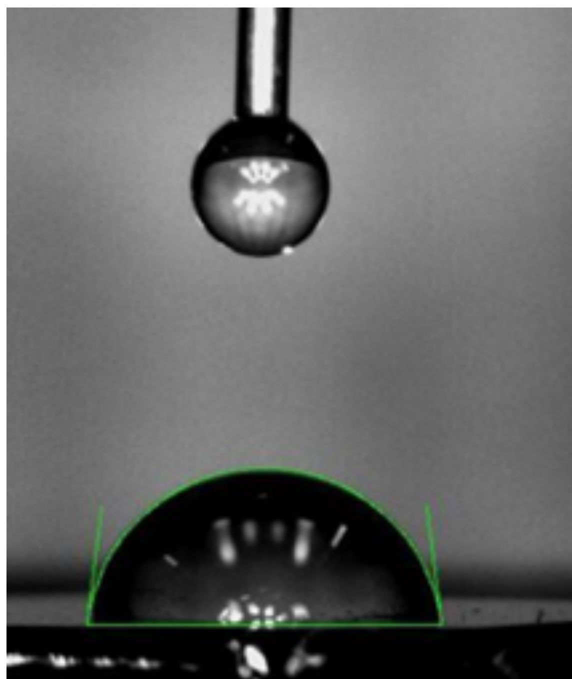

Figure A.6. Screenshot of a LB-ADSA contact angle analysis

BIBLIOGRAPHY

Aarik J., Aidla A., Uustare T, Kukli K., Sammelselg V., Ritala M., and Leskelä M., **2002**. 'Atomic Layer Deposition of TiO_2 Thin Films from TiI_4 and H_2O', *Appl. Surf. Sci.* 193(1): 277–286. https://doi.org/10.1016/S0169-4332(02)00497-X.

Asthana A., Shokuhfar T., Gao Q., Heiden P. A., Friedrich C., and Yassar R. S., **2010**. 'A Real Time Observation of Phase Transition of Anatase TiO_2 Nanotubes into Rutile Particles by in Situ Joule Heating Inside Transmission Electron Microscope'. *Microscopy and Microanalysis* 16(S2): 1360–1361. https://doi.org/10.1017/S1431927610061799.

Bauer S., Shmuki K., Von der Mark K., Park, J., **2013** 'Engineering biocompatible implant surface Part 1: Materials and Surfaces'. *Prog. Mater. Sci.* 58: 261-326. https://doi.org/10.1016/j.pmatsci.2012.09.001

Beckel D., Bieberle-Hütter A., Harvey A., Infortuna A., Muecke U. P., Prestat M., Rupp J. L. M., and Gauckler L. J., **2007**. 'Thin Films for Micro Solid Oxide Fuel Cells'. *J. of Power Sources* 173(1): 325–45. https://doi.org/10.1016/j.jpowsour.2007.04.070.

Bohr M. T., Chau R. S., Ghani T., and Mistry K., **2007**. 'The High-k Solution'. *IEEE Spectrum* 44 (10): 29–35. https://doi.org/10.1109/MSPEC.2007.4337663.

Braun J. H., Baidins A., and Marganski R. E., **1992**. 'TiO_2 Pigment Technology: A Review'. *Prog.in Org. Coat.* 20(2): 105–38. https://doi.org/10.1016/0033-0655(92)80001-D.

Choy K. L., **2003**. 'Chemical Vapor Deposition of Coatings'. *Prog. Mater. Sci.* 48(2): 57–170. https://doi.org/10.1016/S0079-6425(01)00009-3.

Chen T., Cameron T. M., Nguyen S. D., Stauf G. T., Peters D. W., Maylott L., Li W., Xu C., Roeder J. F., Hendrix B. C., Hilgarth M., Niinisto J., Kukli K., Ritala M., and Leskelä M., **2008**. 'Novel Zirconium Precursors for Atomic Layer Deposition of ZrO_2 Films'. *ECS Transactions* 16(4): 87–101. https://doi.org/10.1149/1.2979984.

Chen X., and Mao S. S., **2007**. 'Titanium Dioxide Nanomaterials: Synthesis, Properties, Modifications, and Applications'. *Chem. Rev.*, 107(7): 2892-2959. https://doi.org/10.1021/cr0500535

Chen Y. F., Gong J. Tung W. J., Chou S. W., and Jeng E. S., **2009.** 'Characteristics of N-Channel MOSFETs With Tailored Source/Drain Extension for Mask ROM and EEPROM Applications'. *IEEE Transactions on Electron Devices* 56(9): 2099-2106. https://doi.org/10.1109/TED.2009.2026521.

Cianci E., Lattanzio S., Seguini G., Vassanelli S., Fanciulli M., **2012**, 'Atomic Layer Deposited TiO_2 for implantable brain-chip interfacing devices'. *Thin Solid Films*. *520*, 4745 – 4748.

Coll A., Bermejo S., Hernández D., and Castañer L., **2018**. ‘Al_2O_3/TiO_2 Inverse Opals from Electrosprayed Self-Assembled Templates’. *Beilstein J. Nanotech.* 9(1): 216–223. https://doi.org/10.3762/bjnano.9.23.

Delft, J. A., Garcia-Alonso D., and Kessels W. M. M., **2012**. ‘Atomic Layer Deposition for Photovoltaics: Applications and Prospects for Solar Cell Manufacturing’. *Semicond. Sci. Technol.* 27(7): 074002. https://doi.org/10.1088/0268-1242/27/7/074002.

Diaz B., Harkonen E. Swiatowska J., Maurice V., Seyeux A., Marcus P., and Ritala M., **2011**. ‘Low-temperature atomic layer deposition of Al_2O_3 thin coatings for corrosion protection of steel: Surface and electrochemical analysis’. *Corr. Sci.* 53(6): 2168-2175. https://doi.org/10.1016/j.corsci.2011.02.036

Dotti C. G., Sullivan C. A., and Banker G. A., **1988**. ‘The establishment of polarity by hippocampal neurons in culture’, *J. Neurosci.* 8(4), 1454-1468.

Du, Y., George S. M., **2007**. ‘Molecular Layer Deposition of Nylon 66 Films Examined Using in Situ FTIR Spectroscopy’. *J. Phys Chem. C* 111 (24): 8509–8517. https://doi.org/10.1021/jp067041n.

El Habra N., Visentin F., Gerbasi R., Favaro M., Natile M., Colazzo L., Sambi M., **2015.** ‘Co_3O_4/TiO_2 heterostrucutres obtained by hybrid method’. *Phys. Status Solidi A*, 212(7): 1588-1598. https://doi.org/10.1002/pssa.201532260.

Faraz T., Roozeboom F., Knoops H. C. M., and Kessels W. M. M., **2015**. ‘Atomic Layer Etching: What Can We Learn from Atomic Layer Deposition?’. *ECS J. Solid State Sci. Technol.* 4(6): N5023–32. https://doi.org/10.1149/2.0051506jss.

Faucheux N., Schweissb R., Utzowa K. L., Wernerb C., Groth T.. **2004**. ‘Self-assembled monolayers with different terminating groups asmodel substrates for cell adhesion studies’. *Biomaterial* 25: 2721-2730. https://doi.org/10.1016/j.biomaterials.2003.09.069.

Feldman L. C., Mayer J. W., **1986**. ‘Fundamentals of Surface Thin Film Analysis’. *Elsevier Science*, New York, USA.

Fictorie C. P., Evans J. F., Gladfelter W. L., **1994**. ‘Kinetic and mechanistic study of the chemical vapor deposititon of titanium diocide thin films using tetrakis-(ispropoxo)-titanium (IV)’. *J. Vac. Sci. Tech*. (12): 1108. https://doi.org/10.1116/1.579173.

Finch D. S., Oreskovic T., Ramadurai K., Herrmann C. F., George S. M., and Mahajan R. L., **2008**. ‘Biocompatibility of Atomic Layer-Deposited Alumina Thin Films’. *J. Biomed. Mater. Res. Part A* 87A(1): 100–106. https://doi.org/10.1002/jbm.a.31732.

Fujishima A., Rao T. N., Tryk D. A., **2000** ‘Titanium dioxide photocatalysis’, J. *Photochem. Photobiol. C Photochem. Rev.* 1: 1–21. doi:10.1016/S1389-5567(00)00002-2.

George, S. M. **2010**. ‘Atomic Layer Deposition: An Overview’. *Chem. Rev.* 110(1): 111–131. https://doi.org/10.1021/cr900056b.

George S. M., Dameron A. A., Adamczyk N. M., and Yoon B., **2011**. ‘*Molecular Layer Deposition Process for* Making *Organic Or Organic -Inorganic Polymers'*, 2011. Patent US10092927B2

George S. M., Yoon B., and Dameron A. A., **2009**. ‘Surface Chemistry for Molecular Layer Deposition of Organic and Hybrid Organic−Inorganic Polymers’. *Acc. Chem. Res.* 42(4): 498–508. https://doi.org/10.1021/ar800105q.

Graniel O., Weber M., Balme S., Miele P., Bechelany M., **2018**, ‘Atomic layer deposition for biosensing applications’, *Bionsens Bioelect.* 122: 147-159. https://doi.org/10.1016/j.bios.2018.09.038.

Granneman E., Fischer P., Pierreux D., Terhorst H., Zagwijn P., **2007**. ‘Batch ALD: characteristics, comparison with single wafer ald, and examples’. *Surface coatings technology*. 201 22-23 8899-8907. https://doi.org/10.1016/j.surfcoat.2007.05.009.

Hakan N., **1996**. ‘Initial reactions of whole blood with hydrophilic and hydrophobic titanium surfaces’ *Colloids and Surfaces B: Biointerfaces* 6(4): 329-333. https://doi.org/10.1016/0927-7765(96)01270-2.

Hatanpää T., Ritala M., and Leskelä M., **2013**. ‘Precursors as Enablers of ALD Technology: Contributions from University of Helsinki’. *Coord. Chem. Rev.*, 257 (23): 3297–3322. https://doi.org/10.1016/j.ccr.2013.07.002.

Haukka S., Lakomaa E. L. and Root A., **1993**. ‘An IR and NMR Study of the Chemisorption of Titanium Tetrachloride on Silica’. *J. Phys. Chem.* 97(19): 5085–5094. https://doi.org/10.1021/j100121a040.

Ho Lee J., Khang G., Lee J. W. Lee H. B., **1998**. ‘Interaction of Different Types of Cells on Polymer Surface with Wettability Gradient’. *J. Colloid Interface Sci.* 205(2): 323-330. https://doi.org/10.1006/jcis.1998.5688.

Hoivik N. D., Elam J. W., Linderman R. J., Bright V. M., George S. M., and Lee Y. C., **2003**. ‘Atomic Layer Deposited Protective Coatings for Micro-Electromechanical Systems’. *Sensors and Actuators A: Physical*, Micromechanics section of Sensors and Actuators, based on contributions revised from the Technical Digest of the 15th IEEE International conference on Micro Electro mechanical Systems (MEMS 2002), 103(1): 100–108. https://doi.org/10.1016/S0924-4247(02)00319-9.

https://srdata.nist.gov/xps/

Jones A. C., and Hitchman M. L., **2008**. *Chemical Vapour Deposition: Precursors, Processes and Applications*. Royal Society of Chemistry.

Kautzky. M. C., Demtchouk A. V., Chen Y., Brown K. M., McKinlay S. E., Xue J., **2008**. 'Atomic Layer Deposition Al_2O_3 Films for Permanent Magnet Isolation in TMR Read Heads'. *IEEE Transaction on Magnetics* 44(11): 3576-3579. https://doi.org/10.1109/TMAG.2008.2001795.

Kim Y. S., and Yun S. J., **2005**. 'Nanolaminated Al_2O_3–TiO_2 Thin Films Grown by Atomic Layer Deposition'. *J. Cryst. Growth* 274(3): 585–593. https://doi.org/10.1016/j.jcrysgro.2004.10.007.

Kern W., **1990**. 'The Evolution of Silicon Wafer Cleaning Technology'.*J. Electrochem. Soc.* 137 (6): 1887-1892. doi: 10.1149/1.2086825.

Knez M., Kadri A., Wege C., Gösele U., Jeske H., and Nielsch K., **2006**. 'Atomic Layer Deposition on Biological Macromolecules: Metal Oxide Coating of Tobacco Mosaic Virus and Ferritin'. *Nano Letters* 6(6): 1172–1177. https://doi.org/10.1021/nl060413j.

Knoops, H. C. M., Potts, S. E., Bol, A. A., and Kessels, W. M. M., **2015**. 'Atomic Layer Deposition. Handbook of Crystal Growth'. doi:10.1016/b978-0-444-63304-0.00027-5

Kwok, D. Y., Lam C. N. C., Li A., Leung A., Wu R., Mok E., and Neumann A. W., **1998**. 'Measuring and Interpreting Contact Angles: A Complex Issue'. *Colloids and Surfaces A: Physicochemical and Engineering Aspects* 142(2): 219–35. https://doi.org/10.1016/S0927-7757(98)00354-9.

Leskelä M., Ritala M.. **2003**. 'Atomic layer deposition chemistry: recent developments and future challenges'. *Angew. Chem. In. Ed. Engl*. 42(45): 5548-5554. https://doi.org/10.1002/anie.200301652

Lim G. T., and Do-Heyoung Kim. **2006**. 'Characteristics of TiOx Films Prepared by Chemical Vapor Deposition Using Tetrakis-Dimethyl-Amido-Titanium and Water'. *Thin Solid Films*, 498(1): 254–58. https://doi.org/10.1016/j.tsf.2005.07.121.

Lim, J.S., Kim Y.K., Choi S.J., Lee J.H., Kim Y.S., Lee B.T., Park H.S., Park Y.W., and Lee S.I., **1999**. 'Novel Al_2O_3 Capacitor for High Density DRAMs'. In *ICVC '99. 6th International Conference on VLSI and CAD (Cat. No.99EX361)*, 506–9.

Lin X., Zhou L., Li S., Lu H., Ding X., **2014** 'Behavior of acid etching on titanium: Topography, hydrophilicity and hydrogen concentration', *Biomed. Mater*. 9: 015002. doi:10.1088/1748-6041/9/1/015002.

Mattox. D. M., **2010**. 'Handbook of Physical Vapor Deposition (PVD) Processing'. ISBN: 9780815520375.

Mayer T. M, Elam J. W., George S. M., Kotula P. G., Goeke R. S., **2003**. 'Atomic layer deposition of wear-resistant coatings for microelectromechanical devices'. *Appl. Phys. Lett.* 82: 2883. https://doi.org/10.1063/1.1570926

Mei Y., Saha K., Bogatyrev S. R., Yang J., Hook A. L. Kalcoiglu Z. I., Cho S. W., Mitalipova M., Pyzocha N., Rojas F., Vam Vliet K. J., Davies M. C., Alexander M. R., Langer R., Jaenisch R., Anderson D. G., **2010**. 'Combinatorial development of biomaterials for clonal growth of human pluripotent stem cells'. *Nat Mater* 9(9): 768-78

Moulder J. F., Stickle W. F., Sobol P. E., and Bomben, K. D., **1992**. In J. Chastain (Ed.), 'Handbook of X-ray photoelectron spectroscopy, physical electronics'. Eden Prairie: Perkin-Elmer Corp.

Niinistö L., **1990**. 'Proc. 1st Int. Symp. on Atomic Layer Epitaxy (ALE-1) June 11-13, 1990, Espoo, Finland'. Acta Polytechnica Scandinavica, Chemical Technology and Metallurgy Series.

Niinistö L., Nieminen M., Päiväsaari J., Niinistö J., Putkonen M., Nieminen M., **2004**. 'Advance electronic and optoelectronic material by atomic layer deposition: an overview with special emphasis on recent progess in processing of high-k dielectrics and other oxide materials'. *Physica Status Solidi A*. 201(7): 1443-1452. https://doi.org/10.1002/pssa.200406798.

Peng Q., Gong B., VanGundy R. M., and Parsons G. N., **2009**. 'Zincone-Zinc Oxide−Organic Hybrid Polymer Thin Films Formed by Molecular Layer Deposition'. *Chem. Mater.* 21(5): 820–30. https://doi.org/10.1021/cm8020403.

Pfaff G., and Reynders P., **1999**. 'Angle-Dependent Optical Effects Deriving from Submicron Structures of Films and Pigments'. *Chem. Rev.* 99(7): 1963–82. https://doi.org/10.1021/cr970075u.

Pore, V., Rahtu A., Leskelä M., Ritala M., Sajavaara T., and Keinonen J., **2004**. 'Atomic Layer Deposition of Photocatalytic TiO_2 Thin Films from Titanium Tetramethoxide and Water'. *Chem. Vap. Dep.* 10(3): 143–48. https://doi.org/10.1002/cvde.200306289.

Puurunen R. L., **2003** 'Growth per cycle in atomic layer deposition: a theoretical model'. *Chem. Vap. Dep.* 9(5): 249-257. https://doi.org/10.1002/cvde.200306265.

Puurunen R. L., **2005**. 'Surface Chemistry of Atomic Layer Deposition: A Case Study for the Trimethylaluminum/Water Process'. *J. Appl. Phys.* 97(12):121301. https://doi.org/10.1063/1.1940727.

Puurunen, R. L. **2014**. ‘A Short History of Atomic Layer Deposition: Tuomo Suntola’s Atomic Layer Epitaxy’. *Chem. Vap. Dep.* 20(10-11-12): 332-344. https://doi.org/10.1002/cvde.201402012.

Rahtu, A., and Ritala M.. **2002**. ‘Reaction Mechanism Studies on Titanium Isopropoxide–Water Atomic Layer Deposition Process’. *Chem. Vap. Dep.* 8(1): 21–28. https://doi.org/10.1002/1521-3862(20020116)8:1%3C21::AID-CVDE21%3E3.0.CO;2-0

Ritala M., and Niinistö J., **2009**. ‘Industrial Applications of Atomic Layer Deposition’. *ECS Transactions* 25(8): 641–52. https://doi.org/10.1149/1.3207651.

Ritala M., and Leskelä M. **1994**. ‘Zirconium Dioxide Thin Films Deposited by ALE Using Zirconium Tetrachloride as Precursor’. *Appl. Surf. Sci.* 75(1): 333–40. https://doi.org/10.1016/0169-4332(94)90180-5.

Ritala, M., Leskelä M., Niinistö L., Haussalo P., **1993**. ‘Titanium Isopropoxide as Precursor in atomi Layer Epitaxy of Titanium Dioxide Thin Films’. *Chem. Matter.* 5(8): 1174-1181. https://doi.org/10.1021/cm00032a023.

Roach P., Parker T., Gadegaard N., Alexander M. R. **2010**. ‘Surface strategies for control of neuronal cell adhesion: a review’. *Surf. Sci. Rep.* 65(6): 145-173. https://doi.org/10.1016/j.surfrep.2010.07.001.

Rompelberg C., Heringa M. B., van Donkersgoed G., Drjver J., Roos A., Westenbrink S., Peters R., van Bemmel G., Brand W., Oomen A.G.. **2016**. ‘Oral Intacke of Added Titanium Dioxide and Its Nanofraction from Food Products, Food Supplements and Toothpaste by the Dutch Popolation’. *Nanotoxicology*, 10(10): 1404-1414. https://doi.org/10.1080/17435390.2016.1222457.

Samavedi S., Poindexter L. K., Van Dyke M., Goldstein A.S., **2014**. ‘Chapter 7: Synthetic Biomaterial for Regenerative Medicine Applications’. *Regenerative Medicine Applications in Organ Transplantation*. 7: 81-89. https://doi.org./1016/B978-0-12-398523-1.00007-0

Shirley, D. A. **1972**. ‘High resolution X-ray photoemission spectrum of the valence bands of gold’ *Physical Review B: Condense Matter*, 5: 4709-4713 https://doi.org/10.1103/PhysRevB.5.4709

Siltron L. G., and Kyong-Min K., **2000**. ‘Silicon-pulling technology for 2000+’. *Solid State Technology* 43 (1): 69-73.

Sneck, S., **2007**. ‘NanoTechnology in Northern Europe Conference’, 2007.

Suntola T., Antson J., Pakkala A., and Lindfors S., **1980**. ‘Atomic Layer Epitaxy for Producing EL Thin Films’ *Proc. SID Symp. Dig. Tech. Papers*.

Suntola T., **1989**. ‘Atomic Layer Epitaxy’. *Material Science Report,* 4(5): 261-312. https://doi.org/10.1016/S0920-2307(89)80006-4

Suntola T., **1992**. ‘Atomic Layer Epitaxy’. *Thin Solid Films*, 216(1): 84–89. https://doi.org/10.1016/0040-6090(92)90874-B.

Tiku S. K., and Smith G.C., **1984**. ‘Choice of Dielectrics for TFEL Displays’. *IEEE Transactions on Electron Devices* 31(1): 105–8. https://doi.org/10.1109/T-ED.1984.21482.

Vassanelli S. **2011**. ‘Brain-Chip Interfaces: The Present and The Future’. *Procedia Computer Science*, Proceedings of the 2nd European Future Technologies Conference and Exhibition 2011.

Vila-Comamala J., Jefimovs K., Raabe J., Pilvi T., Fink R. H., Senoner M., Maaßdorf A., Ritala M. and David C., **2009**. ‘Advanced Thin Film Technology for Ultrahigh Resolution X-Ray Microscopy’. *Ultramicroscopy* 109 (11): 1360–64. https://doi.org/10.1016/j.ultramic.2009.07.005.

Visentin F., El Habra N., Favaro M., Battiston S., Gerbasi R., Crociani L., Galenda A. ‘Hybrid synergic methodology to prepare ALD Honey-Comb Anatase Film’. *Chem. Vap. Dep.* **2015**, 21 (10-12):300-306. https://doi.org/10.1002/cvde.201507183.

Wang, J. J., Deng X, Varghese R., Nikolov A., Sciortino P., Liu F., Chen L., and Liu X., **2005**. ‘Filling High Aspect-Ratio Nano-Structures by Atomic Layer Deposition and Its Applications in Nano-Optic Devices and Integrations’. *Jo. Vac. Sci. Tech. B: Microelectronics and Nanometer Structures Processing, Measurement, and Phenomena* 23(6): 3209–3213. https://doi.org/10.1116/1.2132326.

Wu S., Weng Z., Liu X., Yeung K. W. K., Chu P. K. **2014**, ‘Functionalized TiO_2 Based Nanomaterials for Biomedical Applications’, *Adv. Func. Mater.* 24: 5464-5481. DOI: 10.1002/adfm.201400706.

Yamamoto Y., Saito K, Takahashi K., and Konagai M., **2001**. ‘Preparation of Boron-Doped ZnO Thin Films by Photo-Atomic Layer Deposition’. *Solar Energy Materials and Solar Cells*, PVSEC 11 Part I, 65 (1): 125–32. https://doi.org/10.1016/S0927-0248(00)00086-6.

ACKNOWLEDGEMENTS

I would first like to thank the CNR-ICMATE Padova Director Prof. Lidia Armelao for giving me the opportunity to intern at her institute, and Prof. Patrizia Canton, my thesis supervisor at Cà Foscari University of Venice.

I wish to express my sincere and deepest gratitude to Dr. Naida El Habra, my CNR-ICMATE tutor, for providing me with all the necessary research facilities and for her continuous encouragement. I am profoundly grateful for the priceless expertise she shared, being an invaluable and veritable guidance throughout my time as intern.

My gratitude extends to all CNR-ICMATE staff and personnel. I am particularly grateful to Dr. Alessandro Galenda, whom I had the pleasure to share the research facilities.

I wish to thank Prof. Stefano Vassanelli of Padova University for giving me the opportunity to access the Neurochip Laboratory as well as Dr. Marta Maschietto for the work produced.

I would to thank everyone of the specialist involved in this research for their contribution in their respective tasks: Prof. Cinzia Sada, for SIMS analyses, Prof. Tiziana Cesca for spectroscopic ellipsometry measurements, Dr. Marta Maria Natile for XPS characterizations and Sig. Elvio Bullita for the development of the ALD visual basic software.

Finally, I must express my very profound gratitude to my family and Alessia for providing me with unfailing support and continuous incitement throughout my years of study and during the process of researching and writing this thesis.